Suitability of the Yucca Mountain Site to Accommodate a permanent Repository for High-Level Radioactive Waste and Spent Nuclear Fuel: an Independent Assessment

Part One

Synthesis: Contemporary State and Evolution of the Geologic System at Yucca Mountain

By

J.S Szymanski

and

T.R. Harper

Table of Contents

Chapter 1.1. General Geology and Hydrology

1.1.1. General Geology

Yucca Mountain is located at latitude 37° N and longitude 116° 30' W (Figure 1-1), in the Basin and Range Province of the United States within a region known as the Great Basin. This tectonically and volcanically active region is characterized by the presence of major geophysical anomalies, small-scale basalt volcanism of Plio-Quaternary age, active faulting with moderate to high seismicity, high heat flow, and thermal springs. In the area adjacent to Yucca Mountain the climate is arid, the population density is scarce, the land is under control of the Federal Government, and the present-day water table is at a depth of about 500 m.

The mountain ranges of the Great Basin are aligned mostly north south, and are composed of tilted, fault-bounded blocks. These blocks may extend more than 80 km in length and are generally between 8 and 25 km wide. Relief between the valley floors and mountain ridges is typically between 300 and 1500 m. The valleys occupy approximately 50-60 percent of the total area and are filled with thick deposits of alluvium and colluvium, which have been derived through denudation of the adjacent mountain ranges. The ranges are separated, north to south, by roughly 25-30 km, and many of them arc toward each other and merge.

The physiographic pattern of the region is a result of a generally east to west directed extension of the lithosphere, which began in the mid-Tertiary and continues to the present-day. Rocks of every age, from pre-Cambrian to Quaternary, have been affected by this extension.

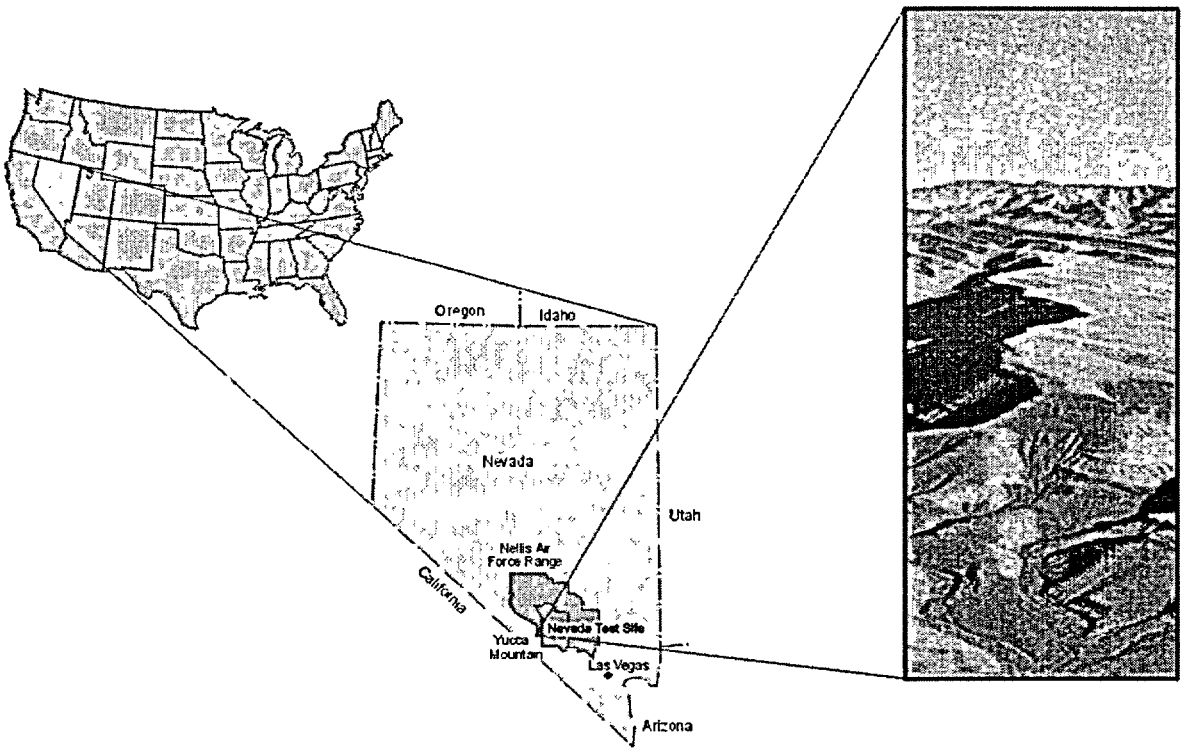

Figure 1-1. Location of Yucca Mountain. Modified from U.S. DOE (1998; 1999).

Long-term extension rates across the southern Great Basin, at latitude 37° N, are of the order of $0.07 \cdot 10^{-6}$ per year, as given in Wernicke et al. (1982). These rates, which have been calculated for the entire region, are averages over the past 15 Ma. However, at any given time, the straining seems to be confined to relatively narrow belts, as now appears to be the case for the area around Death Valley, rather than being uniformly distributed across the region. Local short-term deformation rates are different from the long-term averages, and they vary in time.

Seismicity in the southern Great Basin has a widespread and diffuse background, which is punctuated by areas containing clusters of intense activity separated by larger nearly a seismic areas. Most events are of low to moderate magnitude with the focal depth ranging between 1 and 17 km. The depth distribution has two broad peaks; one between 0 and 2 km and the other between 5 and 8 km, with a distinct minimum at a depth of about 3.5 km. The depth profiles from active areas frequently show event patterns extending from the ground surface down to a depth of 10 km or more. Fault plane solutions indicate that strike-slip faulting is the dominant mode of elastic release of the accumulated and accumulating strain energy. For most of the radiation patterns, the B-axis or pole to a plane containing slip vectors plunges steeply.

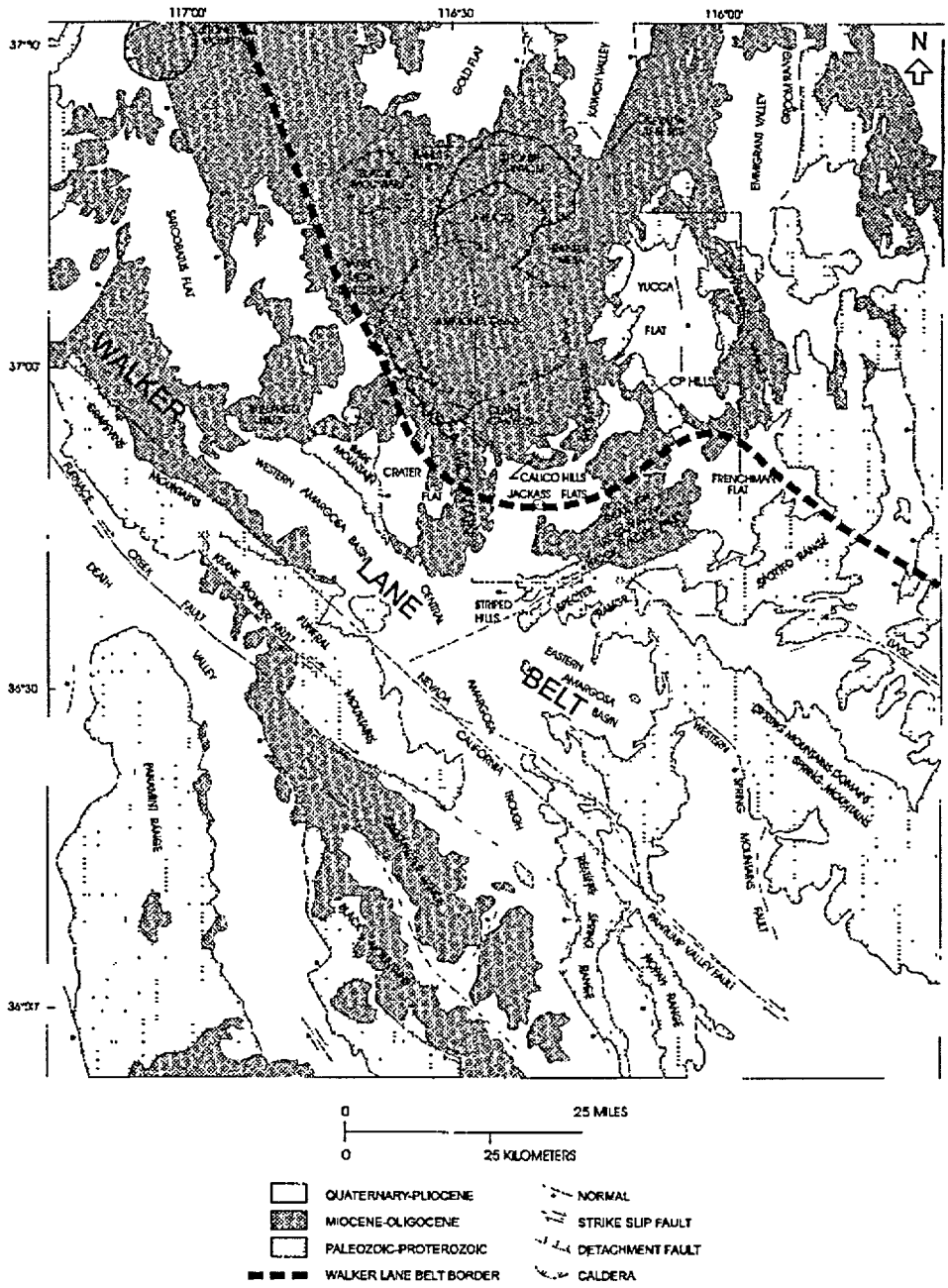

Figure 1-2. Generalized geologic map of the area of Yucca Mountain. Note overprinting of the Walker Lane dextral shear belt by late Tertiary rocks of the southern Nevada volcanic field and downdropping of the basement at and around Yucca Mountain. From U.S. DOE (1998).

The southern Nevada volcanic field is a sub-region of the southern Great Basin. Yucca Mountain is situated within this sub-region, along its south-central margin. This volcanic plateau began forming about 25 Ma ago. It owes its existence to repeated eruptions of large volumes of acid and intermediate lava and ash-flow tuff from a number of strato-volcanoes adjacent to Yucca Mountain, as shown in Figure 1-2.

Some of the ash-flow sheets cover an area of several thousand km^2 and had initial volumes measured in terms of several hundred km^3. This voluminous siliceous volcanism ceased in the late Miocene-Pliocene, after which time development of the volcanic field has continued in the form of volcanic centers, out of which small volumes of basalt magma were erupted.

The most recent eruptions occurred over a time span from 3.7 Ma up to essentially the present. These Plio-Quaternary eruptions of mafic magma represent a replacement of the late Tertiary siliceous volcanism. They form a northwest trending belt that extends from Amargosa Desert, through Crater Flat, to the east Sarcobatus Flat, for a distance of nearly 100 km, as shown in Figure 1-2.

Just a few kilometers to the west of Yucca Mountain, the belt includes basalt lava flows that were erupted about 3.7 Ma ago as well as four 0.7-1.2 Ma old cinder cones. The Lathrop Wells volcanic complex, which is located in the southernmost part of Yucca Mountain, represents the most recent episode of mafic volcanism, and includes fissure eruptions, spatter and scoria cones, and lava flows. Average age of this episode is about 75 Ka.

Deposits of gold and silver are common in the southern Nevada volcanic field. These deposits were worked in the early 1900's and during the depression and some are still actively mined. They were emplaced within or adjacent to the late Tertiary volcanic centers and the chief ore-bearing rocks are extrusive and intrusive complexes of intermediate composition. Yucca Mountain is located between two mining districts, Bare Mountain about 20 km to the west and Whamonie about 20 km to the east, Figure 1-2. The Whamonie district was mined primarily for silver, but also has high concentrations of gold, cobalt, and chromium. The Bare Mountain district was mined primarily for gold and fluorite, but also has a high concentration of arsenic, cadmium, lead, and zinc. The age of the Bare Mountain deposit was considered by Weiss et al. (1993) as between 11 and 14 Ma.

Basement of the southern Nevada volcanic field consists of two major rock assemblages. The older assemblage is crystalline and consists of Archeozoic and Proterozoic igneous and metamorphic rocks. The younger assemblage consists of a nearly 10-km thick section of upper pre-Cambrian and Paleozoic sedimentary rocks formed in the Cordilleran geosyncline. The basal rocks are dominantly clastic, with quartzite being the dominant lithology. The overlying rocks are mainly carbonates, which in turn are overlain by clastic rocks of the Eleana Formation. These Devonian and Mississippian rocks include coarse gravels that were derived from erosion of thrust plates, which begun forming at that time in an area to the northwest. Following this orogenic episode, the carbonate deposition resumed and persisted throughout the remainder of the Paleozoic Era.

There are no Mesozoic sedimentary rocks in the southern Nevada volcanic field. The Mesozoic Era is represented only by a few scattered granite plutons. Several thrust-fault structures of Mesozoic age are

present at the Nevada Test Site and in the adjacent mountain ranges. The combined displacement across these structures amounts to several tens of kilometers. In places, the upper pre-Cambrian and lower Paleozoic rocks are located over the younger carbonate and clastic rocks.

Formation of the southern Nevada volcanic field is the most significant rock-forming process of the Cenozoic Era in this area. Chemical and radiometric data from the associated rocks indicate that similar igneous activity affected a large area, extending to central Nevada and to central Sierra Nevada. Older parts of the volcanic section are developed in the form of intrusive and extrusive complexes of intermediate composition. The subsequent siliceous volcanism is in the form of several major strato-volcanoes (calderas), from which numerous sheets of welded and non-welded tuffs were erupted, including those that comprise Yucca Mountain.

The older sheets are per-alkaline in chemical composition, intermediate between trachyte and comendite, whereas the younger sheets are calc-alkali in composition, which ranges between that of rhyolite and that of quartz latite. The gradual cessation of voluminous siliceous volcanism dates back to the late Miocene, and it is associated with a trend of the calc-alkali compositions evolving with the decreasing age to the more per-alkaline and sub- alkaline compositions.

The youngest stratigraphic units are composed of thick accumulations of alluvium and colluvium in tectonic depressions, with thin veneers of colluvium typically covering the hillsides. Eolian sands are generally minor components of the unconsolidated deposits.

1.1.2. Surface and Vadose Zone Hydrogenic Deposits: Statement of the Issue

Early in the site characterization process, alkaline- and saline-water spring and marsh deposits were discovered to the southwest and south of the proposed repository at Yucca Mountain. Initially, these deposits were studied by Hoover et al. (1981) and dated by Szabo et al., 1981. They carry ^{234}Th/U ages that typically are less than 500 Ka and are developed in a variety of forms. Szabo et al. (1981) furnished the following description of these forms: "*They commonly fill fractures along faults, form dense, strongly cemented deposits in alluvium and are precipitated from spring water. The carbonates were broadly classified into five groups. The hard, dense, and finely crystallized carbonates precipitating from groundwater are referred to as travertines The softer and more porous forms of the precipitated carbonates are defined as tuffaceous travertines The surficial conglomerates or rock fragments and minerals, strongly cemented by authigenic carbonate are called calcretes. The secondary accumulations of cementing carbonate in the host material of a soil environment are identified as soil caliches. Finally, the dense calcium carbonate in fractures in drill holes is referred to as calcite veins.*" (emphasis added). Concurrently, Knauss (1981) confirmed the U-series ages and provided similar description of the carbonate and opal accumulations throughout the Nevada Test Site.

Furthermore, a few meters thick deposit of gypsum was found about 15 km to the east of Yucca Mountain, near the Whamonie mining district, Figure 1-2. This deposit occurs in a topographic setting that precludes a playa deposition, but is, nonetheless, in an area where the vadose zone is more than 500-m thick. It consists of almost pure gypsum with minor calcite, and "... *leaves little doubt that it represents a warm-water paleo-spring discharge*", according to Vaniman et al., 1988, (emphasis added).

Initially, the Whamonie deposit was discovered by the USGS researchers because of the search for a potential repository site at the Nevada Test Site (NTS). A USGS letter to the DOE Nevada Operations Office recommended abandoning the search in this part of the NTS. This letter described this deposit as "... *local surface deposits from recent warm springs that indicate upward seepage of ground water, possibly from great depth*".

The preceding descriptions of obviously very young spring deposits pose a major conceptual problem. How to explain the occurrence of spring activity at levels that are significantly higher than can be attributed to the highest possible climate-related groundwater levels? There are only two ways of resolving this problem. One must accept the paleo-spring origin and then reject the equilibrium system viewpoint or conversely, demonstrate another (non-spring) origin and then reject the competing non-equilibrium system viewpoint. This, in a nutshell, is the issue with which this report is concerned. As stated by Broad (1990), the resolution in favor of the non-equilibrium system viewpoint "...*could mark the end of the Yucca Mountain Project. The retreat would be a stunning setback for the Government and the nuclear-power industry, which is poised for a revival* "

The record shows that the issue was recognized, although not resolved, by early researchers of Yucca Mountain. For instance, Wingrad and Doty (1980) stated: *"Two calcitic fracture fillings found in Paleozoic carbonate rocks at sampling Site #4 are examples of veins apparently having little relation to modern or pluvial groundwater levels despite uranium-thorium dates, of 72,000 and 100,000 years. These samples were collected by W. J. Carr (U. S. Geological Survey, Denver, Colo) at an altitude of approximately 1140 m, or about 200 m above the level of the playa in Frenchman Flat. While we tentatively accept the ages, the assumption that this calcitic material was precipitated within a regional zone of saturation during pluvial times is premature."* (emphasis added).

Surface deposits, which are composed of carbonate, opaline silica, and sepiolite, were found in many locations at and around Yucca Mountain. By the end of the 1980's, however, the early interpretation of these deposits as spring and seep deposits or travertines (e.g., Szabo et al., 1981) had changed. From then on, these deposits were considered as "*pedogenic*", or formed as a result of the soil-forming processes through a dissolution and re-precipitation of eolian carbonaceous dust by rainwater (Quade and Cerling, 1990 and Stuckless et al., 1991, for example). Paces et al. (1993), Quade (1993), Forester et al.

(1999), Paces and Whelan (2001), and many other researchers later exhaustively studied these deposits, and all of them reached a unanimous conclusion that they are products of evaporated rainwater. However, some researchers have challenged this new pedogenic interpretation (Archambeau and Price, 1991; Harmon, 1993; Hill et al., 1995; Dublyansky et al., 1998, for example).

Coarse-crystalline secondary minerals, calcite, opal, chalcedony, quartz and fluorite were routinely reported as vein filling minerals from cores of boreholes drilled in the Yucca Mountain vadose zone. Mostly because of the stable and radiogenic isotope similarity between the subsurface calcite and calcite from the shallow sub-surface, these minerals were attributed to a "pedogenic" origin (Vaniman and Whelan, 1994; Whelan et al., 1994).

In 1995, after the excavation of the Exploratory Studies Facility (ESF; a 7.8 km-long horseshoe-shaped tunnel), many more occurrences of these minerals become available for studies. One important outcome of the ongoing studies was the discovery of two-phase fluid inclusions entrapped inside them. These fluid inclusions provided information on the temperatures and salinities of the mineral-forming waters. Both turned out to be conspicuously elevated, up to 85°C and up to 21,000 ppm respectively (Dublyansky, 1998; Dublyansky et al., 2001; Wilson et al., 2000; Whelan et al. 2000).

Interpretation of these deposits remains subject to controversy. Some researchers maintain that these deposits record downward percolation of meteoric waters (e.g., Paces et al., 1999 and 2000). To explain the elevated homogenization temperatures, they assert that the vadose zone of Yucca Mountain was conductively heated by a magma body solidifying under the Timber Mountain Caldera (see Figure 1-2). The mountain would have to remain hot for some 6 Ma (Marshal and Whelan, 2000; Whelan et al. 2001), an impossibility from any perspective in our opinion. The other scientists claim that these minerals are positive proof of the upwelling of thermal waters along the local fault zones, (Dublyansky et al., 2001, Smirnov and Dublyansky, 2000 and 2001).

The controversial mineral deposits briefly outlined here are discussed in detail in the Part Three of the report.

Chapter 1.2. Late Cenozoic Volcanism around Yucca Mountain: Geothermal Implication

1.2.1. Introduction

In many tectonically active regions of the Earth, volcanism is closely associated with hydrothermal activity, which endures for prolonged periods and assumes a variety of forms. Necessary conditions for these processes include high temperatures in the crust and large fluxes of endogenic heat. Yucca Mountain is in such a tectonically active region, where the onset of orogenic activity is always accompanied by the increased transport of heat from the mantle into the crust across the Moho discontinuity.

The increased heat input has the effect of steadily augmenting the radiogenic heat production in the crust, which eventually leads to the development of thermal disequilibrium therein. The accumulated and accumulating heat must be transported up through the crust, eventually out the surface, and into the atmosphere. Typically, when the thermal disequilibrium sets-in, the transport involves heat conduction as well as advection, which manifests as movement of bodies of volatile and fluid phases. One such mechanism is volcanism, which involves advective transport of heat in the form of siliceous magma. The other is hydrothermal circulation, which also involves advective transport of heat, though one where the transporting medium is an aqueous solution, motions of which are in the form of a convection cell or a hydrothermal plume.

The late Quaternary calcite-silica deposits, present throughout the Yucca Mountain area, have been briefly described in the section 1.1.1 above. We have indicated that a possibility exists these hydrogenic deposits are the products of intermittent eruptions of hydrothermal plumes. The ascent of such plumes would be in part a result of the conversion of endogenic heat into work performed, in the form of non-

equilibrium flow of crustal fluids, and an expression of the thermal disequilibrium-activated advective heat transport through the crust.

Because of the intimate link between hydrothermal and volcanic processes, a review of the history of volcanism in southern Nevada is a necessary first step in addressing the issue of hydrothermal activity and the origin of the controversial hydrogenic deposits. Such a review will be a useful background and perspective for comprehending the present-day thermodynamic environment and its evolution, the potential role of fault ruptures in facilitating the occurrence of hydrothermal events, and eventually the total conceptual model, as constructed in Part Two and then tested in Part Three of the report.

1.2.2. Siliceous Volcanism

Yucca Mountain is an irregularly shaped volcanic upland, 6 to 10 km wide and about 40 km long. The mountain is composed of late Miocene high-silica rhyolite and quartz latite, developed mainly in the form of ash-flow and ash-fall tuffs. These tuffs comprise the two principal stratigraphic units of the area, namely the Crater Flat Tuff and the overlying Paintbrush Tuff. In addition, a section of non-welded tuffs, so-called tuffs of Calico Hills, is sandwiched between the principal units. The basement is composed of a late Proterozoic-early Paleozoic sequence of sedimentary rocks from the Cordilleran geosyncline, which overlies an early-to-mid pre-Cambrian sequence of igneous and high-grade metamorphic rocks.

The upland of Yucca Mountain is part of the southern Nevada volcanic field, which was formed by intense siliceous volcanism over the late Tertiary period. Immediately around Yucca Mountain, this activity ceased with eruption of the Timber Mountain Tuff, about 11.5 Ma ago. Smaller scale volcanism, extension and faulting, moderate to high seismicity, high heat flow, and thermal springs are all associated with this region now. The youngest eruptions post-date the Timber Mountain Tuff and involved mafic, acid, and intermediate magmas. The development of the southern Nevada volcanic field was initiated about 25 Ma ago, and it has proceeded in three stages.

The first stage is represented by rocks that crop out between latitude 37^0 30' and 38^0 00' N, within an area that spans central Nye County of Nevada. This area extends westward from the Belted and Reveille Ranges to the Goldfield and Tonopah mining districts along its western limit, as shown in Figure 1-3.

The intrusive and extrusive rocks from the first stage are mainly intermediate in chemical composition and occur in the form of up to 1-km thick lava flows, dikes, sills, laccoliths, and volcanic plugs. The petrography ranges from basalt andesite to quartz latite and dacite. Importantly, some of the extrusive and intrusive complexes display a trend to higher silica content with decreasing age, which implies a gradually increasing involvement of the crust-derived melts.

Two major ash-flow units have been dated, specifically the Tuff of Monotony Valley, at the bottom of the section, and the Fraction Tuff, at the top. These give a bracket for the age-range of the first stage of between 17.8 and 22.3 Ma, as given in Anderson and Ekren (1968).

The intermediate rocks occupy an area of about 15,000 km^2 and occur in the form of clusters. Each cluster covers an area up to 40 km^2, and these rocks seem to have been extruded from nearby or subjacent fissure vents. Considering the widespread occurrence and compositional uniformity of these rocks, Anderson and Ekren (1968) interpreted this feature as evidence for the presence of a broad magma body that was tapped at numerous locations by fissure vents.

The second stage involved siliceous volcanism, which initially was per-alkaline and then, evolved to calc-alkali in chemical character. As shown in Figure 1-3, the corresponding volcanic centers, or calderas, are located between latitude 36^0 45' and 37^0 30' N, within an area which spans south central Nye and Lincoln Counties. This area extends westward from the southern Delamar Range to the Beatty and Bullfrog mining districts located along its western edge.

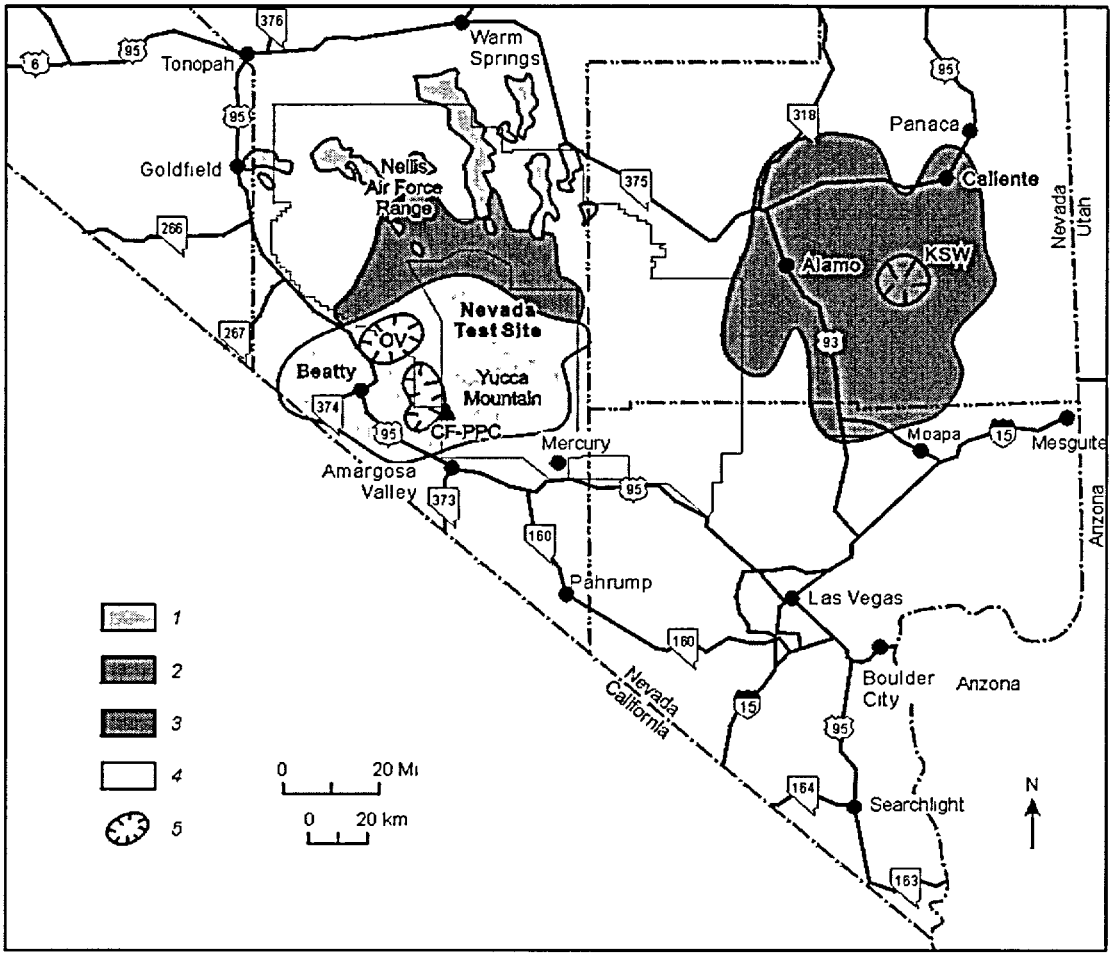

Figure 1-3. Geologic map showing distribution of volcanic rocks from the first and second stage of development of the Southern Nevada volcanic field. Compiled from Ekren (1968), Anderson and Ekren (1968), and Noble et al. (1968).

First stage of development of the Southern Nevada volcanic field: 1 – Miocene rocks of intermediate composition and superjacent and subjacent ash-flow tuffs (17.8 to 22.3 Ma). *Second stage of development of the Southern Nevada volcanic field*: 2 – rocks of Kane Springs Wash center (14.8 Ma); 3 – rocks of Silent Canyon Caldera – Belted Range Tuff (14 Ma); 4 – rocks of Oasis Valley Caldera – Paintbrush Tuff (13-13.6 Ma); and 5 – approximate location of calderas.

KWS – Kane Spring Wash (14.8±0.6 Ma); SC – Silent Canyon Caldera (14 Ma); CF-PPS – Crater Flat/Prospector Pass Caldera (13.6 Ma); and OV – Oasis Valley Caldera (~13 Ma).

From east to west, the centers include the Kane Springs Wash Caldera (Noble et al., 1968), the buried Silent Canyon Caldera (Orkild et al., 1968), and the Crater Flat-Prospector Pass and Timber Mountain-Oasis Valley Caldera complexes (Carr et al., 1984), as shown in Figure 1-3. Most of the rocks that were erupted from these centers were initially trachyte-to-dacite and then high-silica rhyolite and quartz latite. They occur in the form of extensive interbedded sheets of ash-flow tuff, ash-fall tuffs, and occasional lava flows. They comprise the four principal stratigraphic units of this area. These are: the

Kane Wash Tuff (erupted from the Kane Springs Wash Caldera), the Belted Range Tuff (erupted from the Silent Canyon Caldera), the Crater Flat Tuff (erupted from the Crater Flat-Prospector Pass Caldera), and the Paintbrush Tuff (erupted from the Timber Mt.-Oasis Valley Caldera complex).

The material that was erupted from a single caldera had an estimated volume of up to several hundreds of km^3 and covered an area up to several thousands of km^2. Noble (1968), Noble et al. (1968), and Kilter (1968) reported K/Ar ages for all of the four units. These ages range narrowly between about 13 Ma, for the youngest Tiva Canyon Member of the Paintbrush Tuff, and 14.8 Ma, for the oldest Tub Spring Member of the Belted Range Tuff, respectively.

It thus appears that the onset of voluminous siliceous volcanism was nearly coeval over a large area of southern Nevada, and that the centers (calderas) remained active within a narrow interval of time, spanning about 1.5 Ma. The early eruption of intermediate rocks (chiefly lava flows and porphyry complexes with andesite composition) during the first stage of volcanic activity, in the area immediately to the north, preceded this volcanism.

The spatial migration and the evolving chemical composition of rocks, which were erupted between 22.3 Ma and about 13 Ma ago, both imply a trend of increasing heat in the crust and an increasing extent of the crust anatexis (melting). The gradually diminishing proportion of the mafic component provides evidence that the increasing heat content in the crust was a result of the advective input of endogenic heat, in the form of basalt magma. The increasing advective heating, in turn, implies a gradually increasing degree of partial melting in the mantle source.

The third stage of development of the southern Nevada volcanic field is characterized by the eventual cessation of siliceous volcanism and its replacement by eruptions of small volumes of basalt magma. By contrast to the preceding stages, this stage has produced volcanic rocks that display greater variability of chemical and lithological composition, which ranges from calc-alkali through per-alkaline or sub-alkaline to mafic, and includes high silica rhyolite, quartz latite, andesite, dacite, and basalt.

As a whole, the rocks display a trend to lower silica and higher iron content and to a lower Na_2O+K_2O/Al_2O_3 ratio with decreasing age. Thus, this trend is opposite to the one that characterizes the rocks erupted over the preceding two stages. This more recent trend expresses the gradually diminishing degree of melting in the crust, and the increasing proportion of a mafic component in the melt. By contrast, the preceding trend expresses the gradually increasing degree of melting in the crust, whilst expressing the decreasing proportion of a mafic component in the composite melt.

The late centers of siliceous volcanism are located between latitude 36^0 45' and 37^0 45' N, within an area that extends to the northwest from Mercury, Nevada, to about 50 km to the west of Goldfield,

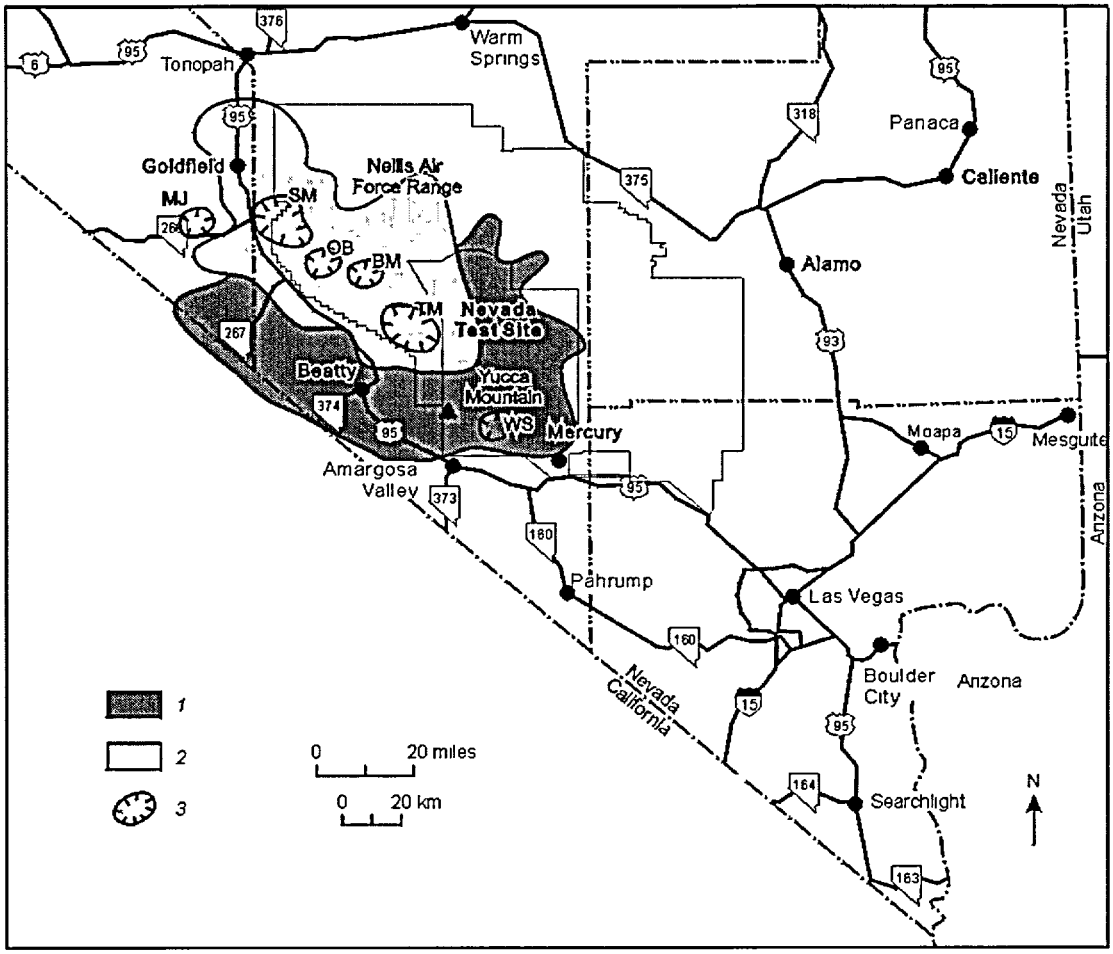

Figure 1-4. Geologic map showing distribution of siliceous volcanic rocks from the third stage of development of the Southern Nevada volcanic field. Note progressive migration of the pyroclastic centers to the northwest. Compiled from Ekren (1968) and Noble et al. (1991).

1 – Timber Mountain Tuff (~11 Ma); 2 – Thirsty Canyon Tuff and Stonewall Flat Tuff (7.4-8.8 Ma); and 3 – pyroclastic center. WS – Whamonie Salyer Center (~13 Ma); TM – Timber Mountain Caldera (~11 Ma); BM – Black Mountain Caldera (8.5-9.0 Ma); OB – Obsidian Butte (8.8±0.3 Ma); SM – Stonewall Mountain Caldera (7.5 Ma); and MJ – Mt. Jackson (3.0-4.5 Ma).

Nevada. These centers form a NW-SE trending alignment, which corresponds to the northeast margin of the Walker Lane wrench system. From southeast to northwest, they include Whamonie-Salyer center, Timber Mountain Caldera, Black Mountain Caldera, Obsidian Butte center, Stonewall Mountain Caldera, and Mt. Jackson-Montezuma Range volcanic center, as shown in Figure 1-4.

The best known and largest among the late pyroclastic centers is the Timber Mountain Caldera, a 35- by 40-km elliptical collapse structure elongated to the northwest. It is located between the Silent Canyon Caldera, to the north, and Yucca Mountain, to the south. A series of three ash-flow tuffs were extruded from this caldera. These compositionally similar ash-flow sheets carry K/Ar ages of about 11.5

Ma and are zoned from high-silica rhyolite, at the bottom, to quartz latite, at the top. They are distributed in and around the parent caldera, covering an area of tens of thousand km^2. The erupted volume is measured in terms of several hundred km^3.

Noble et al. (1991) considered that two distinct suits represent the latest siliceous volcanism. The older suit consists of high-silica tuffs and mainly siliceous lava flows. These rocks are informally referred to as the tuff and lava flows of Bullfrog Hills, rhyolitic tuff and lava of Rainbow Mountain, tuff of Cutoff Roads, and rhyolite of Shoshone Mountain. They carry K/Ar ages between 9.3 and 10.4 Ma. These rocks display close chemical affinity with the Timber Mountain Tuff, thus Noble et al. (1991) regarded them as a part of the Timber Mountain volcanism. However, in contrast to the Timber Mountain Tuff, these tuffs and lava flows were erupted from fissure vents, contemporaneously with the activity of faults nearby.

The younger suite is mostly confined to the Black Mountain, Obsidian Butte, and Stonewall volcanic centers, which are located 30-70 km to the northwest of Yucca Mountain, as shown in Figure 1-4. Sub-alkaline to per-alkaline ash-flow tuffs and highly potassic, siliceous to intermediate lava flows were erupted from these centers. The rocks comprise two principal units, the Thirsty Canyon Tuff and the Stonewall Flat Tuff. They carry K/Ar ages between 7.4 and 8.8 Ma (Noble et al., 1991).

Evidence for the continuation of siliceous volcanism to the northwest, along the northeastern margin of the Walker Lane structure, has been found to the southwest of Goldfield, Nevada, in the area of the Mt. Jackson-Montezuma Range. The Mt. Jackson volcanic center is located about 100-km to the northwest of Yucca Mountain, as shown in Figure 1-4. This center contains volcanic domes that are composed of phenocryst-rich lava flows ranging in composition from high-silica rhyolite to dacite (McKee et al., 1989). Several of the domes cut across basalt that was erupted from the same vents. A sample of the Mt. Jackson rhyolite was found to carry $^{40}Ar/^{39}Ar$ age of 2.93 +/- 0.16 Ma, as reported by McKee et al., 1989. Radiometric ages younger than 4.5 Ma were also found to be associated with rhyolitic tuffs and lava flows of the Montezuma Range (McKee et al., 1989).

It thus appears that the most recent stage of development of the southern Nevada volcanic field has been associated with a well-expressed evolutionary trend. This trend involves systematic migration of the pyroclastic centers to the northwest, parallel to and within the Walker Lane structure, as shown in Figure 1-4. Over the time span from 11 to 3 Ma, the centers have migrated to the northwest, for a distance of about 100-km. This migration was from the areas of Whamonie-Salyer (active 13 Ma ago) and Timber Mountain (active 11 Ma ago), through Black Mountain (active 8.5-9.0 Ma) and Obsidian Butte (active 8.8 Ma ago), to Stonewall Mountain (active 7.5 Ma ago), and then to the Mt. Jackson-Montezuma Range area (active 3.0 Ma ago).

This remarkable trend expresses, in our opinion, the time and space progression of high heat content in the crust. Thus, this trend expresses the transitory character of the advective heat flux, from the mantle into the crust, in the form of basalt magma. It is telling us that, at a given time and location, this flux increases until it is sufficient to support the establishment of a magma chamber in the crust, whose size is large enough to support the pyroclastic activity. Thereafter, adjustment of the size of the magma chamber and the intensity of pyroclastic activity establish a balance between the input and output of heat, accordingly.

After a relatively brief period of the pyroclastic activity, the advective heat flux diminishes, eventually becoming insufficient to support the continuation of large-scale melting in the crust. The process is then repeated, but now at a different and more distant northwest location. The increasing and then decreasing intensity of the advective heat flux, at a given location, reflects the temporal variability of the degree of partial melting in the mantle source at this location.

It thus appears that the evolution in time and space of the siliceous volcanism expresses, and is controlled by, fundamental processes that govern the melting of the mantle material and the derivation there from of basalt magma. This conclusion has profound geodynamic and hydrologic implications, which we will discuss throughout the subsequent sections.

It is important to understand that the cessation of the pyroclastic form of siliceous volcanism does not necessarily mean complete termination of melting in the crust, which could remain in the form of volumetrically small bodies and manifest as inconspicuous fissure eruptions. In fact, such eruptions may have occurred at Yucca Mountain.

Possible evidence for one of such eruptions has been found in southeastern Crater Flat, a few km to the southwest of the proposed repository. At this location, numerous rounded fragments of siliceous pumice were found embedded in a sandy alluvium, underneath a 3.7 Ma old basalt flow. Zircon from the pumice yielded a fission track age of 6.3 +/- 0.8 Ma (Carr, 1982). Because the age of this pumice does not correlate with any of the local tuff units, Carr (1982) considered it as possibly expressing the presence of an unknown fissure eruption of siliceous magma, now buried somewhere in the Crater Flat area.

In addition, Dublyansky and Lapin (1996) have reported the presence of epigenetic, relative to the Paintbrush Tuff, siliceous tuffs in the southern part of Yucca Mountain. Chemical composition of these rocks differs from those of the Tiva and Topopah Spring Members, which host them. These rocks also differ from the youngest locally known ash-flow unit, which is the Timber Mountain Tuff. Relative to the host tuffs, they are strongly enriched in CaO, MgO, and Fe_2O_3 and depleted in Na_2O and K_2O. Thus, they are more per-alkaline to sub-alkaline in composition than their calc-alkali hosts are which indicates that these rocks could represent the younger volcanic suite of the third stage of development of the southern

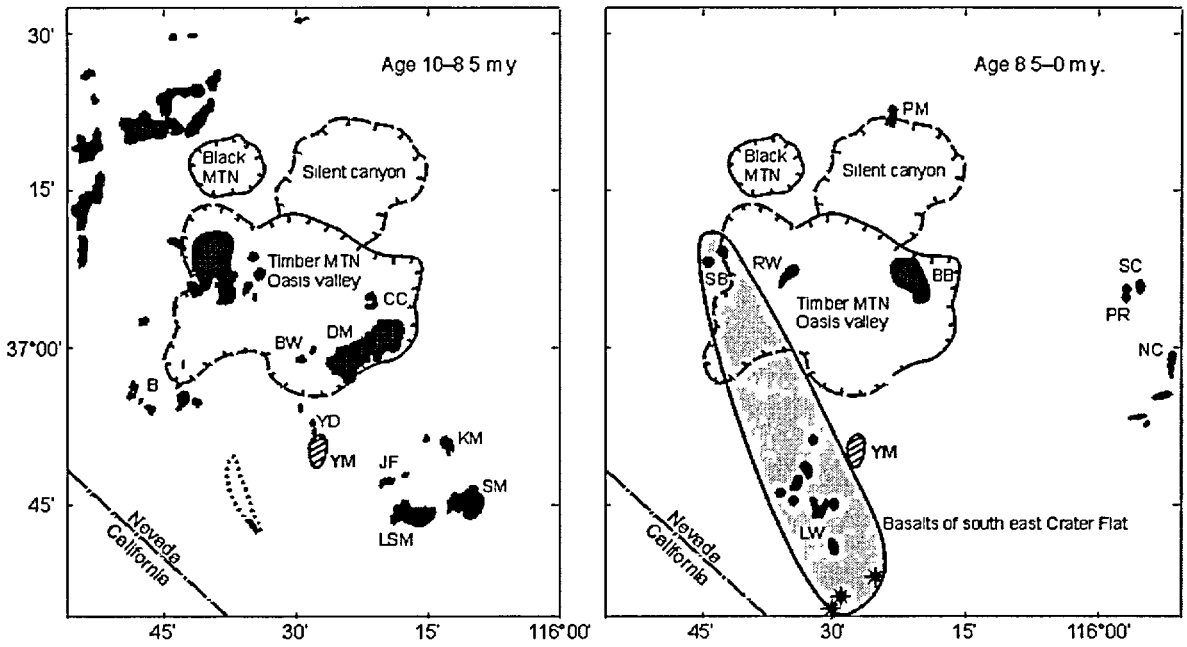

Figure 1-5. Geologic map showing distribution of mafic rocks (basalts) in the area of Yucca Mountain. Note north – northwest trending belt of the basalts (shaded area) just to the west of Yucca Mountain; ages of these basalts range from 3.7 Ma up to essentially the present. Modified from Crow (1990).

YM - Yucca Mountain. *Rocks older than 8.5 M* LSM – Little Skull Mountain; SM – Skull Mountain; JF – Jackass Flat; KM – Kiwi Mesa; YD – dike of Yucca Mountain; DM – Dome Mountain; BW – Beatty Wash; CC – Cat Canyon; B – Beatty. *Rocks younger than 8 5 Ma* LW – Lathrop Wells; PM – Pahute Mesa; RW – Rocket Wash; SB – Sleeping Butte; SC – Scrap Canyon; BB – Buckboard Mesa; PR – Paiute Ridge; NC – Nye Canyon; and stars are approximate locations of aeromagnetic anomalies inferred to represent buried basalt centers or intrusive rocks.

Nevada volcanic field. Although the age for these rocks is not known, it is possible that they are siliceous temporal equivalents of the basalt, which comprises Plio-Quaternary cinder cones and lava flows in Crater Flat, a few km to the southwest of Yucca Mountain.

The possible presence of epigenetic siliceous volcanic rocks is potentially very important, because it could signify that, in spite of the initial decline about 11 Ma ago, intense heating of the crust by the mantle has now resumed, but in a different form. The conductive heat flux may now be sufficiently intense to give rise to a near-solidus temperature in the mid-lower crust and, through that, to a very high intensity of the local heat flow, the possibility of which lies at the heart of our investigations.

1.2.3. Mafic Volcanism

The most visually apparent feature of the area around Yucca Mountain is the presence of a number of volcanic centers from which basalt magma has erupted, in some instances more than once. The eruptions post-date the ash-flow tuffs and their ages span a period from late Miocene to late Quaternary. They occurred at many locations that are scattered all around this area, as shown in Figure 1-5.

Figure 1-5-*a* shows that the centers occupy the same area that previously had been so profoundly affected by the pyroclastic siliceous volcanism. Further, these centers form a cluster elongated to the northwest, parallel to and within the Walker Lane structure. In addition, a conspicuous NNW-SSE trending chain of the Quaternary centers occupies the area of Crater Flat-Amargosa Desert, just a short distance to the west of Yucca Mountain, as shown on Figure 1-5-*b*.

A variety of emplacement forms has been identified in the area including lava flows, cinder cones, dikes, and sills. The rocks are mainly alkali in chemical composition with a groundmass of olivine and calcic clinopyroxene. Alkali basalt, hawaiite, hypersthene hawaiite, and basaltic andesite are the major rock types.

The neodymium isotope ratio (ε_{Nd}) varies between about + 5 and about -10, whereas the strontium isotope ratio ($^{87}Sr/^{86}Sr$) ranges between 0.704 and 0.706, as given in Smith et al., 1997. This isotope variability suggests that the parental magmas were varying mixtures of two end-members.

One end-member is associated with a high value of the ε_{Nd} ratio (about + 8) but a low value of the $^{87}Sr/^{86}Sr$ ratio (about 0.703). This end-member therefore would represent a primitive asthenospheric (in a geochemical sense) source, as given in Zindler and Hart (1986) for example.

The other end-member has a low value of the ε_{Nd} ratio (about -9 ± 2) and a higher value of the $^{87}Sr/^{86}Sr$ ratio (about 0.7073 to say 0.7097), which is consistent with a lithospheric source, as given in Farmer et al., 1991.

Vaniman et al. (1982) and Crowe (1990) have demonstrated that the late mafic volcanism is associated with an important evolutionary trend. One aspect of this trend is a conspicuous decrease in the rate of magma generation, which is expressed by the fact that the volumes erupted in a single event, have been steadily declining over the past 4 Ma. Typically, the volume, which is representative of an older event, exceeds 3 km^3, whereas for the younger events the representative volume is less than 1 km^3.

The other aspect of the evolutionary trend is the tendency toward more mafic composition with decreasing age. The older rocks exhibit a wide range of composition, from andesite to basalt. The younger rocks, however, are compositionally more uniform, ranging from alkali basalt to hawaiite.

In addition, Vaniman et al. (1982) have demonstrated that the evolving character of basalt magma is also expressed by systematic change of the trace element concentrations. This progressive change involves the abundance of light rare earth elements (LREE), relative to heavy rare earth elements (HREE), the younger rocks being enriched in LREE. It also involves the abundance of strontium, the younger rocks

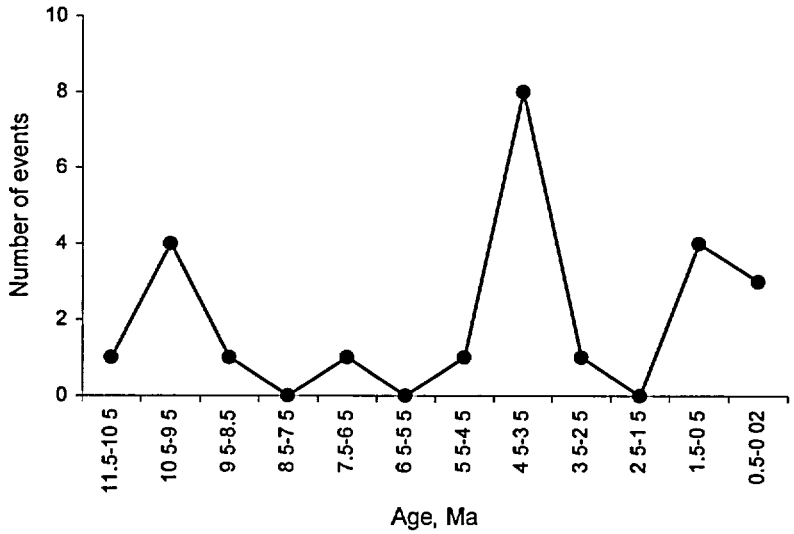

Figure 1-6. Frequency distribution of K/Ar and $^{39}Ar/^{40}Ar$ ages of basalts from the vicinity of Yucca Mountain. Re-plotted from Smith et al. (2002).

being enriched in Sr. Also, this progression manifests in the abundance of rubidium and potassium, where, relative to the older rocks, the younger are depleted in these alkalis.

The absence of a trend toward more K- and Rb-rich composition of the younger rocks was regarded by Vaniman et al. (1982) as evidence for the stability of phlogopite in the melt refractory residuum. Both K and Rb contents of phlogopite are high and hence, if stable, this hydrous mica acts as a moderator that controls the alkalis content of mafic magma, which segregates from the phlogopite-bearing residuum.

As a whole, the evolutionary trends were interpreted by Vaniman et al. (1982) to indicate a gradual decrease of the degree of partial melting in the mantle source. Thus, it is evident that the decreasing degree of partial melting in the mantle source correlates temporarily with the reduction in the intensity of the advective heat flux from the mantle into the crust. This reduced intensity has been inferred earlier as being responsible for the cessation of pyroclastic siliceous volcanism in the southern Nevada volcanic field.

That the eruptions of mafic magma have continued intermittently, over the Plio-Quaternary time span, is perhaps best demonstrated by a graph of radiometric ages. Such a graph is shown in Figure 1-6. The figure is based on K/Ar and $^{40}Ar/^{39}Ar$ ages from samples of mafic rocks that overlie or intrude the late Miocene tuffs. It shows that the eruptions have persisted in the area up to essentially the present time.

Though the volume of individual eruptions has been steadily declining in the most recent past, the corresponding eruption frequency appears to have been steadily rising. The divergence suggests that the

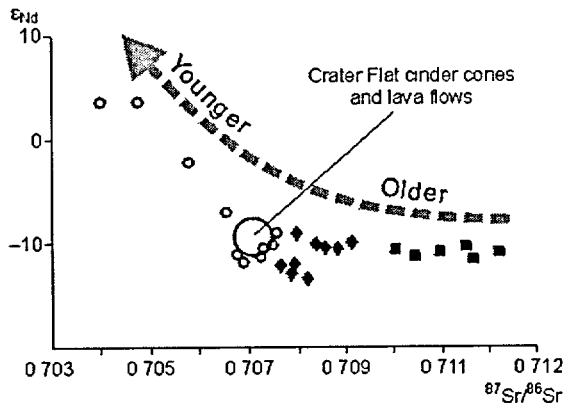

Figure 1-7. Epsilon Nd *vs.* $^{87}Sr/^{86}Sr$ data from mafic and siliceous rocks of the Southern Nevada volcanic field. Note convergence of the field from the second stage, first with that from the third stage, and then with the field from the latest mafic volcanism. Modified from Smith et al. (1997).

Squares – calc-alkalic rocks from the second stage of development of the Southern Nevada volcanic field (Paintbrush high-silica rhyolite and quartz latite); *diamonds* – peralkaline to sub-alkaline rocks from the third stage of development of the Southern Nevada volcanic field (Whamonie-Salyer andesite and Timber Mountain rhyolite); and *circles* – Late Miocene and Plio-Quaternary alkali basalt.

crust has been steadily losing its ability to confine the increasingly smaller bodies of mafic magma to the upper mantle. This gradual deterioration, in turn, seems to be indicating a progressive thinning and corrosion of the lithosphere by the thermally (melting) and gravitationally (rising) unstable body beneath it. In addition, these temporal changes indicate a gradual alteration of factors, which control the degree of partial melting in the mantle source.

1.2.4. Thermodynamic Significance of the Diminishing Degree of Partial Melting in the Mantle Source

That the early (acid-to-intermediate) and late (mafic) magma suits, from the third stage of development of the southern Nevada volcanic field, are co-genetic is implied by the evolving chemistry of these suits. This is expressed through the progressive replacement of the acid (calc-alkali) compositions by, first, the intermediate (per-alkaline to sub-alkaline) compositions and, then, by the mafic compositions. The trend, we believe, expresses the intermixing of basalt and siliceous magmas, on one hand, and the increase (with time) of the relative involvement of the mafic component concurrently with the decrease of the relative involvement of the siliceous component, on the other.

Radiometric ages from the late silicic pyroclastic centers (see Figure 1-4) and from the mafic centers (see Figure 1-6) also imply that the magma suites are co-genetic, which means that both of these suits are a result of the fundamental geodynamic instability in the upper mantle. This instability has been continuously affecting the area of Yucca Mountain by controlling, over the past millions of years, evolution of thermal state in the crust. The most important factor in this regard appears to be the diminishing degree of partial melting in the mantle source, which controlled temporal variability of the advective flux of heat into the crust in the form of basalt magma. The diminishing with time intensity of this flux manifests as the progressing reduction of melting in the crust and derivation there from of siliceous magma.

In addition to the evidence from the radiometric ages and from the changing chemical compositions, the co-genetic character and the linkage to the fundamental geodynamic instability in the

upper mantle is also indicated by the isotope characteristics of the magma suites. To illustrate this point, the ε_{Nd} vs. $^{87}Sr/^{86}Sr$ fields for the volcanic suites are shown in Figure 1-7.

The figure shows a cross-plot between ε_{Nd} and $^{87}Sr/^{86}Sr$ isotope ratios for the siliceous magma (as represented by the Paintbrush Tuff, the Wahmonie-Salyer andesite, and the Timber Mountain Tuff) and for the subsequent mafic magma. This figure therefore compares the isotope properties of siliceous magma, representing the second (Paintbrush Tuff) and third (Wahmonie-Salyer and Timber Mountain Tuff) stages of development of the southern Nevada volcanic field, with that of mafic magma representing the third stage of development of this field. The gradual change of the isotope ratios, which is shown in the figure, indicates that, indeed, it is the intermixing of melts, which were derived from the mantle, with the crust-derived melts that has generated the calc-alkali and per-alkaline to sub-alkaline magma suits.

The trend of approximately constant ε_{Nd} values but diminishing $^{87}Sr/^{86}Sr$ values, which represents the increasingly younger siliceous magma suits, is important because it shows the gradually diminishing involvement of melts derived from the crust. This trend confirms the evolving (diminishing) character of the advective heating of the crust by the upper mantle and, in addition, it manifests the diminishing degree of partial melting in the mantle source, as Vaniman et al. (1982) have suggested.

The decreasing $^{87}Sr/^{86}Sr$ values but increasing ε_{Nd} values, which are shown in Figure 1-7 as following the transition from the per-alkaline magmas to the mafic magma, indicate that the degree of partial melting in the mantle source has been diminishing over the entire late Miocene-late Quaternary time span. It is this diminishing degree of melting in the mantle source that is directly responsible for cessation of the voluminous siliceous volcanism in the southern Nevada volcanic field.

The Nd and Sr isotope ratios *vs.* time trend provides direct evidence that the mantle instability has persisted in this area at least since late Miocene. This trend also implies that this instability has controlled the evolution of thermal state in the crust. This instability has controlled therefore, at least partly, the evolution and behavior of the geologic system at Yucca Mountain over its entire life span. It can therefore be expected that this control will continue for a long time into the future.

In summary, the most salient feature of the geodynamic setting of Yucca Mountain, which has been revealed thus far, is the progressive decline in the degree of partial melting in the mantle source. The implications of this decline must be considered when assessing the anticipated long-term performance of the proposed disposal facility. The proponents, of course, will claim that any decrease in the degree of partial melting means that the volcanic hazard is diminishing.

Although this reasoning may appear to some as logical and valid, we see it as grossly misleading. This is because it is not mafic volcanism, which poses the greatest and most direct treat to the proposed

facility. Rather, what really matters in this regard is the evolving thermal state of the mid-lower crust, which is being expressed by this volcanism. In the course of its evolution, this state will inevitably change in such a manner that advective transport of the accumulated heat, by means of short-lived but energetic hydrothermal plumes, will become a thermodynamic necessity. To understand this issue it is essential to develop first some understanding of melting in the upper mantle and the processes that control it.

1.2.5. Melting in the Upper Mantle as a Heat Dissipative Process

Heat, which is produced and/or released in the Earth's interior, is continuously being converted into work, which manifests as structural and chemical evolution of both the lithosphere and the underlying mantle. The integrated (over time) result of this evolution is, of course, the presently observed structural and geologic framework in all its aspects.

After flowing upward through the lithosphere and performing work therein, the remainder of the endogenic heat arrives at the surface, where it is dissipated into space as infrared radiation. The heat is transported by conductive as well as advective means. Advective transport involves hydrothermal and volcanic processes, which are often closely related to each other, although volcanism is not essential for the occurrence of hydrothermal processes.

Both of the heat transport processes take the form of flows of liquid and gas phases, which are supported either by convectively recharging heat sources, such as a magma body, or by conductively recharging heat sources, such as a hot rock. In both of these cases, the resulting motions may be steady state, periodic, a periodic, and/or critically eruptive (accompanied by a positive feedback process, effervescence and vaporescence in particular) depending on the evolutionary stage of the process.

Advective transport of heat in the form of volcanic processes requires solid $\rightarrow$ liquid phase transitions, whereas hydrothermal transport does not, although both processes may be accompanied by liquid $\rightarrow$ gas phase transitions. Otherwise, they are close analogs of each other, in a thermodynamic sense. However, for each process, the initiation thresholds, the work performed and the entropy produced and lost, as a result of irreversible processes, are quite different in forms and magnitudes.

Lindemann's Law of Melting (see Stacey, 1977, for example) can be used to understand the rock $\rightarrow$ magma phase transition. In this model, melting occurs when the amplitude of atomic vibrations about their equilibrium position, for the most volatile mineral phases, becomes larger than a given fraction of the inter-atomic distance. In order to increase the vibration amplitude, so that it is sufficient to initiate the fractional melting, it is necessary to raise the temperature of a rock to above the so-called solidus (T_m).

The solidus increases as a function of depth (pressure, p) but, because it is necessary to extrapolate outside the static experimental range, the $T_m(p)$ relation is subject to uncertainties of up to a few hundreds

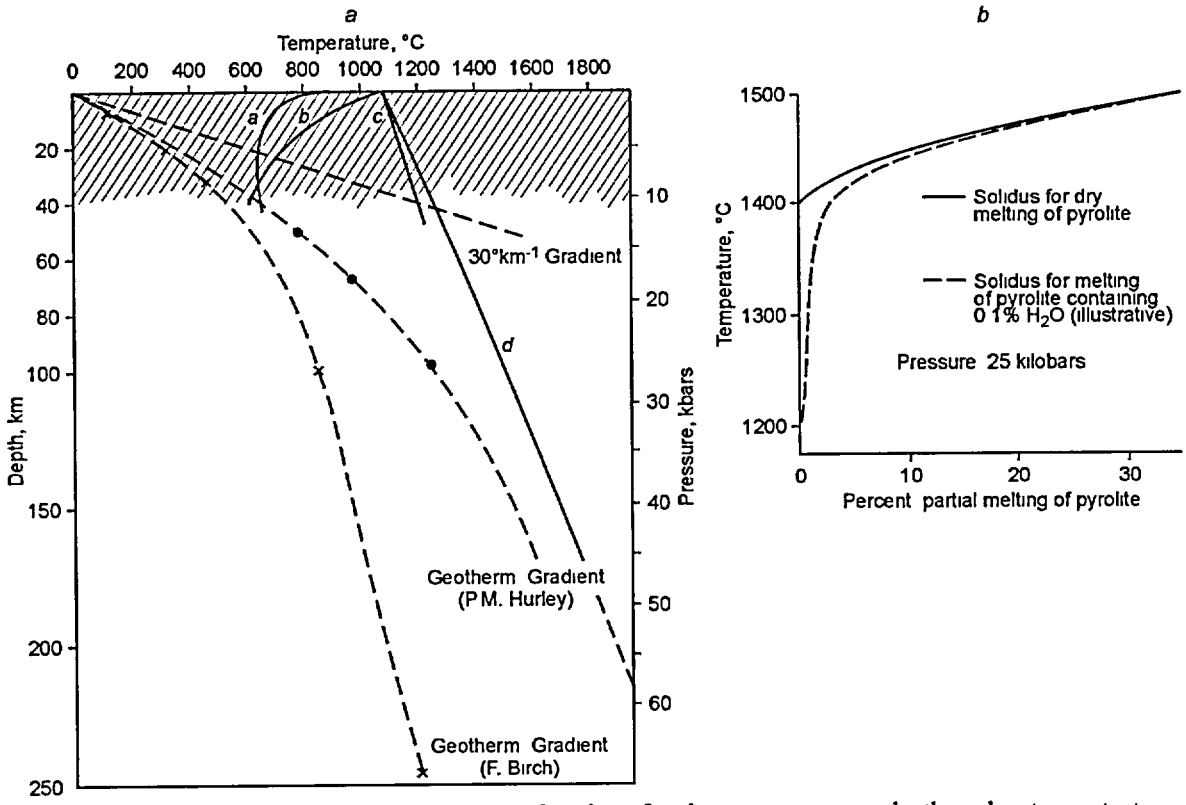

Figure 1-8. Variability of solidus temperature as a function of rock type, pressure or depth, and water content.

a – Solidus temperatures as a function of depth for the crust and the upper mantle: a – water saturated granite; b – water saturated basalt; c – pyroxene; and d – pyrolite. Modified from Wedepohl (1967) and Green and Ringwood (1967). *b* – Degree of melting as a function of temperature for pyrolite under anhydrous conditions and in the presence of 0.1% H_2O at 25 kbars. From Ringwood (1969).

of °C at high pressures. The generally accepted variability of $T_m(p)$ for common rocks which comprise the lithosphere is shown in Figure 1-8-*a*. In addition to being pressure-dependent, the mantle solidus is also dependent on the presence of volatile phases such as H_2O and CO_2, which may depress it by up to about 200 °C, as shown in Figure 1-8-*b*.

Melting experiments by Green and Ringwood (1967) have shown that the degree of partial melting increases sharply as the temperature exceeds the solidus even by a small amount. They further show that the temperature interval between solidus (say about 1% of melting) and liquidus (100% of melting) is quite small. For example, at a pressure between 20 and 30 kbar, this interval is smaller than 100 °C for olivine tholeiite. It is probable that a completely dry pyrolite (i.e., hypothetical primitive mantle matter, see Ringwood, 1969) would become 30% molten within this interval.

Thus, in the case of the seismic Low Velocity Zone (*P*-wave velocity of say 7.6 $km \cdot s^{-1}$), only relatively small increases of the temperature, which already exceeds the solidus temperature, would be required to initiate basalt volcanism. In fact, a temperature increase as small as 20 °C could induce partial

(i.e., about 5% or more) melting sufficient for segregation of bodies of basalt magma, which could then buoyantly rise to the Earth's surface. However, this would only be the case if the Low Velocity Zone was completely anhydrous, which it is not.

The matter comprising the Low Velocity Zone contains small amounts (0.1 %) of H_2O as a free phase, mostly in the form of small bubbles and films along mineral grain boundaries, as Ringwood (1969) has argued. Even such tiny amounts of H_2O have the effect of lowering the solidus by about 200 °C (Figure 1-8-*b*). Initially, at a time when the degree of melting is very low (say about 1%, or incipient), most of the H_2O originally present in the pyrolite occurs in the melt.

As the degree of melting increases, the H_2O concentration in the melt decreases. This lowers H_2O pressure in the melting system and has the effect of decreasing the degree of melting, because it raises the crystallization temperature. The net effect is that, under the presence of small amounts of H_2O, a relatively large increase of the temperature (up to 200 °C) would cause only a small increase in the degree of partial melting (Figure 1-8-*b*).

Thus, in the case of a slightly hydrous mantle, this effect permits the large volumes to remain in a quasi-stable state of incipient melting in spite the inevitable small changes of the temperature. However, for the upper mantle, which exists in an anhydrous state, the situation is very different (Figure 1-8-*b*).

To induce magma generation, the necessary but not sufficient condition is to increase the heat content to a level at which the temperature exceeds the solidus. To satisfy the sufficient condition, however, requires an additional increase in the temperature in order to overcome the latent heat of melting and to exceed the magma segregation threshold. Three geodynamic processes are capable of causing the onset and continuation of magma generation.

The first is the sinking of relatively cool rocks into the Earth's interior; such as in the case of subduction of oceanic lithospheres, or of the foundering of blocks of the crust, which undergo the basalt (gabbro) → eclogite phase transition.

The second process involves a spontaneous rise of the temperature, which could be a result of increased radiogenic heat production in a tectonically thickening continental crust, for example. If the increased heat production were of sufficient magnitude, anatexis of the sial would begin in the lower crust, thus producing bodies of acid magma having a low density and a tendency to rise. The upwardly migrating magma would cause granitization of the rocks through which it passes. The ultimate fate of the rising body is eventual solidification in the mid-upper crust, in the form of a granite batholith, and/or to partially discharge at the surface, in the form of ash-flow tuffs forcefully ejected from a strato-volcano.

The third process is directly relevant to the area of Yucca Mountain. This process involves the adiabatic transfer of a large body of pyrolite, from a high-pressure (deep) environment to a lower pressure environment, so that the heat content initially remains essentially unchanged. The adiabatic transfer has the effect of lowering the pressure, and thus the effective solidus, without substantially lowering the temperature. As many authors have suggested, for example Van Bemmelen (1972) and Morgan (1972), this process operates throughout the whole mantle, at different spatio-temporal scales, and is a root-cause of all tectonic processes, thereby controlling their fundamental evolution.

The development of the southern Nevada volcanic field, which began about 25 Ma ago, is directly attributable to the initially adiabatic rise of a body of solid pyrolite. This rise may have taken the form of a diapiric upsurge of the Low Velocity Zone (i.e., the geochemical asthenosphere at that time) or a broad arching of the underlying sclerosphere (i.e., Zone C of Bullen, see Bullen and Handon, 1970). In either case, it would have been a result of either physical uplift of a section of the sclerosphere, or a result of local heating of the asthenosphere and the resulting local reduction in the density. Evidently, the gravitationally unstable body was large enough, relative to its velocity, so that it behaved adiabatically during initial stages of the ascent and did not interact appreciably by thermal conduction with the surrounding mantle.

The adiabatic gradient for the Earth's upper mantle is about 0.3 $^{\circ}C \cdot km^{-1}$, which is a factor of about ten smaller than the gradient of pyrolite solidus, as given in Hughes (1982). Therefore, at some point in the ascent, the temperature of the ascending body $[T_s(p_{n-1})]$ would reach and then sufficiently exceed the solidus $[T_m(p_n)]$, so that the incipient melting sets-in. The degree of partial melting would increase as the now crystalline + liquid body rises further. However, the temperature $[T_s(p_{n+1})]$ would be somewhat lower than the adiabatic temperature $[T_s(p_{n-1})]$ initially because of the effects of the latent heat of melting, but, at a later time, because of the additional conductive heat transfer into the overlying lithosphere.

Although the amount and composition of the crystalline and liquid phases would change with the decreasing pressure, chemical equilibrium would be maintained. This is because olivine and pyroxene crystals, which comprise the refractory residuum, continuously buffer the basalt liquid, as Green and Ringwood (1969) have suggested. At some particular depth, the so-called magma segregation depth, the degree of partial melting would be extensive enough and the tectonic environment such that the liquid segregates from the residual crystals, with which it was initially saturated. At and above this depth, the segregated magma would fractionate independently by cooling and crystal settling as it ascends towards the Earth's surface.

Petrography research has greatly increased the wealth of diagnostic data on which our concepts of the origin of basalt magma are founded. In particular, it has been shown that the degree of partial melting

and the depth of magma segregation are the primary factors, which determine the composition of the magma. In this regard, Yoder and Tilley (1962) have established that two types of basalt magma produce mafic rocks, which are olivine-alkali and tholeiite.

[Olivine-alkali basalt usually contains diopside pyroxene only, whereas tholeiite basalt may contain two or three different pyroxenes. The two types can also be distinguished based on their SiO_2/Na_2O+K_2O ratio, which averages about 10 for alkali-olivine basalt and about 15 for tholeiite basalt.]

In regions where basalt volcanism is continuously active, such as the Hawaii Islands, the first melts to extrude typically have tholeiitic composition, and then they are followed by melts of the olivine-alkali type. This sequential occurrence has been confirmed experimentally by Green and Ringwood (1967) who found that olivine-alkali magma could be formed only at a depth ranging between 40 and 80 km. By contrast, high-alumina tholeiitic basalt magma can be fractionated either at a shallow depth, ranging between 20 and 40 km, or below a depth of 80-90 km.

Although the $T_s(p_{n-1})$ - $T_m(p_{n+1})$ difference increases as a pyrolite body continues to ascend, it would be incorrect to infer that the degree of partial melting increases steadily, so that the liquidus conditions are eventually attained. This is because the availability of H_2O as a free phase, which controls the degree of partial melting, decreases with decreasing pressure or depth. This availability is strongly influenced by the stability of hydrous minerals, which remain in the refractory residuum, principally amphibole and to a lesser extent phlogopite.

In this regard, experimental data from Green and Ringwood (1967) show that, in an olivine-rich environment, amphibole is stable at temperatures near the dry solidus, but only under conditions of $P_{H2O} < P_{load}$ at the load pressures up to 15 kbar. This suggests that, at a melting depth of less than 60 km, the small amount of H_2O present will be incorporated in the crystalline structure of amphibole, so that $P_{H2O} < P_{load}$.

The experimental evidence further indicates that amphibole is not stable at a temperature above 1200 °C and at a pressure greater than about 20 kbar, even at a relatively high H_2O-partial pressure. Under these conditions, amphibole transforms into an eclogite mineral assemblage plus H_2O, and the transformation temperature may be decreasing with the increasing pressure.

Thus, the experimental results indicate that the amount of H_2O, which is held in the refractory residuum and hence not available to affect the solidus, changes and does not remain constant during the ascent of a melting mantle body. At a depth more than 60 km, the amphibole → eclogite phase transition allows H_2O to exist as a free phase. This has the effect of allowing the ascending body to keep increasing the degree of partial melting, until a maximum is attained at the 60-km depth.

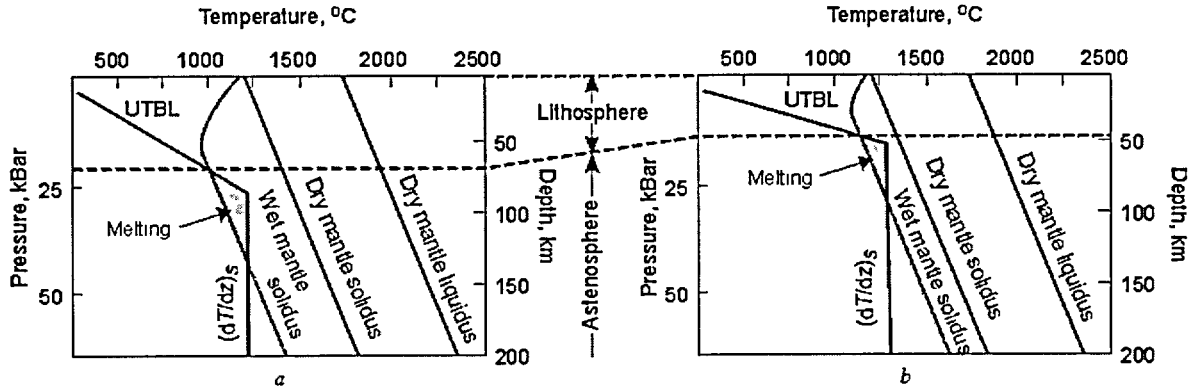

Figure 1-9. Accepted explanation for causes of melting in the upper mantle. Note thinning of the lithosphere by an ascending mantle source ($a - b$) and the difference between the adiabatic gradient and the gradient of the mantle solidus. Modified from Huges (1982).

$(dT/dz)_s$ – adiabatic gradient of temperature ~0.3°C km^{-1}; UTBL – upper thermal boundary layer. "Astenosphere" denotes seismic Low Velocity Zone, which may or may not correspond to the primitive mantle.

At a depth of less than about 60 km, however, the pressure is less than 20 kbar and, consequently, the previously unstable amphibole now becomes stable, which has the effect of sequestering the free H_2O. The net effect is that the solidus temperature increases by up to 200 °C, relative to that at the prior and greater depth, and the degree of partial melting and the rates of magma segregation both diminish gradually, as illustrated in Figure 1-9.

The figure shows that the "wet" mantle solidus is up to 200 °C lower than the "dry" solidus, which allows the degree of partial melting in a "wet" mantle body to be relatively high. However, as this body continues to migrate upward, the stability fields of the hydrous minerals eventually affect it. At this stage, the previously free H_2O now becomes increasingly more sequestered by the stable hydrous minerals and, consequently, the rising body becomes increasingly dryer. The solidus temperature increases, from 1200 to possibly 1400 °C, and the degree of partial melting decreases accordingly.

Another effect of the H_2O sequestration is that the stabilization mechanism, which permits the asthenosphere (or Low Velocity Zone) to remain in a quasi-stable state of incipient melting, is no longer operational. The absence of H_2O as a free phase has the effect of causing the degree of partial melting, within the progressively dryer body, to become increasingly sensitive to small changes of the temperature. As shown in Figure 1-8b, an increase as small as 50 °C would produce a very substantial increase in the degree of partial melting, this would lead to voluminous eruptions of basalt magma at the surface. Figure 1-9 further implies that the ascending body has the effect of causing progressive thinning of the geochemical lithosphere, by mechanically and thermally corroding it.

At this point, it is appropriate to point out that the inferred thinning in southern Nevada has been actually confirmed by DePaolo and Daley (2000) who reconstructed the spatio-temporal variability of

depth to the geochemical asthenosphere. [The latter should not be confused with the seismic Low Velocity Zone, which occurs in the Basin and Range Province at a shallower depth.]

The reconstructed variability is based on chemical composition, radiometric ages, and Nd and Sr isotope systematics of the late mafic rocks from the southwestern Basin and Range. The reconstruction shows that the area of Yucca Mountain is located near a north-south trending margin of the so-called Death Valley Extension Area (DVEA), as shown in Figure 1-13. The evidence suggests that, in this area, the geochemical lithosphere had thinned to 50-70 km, by 9 Ma ago, and perhaps to less than 50 km, by 4 Ma ago. The inferred thinning and the resulting extension are shown on Figure 1-10.

The preceding remarks have provided a satisfactory explanation for, first, the increasing and, then, the decreasing degree of partial melting in the mantle source, which is expressed by the evolving volcanism in the Yucca Mountain area. Clearly, it is the ascent of a gravitationally and thermally unstable body in the mantle that is responsible for the systematically changing degree of the partial melting. This ascent is also responsible for the changes in the intensity of advective heating of the crust by the mantle, which manifested as initially on-set and then cessation of the pyroclastic siliceous volcanism.

However, the cessation comes at the price of increasing the temperature within the ascending body, from 1200 to about 1400 °C, and of thinning the tectonic lithosphere. The thinned lithosphere and the increased temperature at its base act in concert to increase the heat content in the mid-lower crust to the near-solidus levels. The increasingly hotter crust will eventually act as a conductively replenished heat source, capable of supporting intermittent hydrothermal activity in the form of Rayleigh-Bénard instability in faults and fractures.

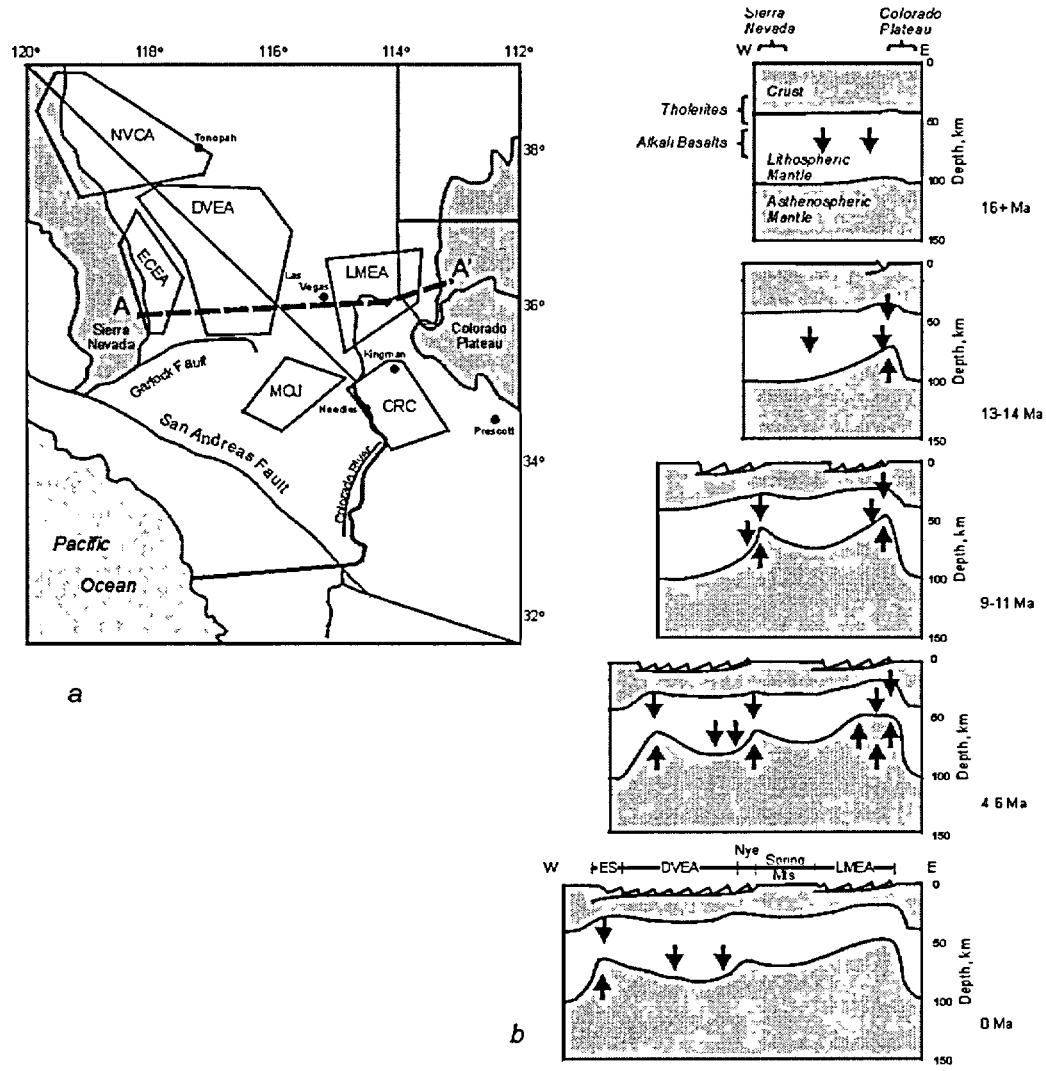

Figure 1-10. Sample location map (*a*) and series of sections across the Basin and Range along line A – A' shown in *a* at different times prior to and during extension (*b*). From DePaolo and Daley (2000).

a – Schematic study area map. Polygons denote geographic locations: LMEA (Lake Mead Extensional Area), DVEA (Death Valley Extended Area), ESEA (Eastern Sierra Extended Area), CRC (Colorado River Extensional Corridor), MOJ (Mojave Extensional area, and NVCA (Nevada-California border region). The dashed line within DVEA delineates the zone along the eastern edge including Nye Canyon that shows isotopic evidence of lithospheric thinning.

b – Schematic cross-sections along the A-A' line at different times. Cross-section end points are fixed in the Sierra Nevada on the west and Colorado Plateau on the east, and the width of the intermediate region (Basin and Range) increases in successive cross-sections based on the estimated extension vectors of Wernicke et al. (1998). Solid arrows indicate constraints on the depth to the lithosphere-asthenosphere boundary, which assumes that the depth to the tholeiite-alkaline boundary is 50 km and alkali basalts form between 50 and 70 km depth. The upper shaded layer is crust, the unshaded layer is lithospheric mantle and the lower shaded layer is asthenospheric mantle.

Chapter 1.3. Geothermal Environment: Evolution and Contemporary State

1.3.1. Thermal State

An understanding of the long-term behavior of the hydrologic sub-system at Yucca Mountain is necessary in order to evaluate the anticipated releases of radioactivity from the proposed repository. This behavior can only be determined through recognition, among other factors, of the geothermal environment within which this system operates. Informative in this regard is a map, Figure 1-11, of the inferred crust-mantle refraction velocity (P_n) in the uppermost mantle of western United States, because this velocity is intimately dependent on the temperature of the local mantle-forming matter.

The map is based on the travel-times of earthquake-generated seismic waves, as compiled by the International Seismological Center and interpreted by Hearn et al. (1990). It shows that an abnormally "soft" mantle, with a P_n velocity as low as 7.6 $km \cdot s^{-1}$, underlies the crust at Yucca Mountain.

Similarly low P_n velocities are known to occur only in regions characterized by recent volcanism, high level of seismicity, high heat flow, and hydrothermal activity (for example, the Rio Grange rift at 35 ^{0}N-111 ^{0}W and Snake River Plain at 43 ^{0}N-113 ^{0}W in Figure 1-11). These low velocities are commonly regarded as firm evidence for a state of incipient or partial melting in the upper mantle and for the gravitational (i.e., buoyant) instability of this mantle (Archambeau et al., 1969; and Anderson and Sammis, 1970).

In particular, the map shows that, at Yucca Mountain, a mantle whose temperature (T) exceeds the solidus temperature (T_m) underlies the crust, so that $T > T_m$. The latter ranges between 1200 and 1400 °C, depending on the availability of volatile phases (principally, H_2O and CO_2, Ranalli, 1987) and on the composition of the melting matter. Under the assumption that the Moho discontinuity is situated at a depth of 25-30 km, the $T > T_m$ relation implies that the long-term average geothermal gradient has the value of $dT/dz = 40$ °C·km^{-1} or more.

[The terms "long-term average geothermal gradient" and calculated there from "long-term average heat flow" are used herein to denote a geothermal gradient and heat flow, values of which are not affected by transient hydrothermal circulations. By contrast, the geothermal gradient and heat flow the values of which have been determined based on the down hole measurements of the *in situ* temperatures are referred to as "short-term surface geothermal gradient" and "short-term surface heat flow". The short-term parameters may be affected by advective transport of heat. They, therefore, may or may not correspond to their long-term average equivalents.]

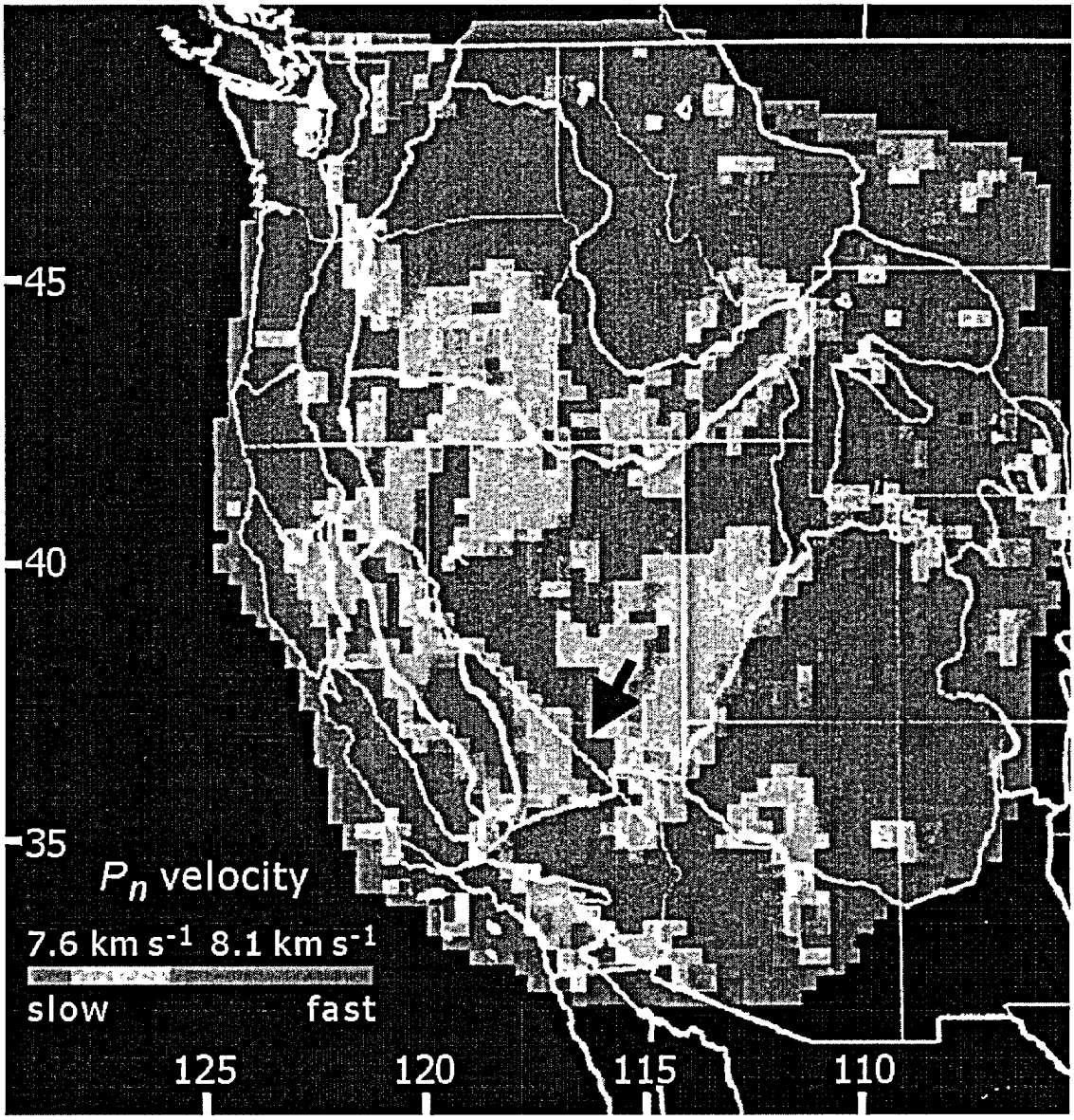

Figure 1-11. Distribution of the P_n velocity (crust-mantle refraction velocity) in the western United States. Reproduced from Hearn et al. (1990). Black arrow shows the location of Yucca Mountain.

The map indicates that at and around Yucca Mountain $P_n \cong 7.6$ km·s^{-1}, which corresponds to the thickness of "seismic" lithosphere of ~30 km.

A mantle refraction velocity (P_n) as low as 7.6 km·s^{-1} further implies that the seismological Low Velocity Zone (LVZ) occurs immediately below the Moho discontinuity, at a depth of only 25-30 km. This means that the lithospheric mantle has been thermally softened, so that its rheological state now resembles that of the underlying asthenosphere. This also means that the thermal lithosphere is very thin. The thermal lithosphere, which is defined as extending to a depth where $T = 0.85 \cdot T_m$ (Ranalli, 1987), is

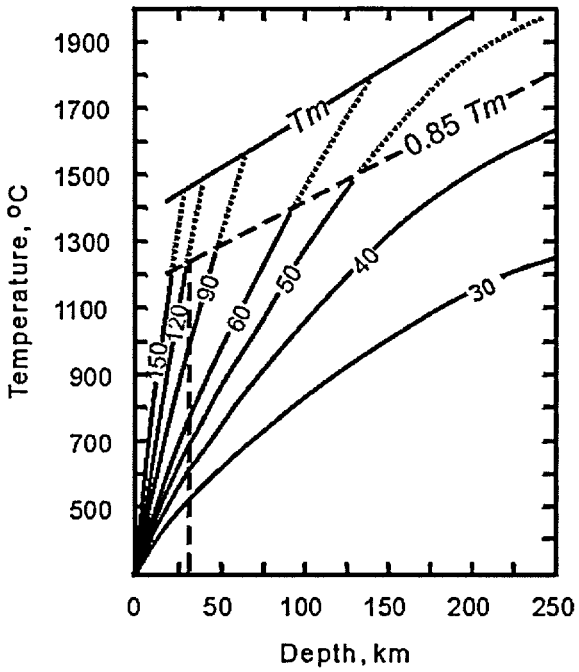

Figure 1-12. Continental geotherms for different values of surface heat flow. Based on the data by Pollak and Chapman (1997), modified from Ranalli (1987).

Tm is mantle solidus. $T = 0.85Tm$ may be taken as defining the thickness of the lithosphere. Curves represent depth distribution of temperature as a function of steady-state heat flow (in mWm^{-2}). Figure 1-11 shows that at Yucca Mountain the thickness of "seismological" lithosphere (i.e., depth at which P_n ~7.6 km s^{-1}) is ~30 km. This relationship suggests that long-term average heat flow at Yucca Mountain attains intensity as high as 120 mWm^{-2} or ~3 HFU (determined by intersection of vertical dashed line with the $0.85Tm$ line).

important. This is because the thickness of this lithosphere could be used to estimate the corresponding intensity of long-term average heat flow, based on global observations as compiled by Pollack and Chapman (1977). The relation between heat flow and thickness of the thermal lithosphere is shown in Figure 1-12.

This figure shows the continental geotherms for different values of surface heat flow. The intersection of geotherms with the curve $T = 0.85 \cdot T_m$ may be taken as defining the thickness of the thermal lithosphere. This figure therefore indicates that the less than 50 km thick thermal lithosphere at Yucca Mountain is associated with a long term average surface heat flow of about 120 mWm^{-2}, or 3 heat flow units (HFU). That the $T = 0.85 \cdot T_m$ condition is satisfied at a depth of less than 50 km is implied by the distribution of P_n velocity, which is shown in Figure 1-11. The inferred heat flow and average geothermal gradient (dT/dz = 40 °C·km^{-1}) both imply that the crust beneath Yucca Mountain is exceptionally hot, with a near-solidus temperature in the lower crust.

The preceding inference is supported by estimates of the depth-extent of magnetic sources in Nevada made by Blakely (1988), based on the statistical properties (wavelengths) of magnetic anomalies. Figure 1-13 shows the spatial distribution of the Curie isotherm, which corresponds to a temperature of about 580 °C depending mainly on the titanium content of magnetic minerals in the crust, and whose depth corresponds to the depth-extent of magnetic sources.

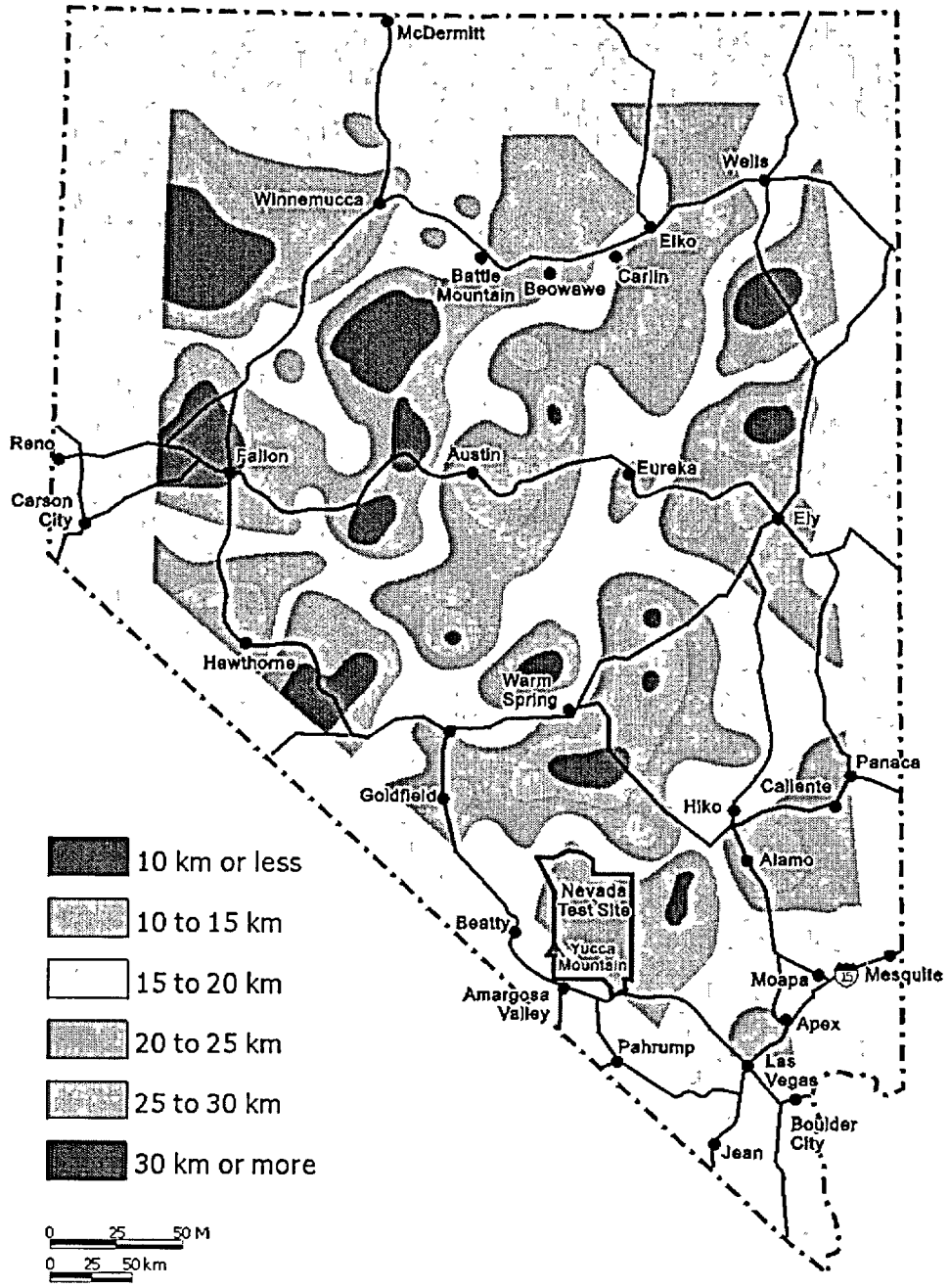

Figure 1-13. The depth of Curie isotherm (T~560°C) in the state of Nevada. Modified from Blackely (1988).

The depth of Curie isotherm is ~10-15 km at Yucca Mountain, which implies average geothermal gradient dT/dz ~36-54°C km^{-1}. Average thermal conductivity for the upper-middle crust is ~3 Wm^{-1}K^{-1}. Average long-term heat flow at Yucca Mountain therefore ranges from 113 to 170 mWm^{-2} (2.7 to 4.0 HFU).

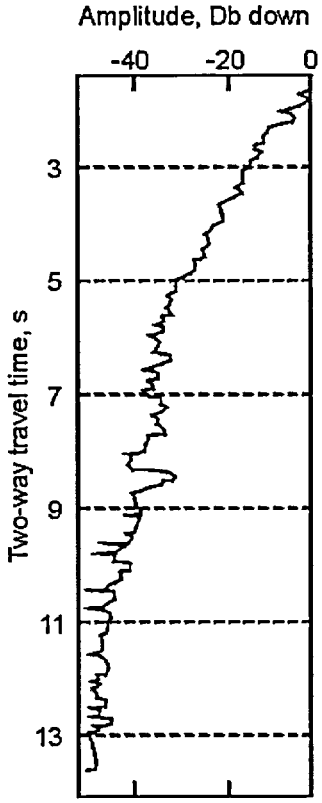

Figure 1-14. Average amplitude *vs.* travel time decay curve. 40 traces from the explosion record for the shot at station 1549. From Brocker et al. (1989)

The figure shows that Curie isotherm occurs at Yucca Mountain at a depth ranging between 10 and 15 km. This indicates that the average long-term geothermal gradient has a value in excess of 40 $°C \cdot km^{-1}$, in agreement with the earlier estimate based on the interpretation of the P_n velocities. The figure further shows that, in Nevada, this isotherm occurs at similar and smaller depths only in the areas of Battle Mountain and Hawthorne-Reno, both of which are known geothermal areas.

Average thermal conductivity for the upper-mid crust at Yucca Mountain may be taken to be about 3.0 $Wm^{-1}K^{-1}$. Thus, the depth of Curie isotherm, ranging between 15 and 10 km, corresponds to an average long-term heat flow of between 113 and 170 mWm^{-2} (2.7- 4.0 HFU), respectively. This estimate is in reasonable agreement with the earlier estimate, based on the inferred thickness of the thermal lithosphere.

Figure 1-13 also shows that the depth of Curie isotherm increases gradually to the north of Yucca Mountain. It attains a depth of about 30 km, over a lateral distance of about 35 km, in the center of the Eureka Low geothermal anomaly. Thus, the mid-crust at and around Yucca Mountain hosts substantial lateral gradients of temperature ($dT/dx(y)$ = 3.2 $°C \cdot km^{-1}$), in addition to hosting an average long term geothermal gradient as large as $dT/dz > 40\ °C \cdot km^{-1}$.

At a pressure equivalent to a depth of about 20 km, the solidus ranges from about 640 °C, for water-saturated sialic crust, to 770 °C, for water-saturated simatic crust (Wedepohl, 1971). Thus, the average geothermal gradient $dT/dz > 40\ °C \cdot km^{-1}$ implies that, in the mid-lower crust, the temperature approaches or exceeds the solidus.

The implied local presence of the super-solidus state in the crust is confirmed by the fact that, locally, the crust has been observed to produce seismic reflections with unusually high amplitudes. Specifically, these reflections were observed in association with the so-called Amargosa Desert "bright spot". This seismic reflection feature has been identified on an explosive source profile for line AV-1 at a seismic depth of 8.4 s (a depth of roughly 20 to 25 km), by Brocker et al. (1989). On a common shot gather, the amplitude of the anomalous reflection was about 9 dB above the average amplitude vs. travel-time decay curve, as shown in Figure 1-14.

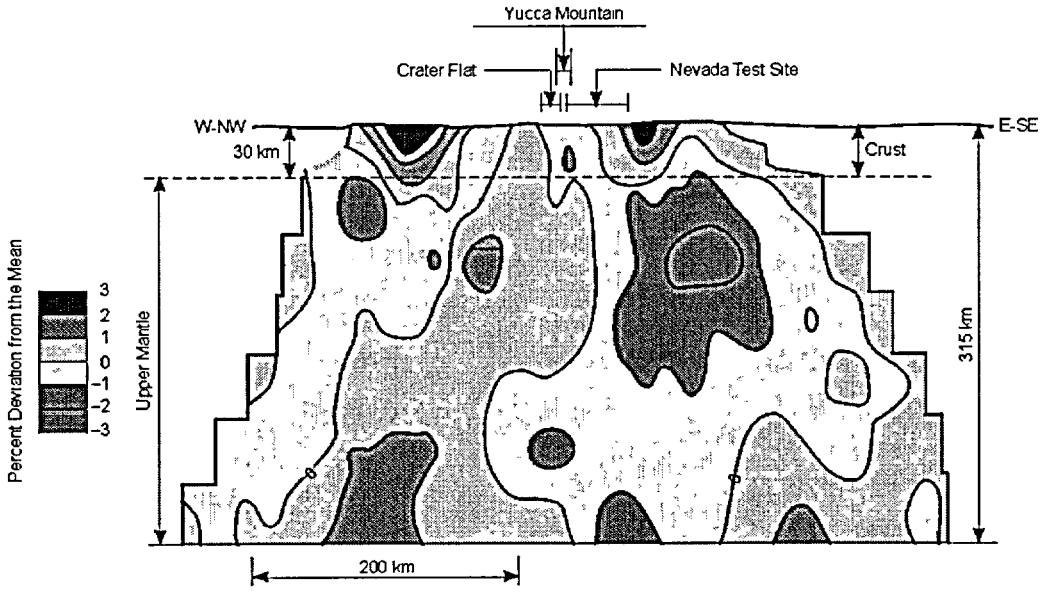

Figure 1-15. Tomographic depth section showing seismic velocity variations (in percent of deviation from the horizontally averaged mean) in the crust and upper mantle beneath and near Yucca Mountain. The low velocity zones in the upper mantle most probably represent partial melting and a source of volcanism in the future. The low velocity zone directly beneath Yucca Mountain may indicate lower crustal heating and possible partial melting. Location of the section is shown in Figure 1-17. From Evans and Smith (1992).

According to Brocker et al. (1989), "*... the Amargosa Desert 'bright spot' is similar to the lower crust spots imaged by COCORP in Death Valley, California, and near Socorro, New Mexico, in the Rio Grande rift. Both of these bright spots have been attributed to reflections from thin and discontinuous magma chambers*." (emphasis added).

High-resolution tomographic images of the crust and upper mantle of Yucca Mountain, which were constructed by Evans and Smith (1992), further corroborate the exceptionally hot state of the crust and upper mantle of this area. These images are reproduced in Figures 1-15 and 1-16.

The figures reveal a pronounced heterogeneity in the *P*-wave velocity of the crust and upper mantle between Crater Flat and western Yucca Mountain. In the uppermost mantle, the *P*-wave velocity is 2-3 % lower than the laterally averaged background. The background velocity itself is representative of a mantle region within which partial melting is taking place. Thus, the anomalous low velocities indicate that the degree of partial melting beneath Crater Flat and western Yucca Mountain is greater than that in the neighboring areas. They also imply that the total input of heat from the mantle into the crust is locally enhanced.

As shown in Figure 1-16, the *P*-wave velocity in the crust beneath Crater Flat and western Yucca Mountain is about 1-2 % lower than the laterally averaged background. Evans and Smith (1992)

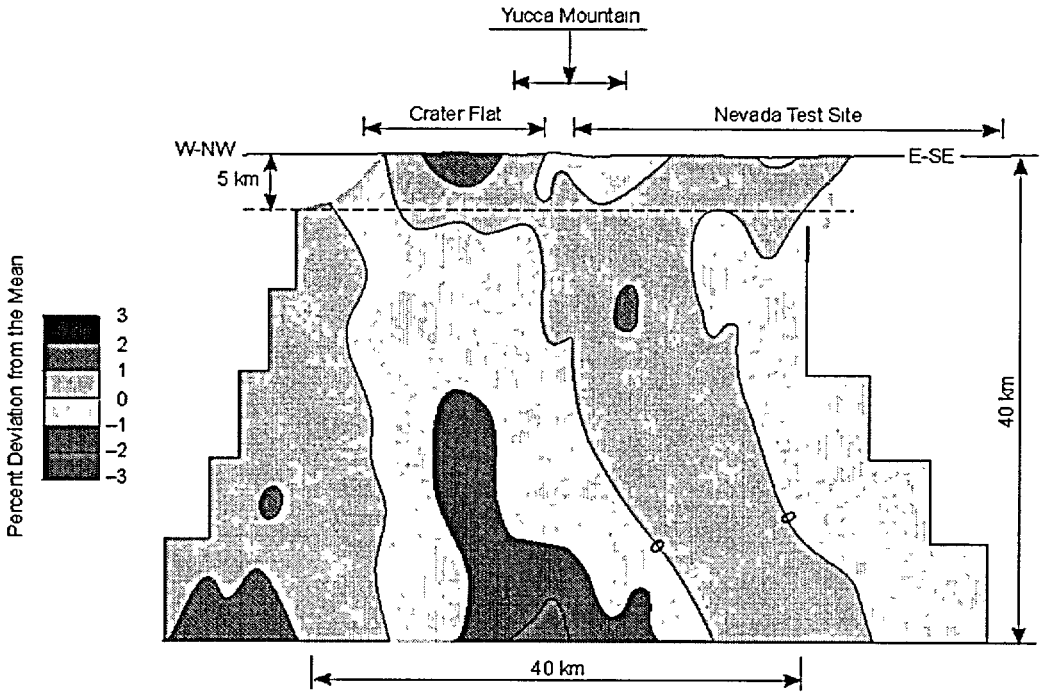

Figure 1-16. Tomographic depth section showing seismic velocity variations (in percent of deviation from the horizontally averaged mean) in the crust beneath and near Yucca Mountain. The low velocity zones beneath Crater Flat and Yucca Mountain may represent crustal heating and a source of volcanism in the future. Location of the section is shown in Figure 1-17. From Evans and Smith (1992).

considered the potential significance of this low velocity zone. They concluded: "*However, the weak middle and lower crustal-low velocity anomaly is significant. It may be caused by many phenomena, including... crustal heating possibly related to current basaltic activity. It is quite similar to the Mineral Mountains anomaly in Utah, which lies beneath vents of Quaternary rhyolite flows and near the Roosevelt Hot Springs geothermal areas. This similarity supports the crustal heating hypothesis at Crater Flat.*" (emphasis added).

A tomographic image, which has been constructed earlier by Monfort and Evans (1982), provides a regional context for the low *P*-wave velocity zone in the crust of Crater Flat and western Yucca Mountain. This important image is reproduced in Figure 1-17.

The image has been constructed based on tele-seismic *P*-wave travel-time residuals from 98 seismic events, which were recorded at as many as 53 seismic monitoring stations. The overall *P*-wave velocity pattern shown consists of low velocity zones (negative velocity perturbations) systematically alternating with zones of relatively higher *P*-wave velocity (positive velocity perturbations). The figure shows that the Crater Flat-Yucca Mountain anomaly lies inside a spatially very extensive *P*-wave velocity anomaly, which extends from at least Pahrump, Nevada, to the northwest, for a distance of about 200-km. This

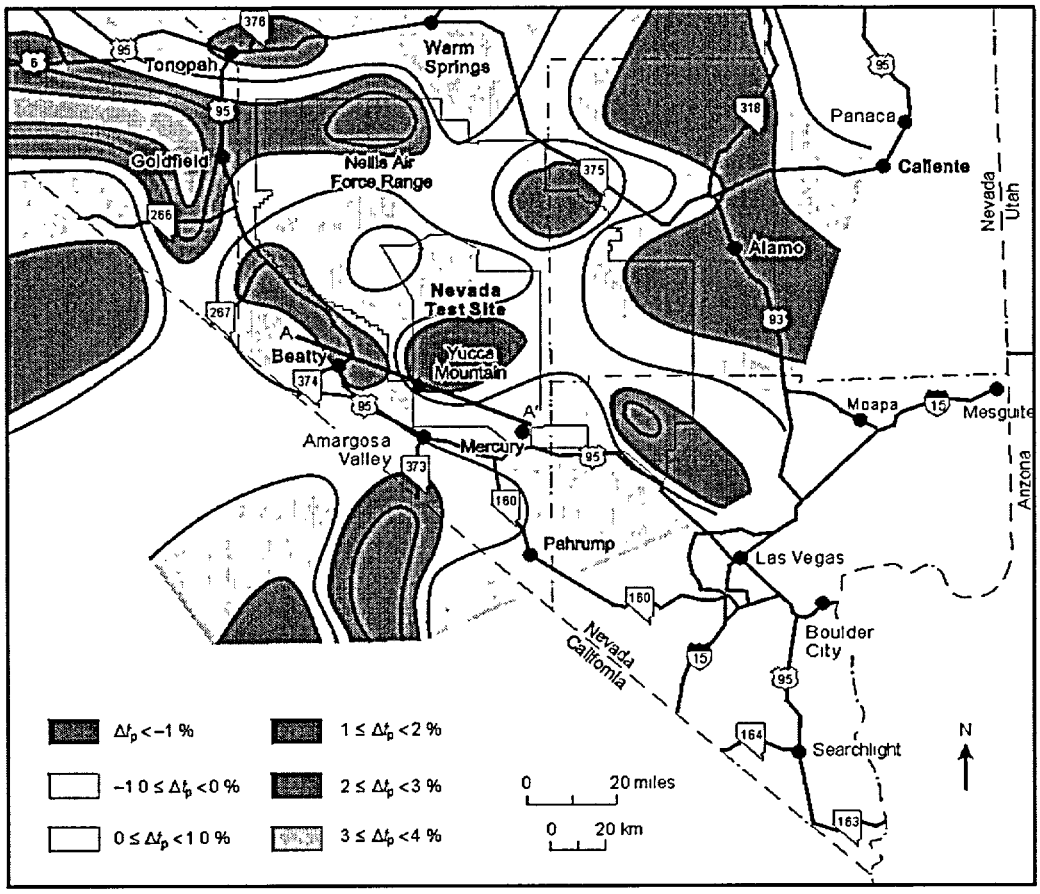

Figure 1-17. Teleseismic *P*-wave velocity perturbations (Δtp) in the mid-lower crust (15-30 km) in the area of Yucca Mountain. Constructed from the data of Monfort and Evans (1982).

Negative velocity perturbation areas shown as warm colored contour areas may represent regions of higher than normal temperatures in the lower crust, particularly when such anomalies are correlated with areas of higher than normal heat flow. Zero velocity perturbation corresponds to mean layer velocity. Line A-A' shows the location of tomographic depth sections shown in Figures 1-15 and 1-16.

anomaly is up to 100 km wide, and it is situated entirely within the southern segment of the Walker Lane wrench system, as shown in Figure 1-17.

From east to west across Yucca Mountain, the *P*-wave velocity perturbations decrease from +1.64 to -1.40 %, over a lateral distance of only about 20-km, as shown on Figure 1-17. The highest negative *P*-wave velocity perturbations (Δt_p < -1.0 %) occur in the area immediately to the northwest of Yucca Mountain. This area corresponds to the northwest trending belt, within which the youngest volcanic centers (basalt) are situated. This spectacular sub-anomaly is up to 10 km wide and extends for a distance of about 75-km, encompassing an area of nearly 1000 km^2.

Further to the northwest, however, the *P*-wave velocity perturbations increase sharply from $\Delta t_p < -1$ s to $\Delta t_p > +3$ %, over a lateral distance of only about 35-km. To the southeast, however, the increase is much smaller and the velocity perturbations remain negative in this area, as shown in Figure 1-17.

The fact that the low *P*-wave velocity zone underlies the most recent basalt eruption centers is clearly very significant. From the southeast to the northwest, these centers include the youngest Lathrop Wells cone and lava flows, the four mid-Quaternary Crater Flat cider cones, and the two late Quaternary Sleeping Butte cones. The low velocity zone also underlies the Amargosa Desert "bright spot" of Brocker et al. (1989) as well as a few conspicuous aero-magnetic anomalies nearby, which most likely represent buried but fairly recent basalt eruption centers.

Thus, the low velocity zone shown in Figure 1-17 has a clear volcanic expression; it is spatially very extensive and exhibits a large degree of seismic heterogeneity. Considering these characteristics, the anomaly must be regarded as expressing the effect of laterally varying temperature on rheology (i.e., rigidity) of the crust. Thus, the anomaly provides further evidence for the near-solidus thermal state of the mid-lower crust.

The thermal origin of the low velocity anomaly is corroborated by the distribution of the depth of Curie isotherm. This anomaly is located in an area where this isotherm is shallow, at a depth between 10 and 15 km, which can be seen by comparing Figures 1-13 and 1-17.

In the central and southeast parts of the anomaly, where the *P*-wave velocity perturbations are fairly uniform and negative, the Curie isotherm occurs at a uniformly shallow depth. To the northwest, however, this depth increases sharply from 15 to 25 km, as shown in Figure 1-13. The increase occurs in an area where the P-wave velocity perturbations become positive and the tele-seismic *P*-wave delays (Δt_p) attain values of more than +3 %, as shown in Figure 1-17.

Thus, two totally independently inferred geophysical anomalies lead to a mutually consistent conclusion, which is that the mid-lower crust in the Yucca Mountain area is exceptionally hot and in a near- or at-solidus thermal state. This crust therefore is capable of acting as a conductively recharged heat source, which could support intermittent hydrothermal activity in the upper crust.

1.3.2. Evolution of the Thermal State

It is important to note that the NW-SE axis of the low *P*-wave velocity anomaly corresponds to the northwest trending chain of the most recently active pyroclastic centers of siliceous volcanism. This remarkable correspondence is illustrated in Figure 1-18.

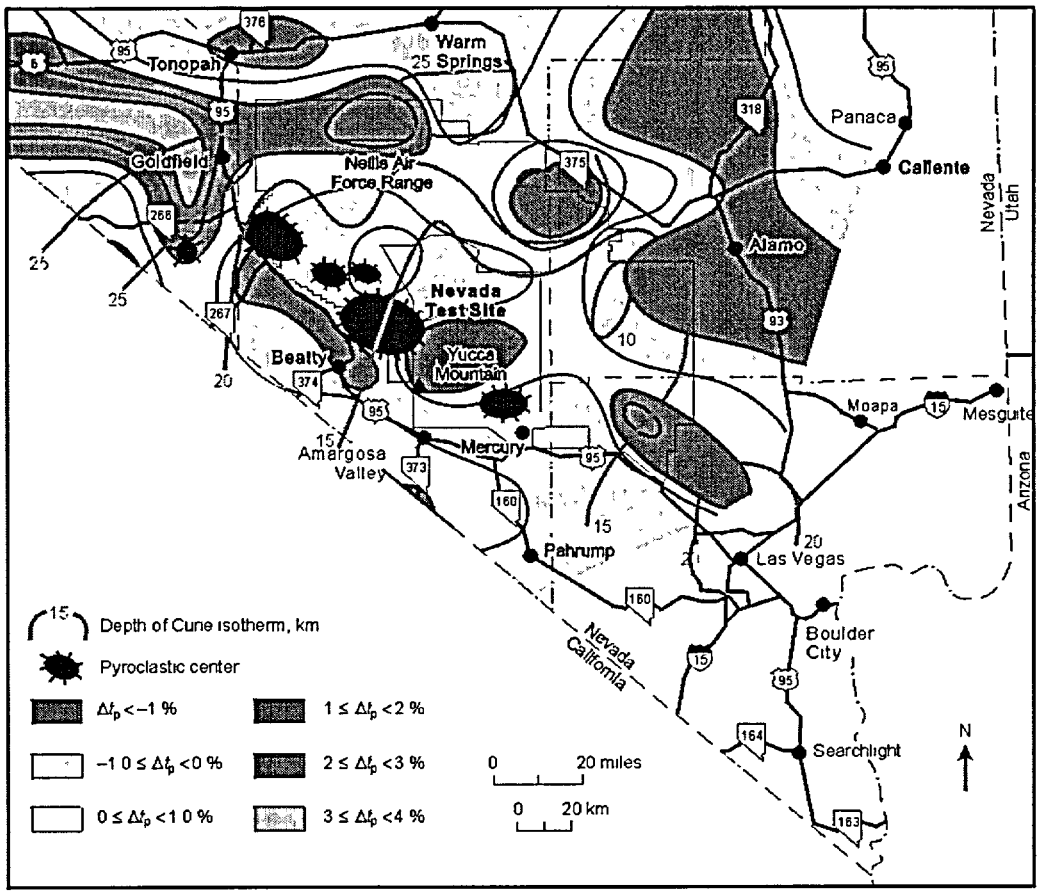

Figure 1-18. The distribution of teleseismic *P*-wave perturbations (based on the data of Monfort and Evans, 1982; see Figure 1-17 for explanations) in relation to the distribution of depth of the Curie isotherm (based on the data by Blackely, 1998; see Figure 1-13) and the distribution of the late pyroclastic centers. Note close correspondence of the distribution patterns.

Pyroclastic centers: WS – Whamonie-Salyer center (~13 Ma); TM – Timber Mountain Caldera (11 Ma); BM – Black Mountain Caldera (8.5-9.0 Ma); OB – Obsidian Butte (8.8±0.3 Ma); SM – Stonewall Mountain Caldera (7.5 Ma); and MJ – Mt. Jackson (3.0-4.5 Ma).

The figure shows that the ages and locations of the centers record a progressive migration, over a time span from 13 to 3 Ma ago, of the pyroclastic siliceous volcanism to the northwest. As noted earlier, the activity has progressed from the Whamonie-Salyer area, first to Timber Mountain and Black Mountain, then to Obsidian Butte and Stonewall Mountain, and finally to the area of Mt. Jackson-Montezuma Range.

By recording the migration, the centers are in fact recording migration of the super-solidus temperature in the crust to the northwest. Because the super-solidus temperature is a result of the advective flux of heat from the mantle, the centers therefore record the migration of the locus of the maximum intensity of this flux. This intensity, in turn, reflects the degree of partial melting in the mantle

source. Thus, the centers pinpoint the timing and the position of the most extensive melting in the upper mantle.

The systematic decrease of ages of the pyroclastic centers implies that the low velocity anomaly, which underlies these centers, has been growing over the past 13 Ma, both to the northwest and sideways as well. The cessation of siliceous volcanism, at each of these centers, and then progressive migration of this activity, to the northwest, is very important. This is because the migration indicates that the intense advective flux of heat into the crust was of a relatively short duration. At a given period, the intense advective heating seems to have been present only at the leading edge of the growing low velocity anomaly. To the southeast, in the interior of this anomaly, the intensity of this heating has quickly diminished thereafter, becoming insufficient to support the continuation of siliceous volcanism.

Nonetheless, the presently observed thermal "softening" of the mid-lower crust and the elevated position of Curie isotherm are both telling us that the present-day heating of the crust by the mantle has not relaxed. The total input of heat from the mantle must have remained sufficiently high to allow for the presence of the near-solidus temperature.

Evidently, the steadily increasing conductive heating of the crust by the upper mantle has effectively compensated for the decreasing intensity of the advective heating. The steadily increasing intensity of the conductive heating is a result of the steadily decreasing depth of the thermally and gravitationally unstable body in the upper mantle and the increasing temperature of this body. Both of these trends have been inferred earlier, based on the evolution of volcanism during the third stage of development of the southern Nevada volcanic field.

It thus becomes apparent that the thermal state of the crust, which underlies the area of Yucca Mountain, has been evolving over the entire life span of this mountain. Figure 1-19 is a schematic diagram illustrating the inferred evolution of the thermal state of a crust. This crust overlies a gravitationally and thermally unstable body in the upper mantle and contains a chain of extinct centers of pyroclastic siliceous volcanism. This inferred evolution is therefore directly applicable to the area around Yucca Mountain.

The evolution is presented in the form of changes in the advective (Figure 1-19-*a*), the conductive (Figure 1-19-*b*), and the total (Figure 1-19-*c*) fluxes of heat from the mantle into the crust across the Moho discontinuity. The resulting changes in temperature of the mid-lower crust, for periods during the pyroclastic siliceous volcanism (Figure 1-19-*d*) and for a long time after the cessation of this activity (Figure 1-19-*e*), are also shown.

At the time when the pyroclastic siliceous volcanism was active, the inferred intensity of the advective component of the total flux of heat is high relative to that of the conductive component (Figure

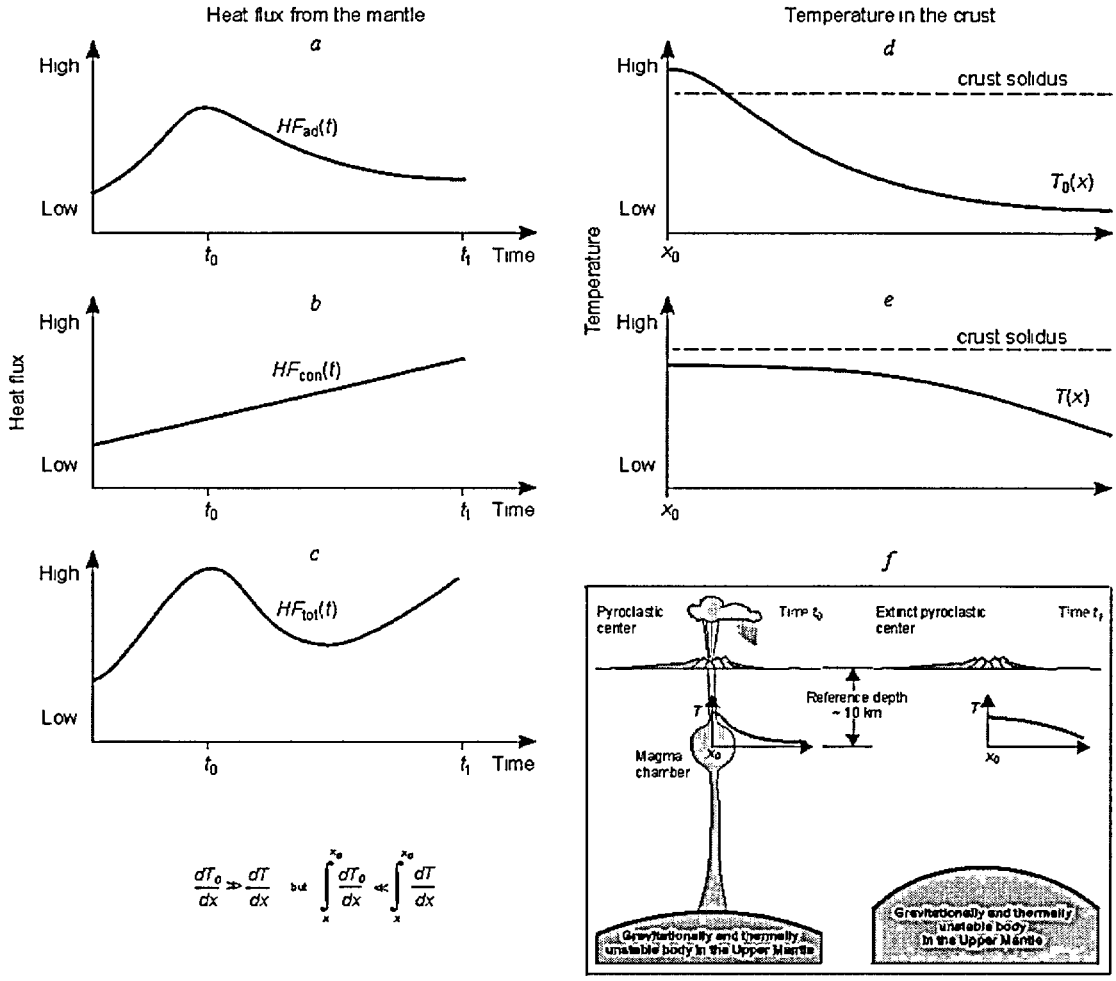

Figure 1-19. Schematic diagram illustrating evolution of thermal state of the crust that overlies a gravitationally and thermally unstable body in the upper mantle and contains extinct pyroclastic center. Note that present-day flux of heat from the mantle into the crust is on the order of 100 to 120 mWt m^2 (see Figure 1-12).

a – advective heat flux; *b* – conductive heat flux; *c* – total heat flux; *d* – temperature during pyroclastic activity; *e* – temperature long time after cessation of the pyroclastic activity; and *f* – cartoon illustrating two modes of the supply of heat into the crust, advective and conductive, shown in *d* and *e*.

t_0 – time of the pyroclastic activity; t_1 – present time; x_0 – location of the pyroclastic center; T_0 – temperature at t_0; T – temperature at t_1; HF_{ad} – advective heat flux; HF_{con} – conductive heat flux from the mantle into the crust.

1-19-*a*). This relationship expresses the high degree of partial melting in the mantle source, on the one hand, and the segregation of the basalt magma at a greater than about 60 km depth, on the other. The partitioning of the total heat flux in this manner results in a high degree of thermal heterogeneity in the crust. This heterogeneity is expressed in Figure 1-19-*d* in the form of a "steep" lateral geothermal gradient (dT_o/dx).

Although the temperature is shown to vary locally in exceeding the solidus, the total amount of heat (i.e., the spatial integral of the $dT_o/dx(y)(z)$ derivative), which is contained at that time in the crust, is low

relative to that over the subsequent period. This is because the super-solidus temperature is present locally, only within the isolated and relatively small magma chambers. Outside these chambers, however, the temperature is well below that over the subsequent period. The relatively low intensity of the conductive component of the total flux, at that time, is responsible for this situation.

When the ascending mantle source encounters the stability fields of hydrous minerals, which have remained in the mantle refractory residuum, the degree of partial melting and the resulting rates of basalt magma segregation both begin to decline. Eventually, they become insufficient to support continuation of the pyroclastic siliceous volcanism. From then on, the advective component of the total flux of heat begins to decline, as shown in Figure 1-19-*a*.

Both the increasing solidus temperature and the decreasing depth of the melting mantle source will have the effect of causing the continual increase of the conductive component, as shown in Figure 1-19-*b*. This increase, in turn, has the effect of eventually arresting the initial decline of the total flux of heat and thereafter of increasing this flux, as shown in Figure 1-19-*c*.

The now dominant conductive heating of the crust by the uprising mantle is spatially more uniform and extensive, relative to the prior heating. Thus, this mode of heating is more effective in raising the overall heat content in the crust. This increasing heat content has the effect of "flattening" the prior lateral gradient (dT_o/dx) and, on top of that, of raising the crustal isotherms. Gradually, the amount of heat contained in the crust increases and, sometime after the cessation of pyroclastic siliceous volcanism, it matches and exceeds the prior amount, as shown in Figures 1-19-*d* and 1-19-*e*.

The inferred evolution of the thermal state begs a question of major importance. What is the current thermal state at Yucca Mountain? Specifically, it is necessary to know whether this state has evolved to the point where another round of advective removal of heat is necessary. Such removal would probably be in the form of intermittent eruptions of hydrothermal plumes initially and, eventually, in the form of volumetrically small eruptions of fissure rhyolites, which then would be followed by massive eruptions of mafic magma in the form of so-called flood basalts.

The prior heat sources were mainly in the form of magma chambers, which supported continuous hydrothermal processes. For these processes, magma convection efficiently replenished the heat losses.

However, heat losses from the present-day heat sources would have to be replenished by the conduction of heat from far field (i.e., from below and from outside the depleted heat sources). This mode of the replenishment has the effect of causing hydrothermal eruptions to be intermittent and short-lived. This character contrasts with that of the prior hydrothermal processes, which were continuously active (multi-path) for a time span measured in terms of 0.5-1.5 Ma. It is important to keep this distinction in

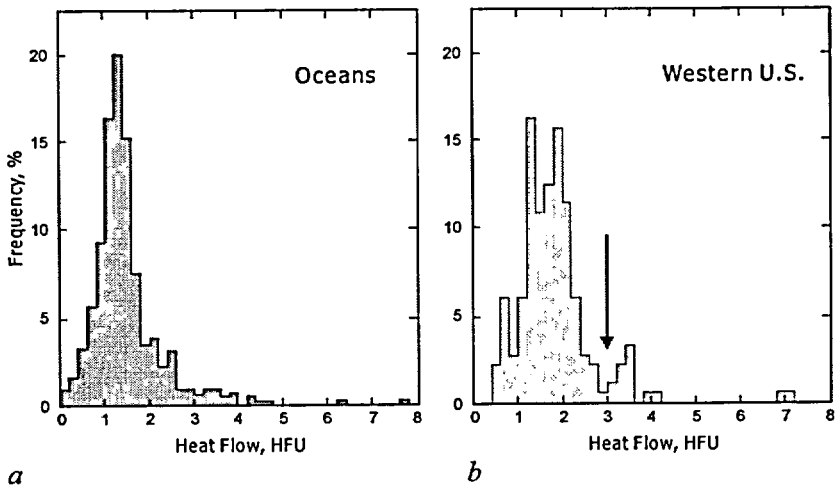

Figure 1-20. Statistical distribution of the conducive heat flow on Earth. Data for oceans are from Von Herzen and Lee (1969); data for western U.S. are from Sass et al. (1971).

Arrow on graph *b* indicates long-term average conductive heat flow at Yucca Mountain inferred on the basis of geophysical data.

mind whilst addressing the origin of calcite-silica deposits, which occur at the surface of Yucca Mountain, and of their crystalline and isotope equivalents in the vadose zone.

The inferred evolution further implies that the remaining time required to conductively replenish the present-day heat sources has diminished as a function of the time elapsed after the cessation of pyroclastic siliceous volcanism. This means that the frequency (or annual probability) of occurrence of the intermittent eruptions now increases with the passage of time.

The first step in addressing the preceding postulates is to examine the contemporary heat flow at and around Yucca Mountain. However, we will defer the final answers in all these regards until subsequent analyses of the geologic record are completed and the associated controversies are finally resolved in Part Three of the report.

1.3.3. Present-Day Surface Heat Flow

Both the intensity of long-term average heat flow and the values of the long-term average geothermal gradients (*dT/dz*, *dT/dx*, and *dT/dy*), which have been inferred based on the geophysical data are conspicuously high. Nonetheless, they are in general agreement with indirect estimates of the actual regional heat flow. In this regard, Swanberg and Morgan (1978) have constructed a map of the actual heat flow in the Great Basin, based on the silica content of groundwater. This map shows that Yucca Mountain is situated within the 2.5 HFU (100 mWm^{-2}) contour. Similar high values of heat flow are observed only rarely, as in oceanic areas near sea-floor spreading centers and in volcanically active continental regions, such as the western USA (Figure 1-20).

Figure 1-20-*b* shows that the intensity of the long-term average heat flow at Yucca Mountain, which has been inferred to range between 2.5 and 3.0 HFU, is very high even by the Great Basin standards.

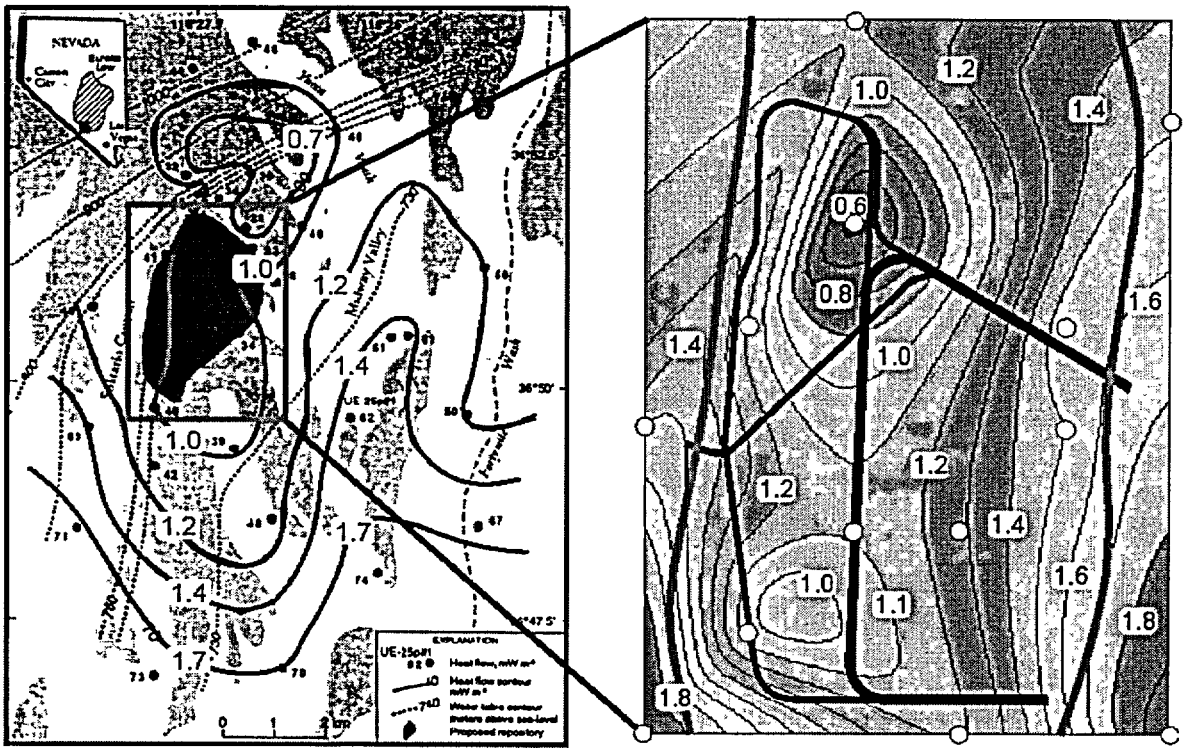

a b

Figure 1-21. Heat flow in the vicinity of Yucca Mountain.

a - Modified from Sass (1998). Light shading indicates outcrops of Tertiary volcanic rocks. Solid isolines show heat flow in HFU. *b* – Heat flow field in the planed radioactive waste repository area. Numbers are in HFU. Calculated from the data of Sass et al. (1987). Yellow circles show locations of boreholes in which temperature measurements were carried out.

However, this long-term average intensity is in sharp conflict with the short-term surface conductive heat flow, which is indicated by direct down hole measurements of the *in situ* temperature. These measurements show that the present-day surface heat flow at Yucca Mountain is very low, and not at all compatible with the volcanically active character of this area and the geophysical observations. This heat flow has intensity ranging only between 0.7 and 1.7 HFU, or between 29 and 71 mWm^{-2}, as shown in Figure 1-21.

We believe that the anomalous high intensity of the inferred long-term average heat flow is a feature that must be considered when evaluating the suitability of Yucca Mountain. This is true, in particular, because the short-term surface measurements do not confirm it, implying that either the inferred long-term values are in error or the surface heat flow is a phenomenon that varies with time.

Because the present-day surface heat flow is very low researchers, who were studying Yucca Mountain for the DOE, have stated on numerous occasions that Yucca Mountain is located in a "friendly"

geothermal environment. Such is the case, they claim, notwithstanding the notorious volcanism that is associated with the region.

To support this dubious notion, these researchers point out that Yucca Mountain is located at or near the southern edge of the so-called Eureka Low - a geothermal anomaly. Within this anomaly, conductive surface heat flow is low by the Great Basin standards. This anomaly is situated some 30 km to the north of Yucca Mountain and is characterized by conductive heat flow of less than 65 mWm^{-2}, or less than 1.5 HFU, as shown in Figure 1-22.

What distinguish Yucca Mountain from the Eureka anomaly are their respective thermal states of the lithosphere. The distinction is based on a number of clear geophysical properties, including the crust-mantle refraction velocity (P_n), the depth of the Curie isotherm, and the tele-seismic *P*-wave travel-time residuals, as illustrated in Figure 1-23.

Figure 1-23-*a* shows that the upper mantle, which underlies the Eureka anomaly, is firmer with a P_n velocity ranging up to 7.9 km s^{-1}, whereas at Yucca Mountain this velocity is significantly lower (P_n as low as 7.6 $km{\cdot}s^{-1}$). The respective depths of the Curie isotherm (Figure 1-23-*b*) also express the distinction. This isotherm occurs at a depth of 10-15 km at Yucca Mountain, whereas the Eureka anomaly occupies an area within which the isotherm is much deeper, at a depth between 20 and 30 km.

The distinction is further emphasized by the distribution of tele-seismic *P*-wave travel-time residuals (Figure 1-23-*c*). The residuals are generally negative at and around Yucca Mountain, whereas underneath the Eureka anomaly these residuals are positive attaining Δt_p values of up to 3 %. Furthermore, the area of Yucca Mountain is situated within the Walker Lane wrench system, whereas the Eureka anomaly is located outside this system. This area, therefore, cannot be associated with the Eureka Low anomaly.

It appears, based on the information presented in Figure 1-23, that the Eureka geothermal anomaly is real, and further that it expresses a local reduction of the conductive flux of heat from the mantle into the crust. This total flux is very much like the one, which has been affecting a few areas near Yucca Mountain, over the past 10-14 Ma, but only in places away from the magma chambers.

Now, however, such is clearly not the case at all at and around Yucca Mountain. Here, the high temperature in the mid-lower crust is a result of the enhanced conductive flux of heat from the mantle. In view of that, the arguments in favor of the proposed radioactive waste repository based on low values of the conductive surface heat flow are superficial and, upon this closer scrutiny, do not carry any weight at all.

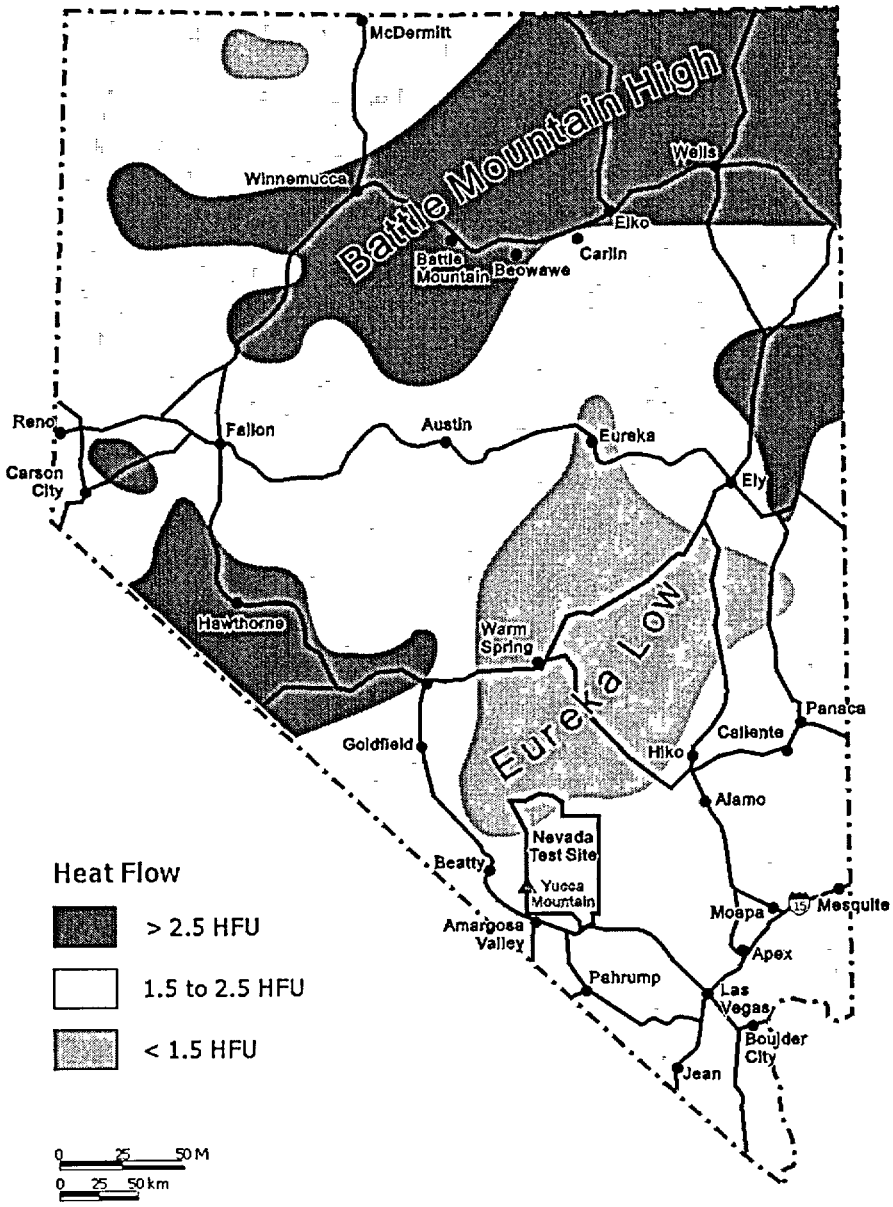

Figure 1-22. Distribution of the surface conductive heat flow in Nevada. From Lachenbruch and Sass (1978).

Contemporary surface heat flow at and around Yucca Mountain ranges from maximum of 2.0 HFU (discharge area) to as low as 0.7 HFU at the northern Yucca Mountain. Heat flow with intensity ~3.0 HFU, anticipated based on the lithospheric thickness, has been encountered only in one well UE-25 a#3 (Sass et al. 1980).

Nonetheless, the comparable low intensities of the present-day surface conductive heat flow, observed at Yucca Mountain (see Figure 1-21) and within the Eureka anomaly, are noteworthy and demand a rational explanation. The large discrepancy between the conductive output of heat, from the topographic surface into the atmosphere, and the inferred input of heat into the upper crust, also demands

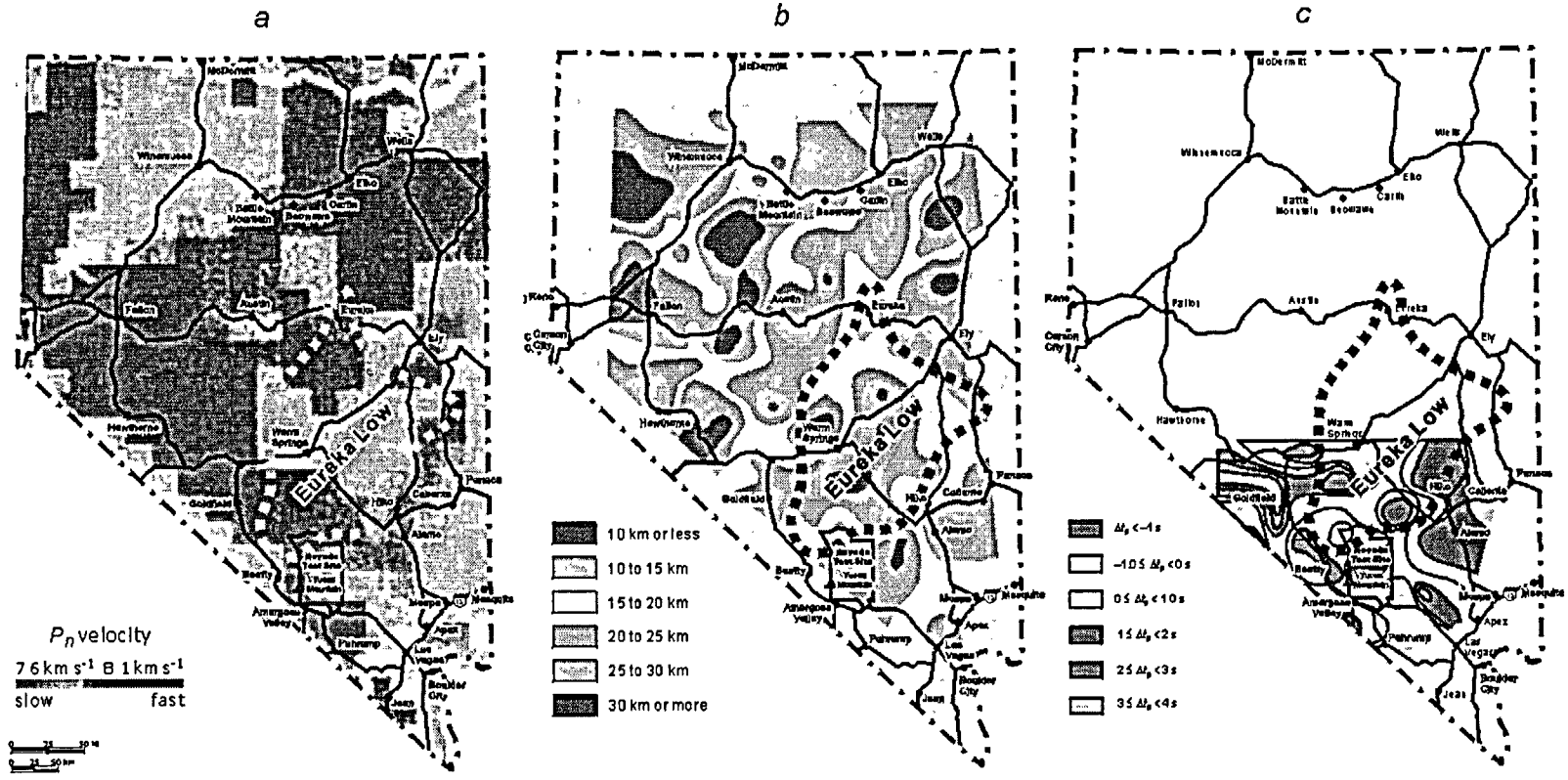

Figure 1-23. Thermodynamic setting of the Eureka Low geothermal anomaly, a comparison with that of Yucca Mountain. Three features distinguish the respective thermodynamic settings. *a* - Distribution of the P_n velocity (crust-mantle reflection velocity) in Nevada. Reproduced from Hearn et al. (1990). *b* - The depth of Curie isotherm (T~560°C) in the state of Nevada. Modified from Blackely (1988). *c* - Teleseismic P-wave delays (Δtp) in the mid-lower crust (15-30 km) in the area of Yucca Mountain. By Monfort and Evans (1982)

By contrast to Yucca Mountain, the Eureka Low anomaly is underlain by the upper mantle, which is rheologically firmer (P_n ~7.9 km s^{-1}; *a*), the Curie isotherm there occurs at greater depth (*b*), and most of the anomaly is situated outside the large P-wave velocity anomaly in the lower crust (*c*).

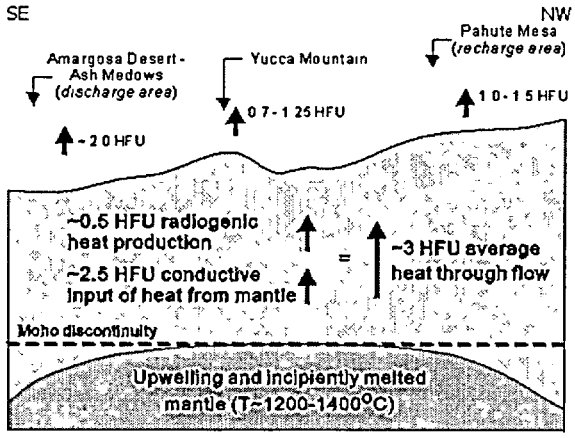

Figure 1-24. Schematic presentation of the heat balance across the hydrological system of Yucca Mountain.

The surface output of heat (0.7 to 2.0 HFU) is substantially lower than a sum of the heat radiogenically produced in the crust (~0.5 HFU) and the conductive input of heat from thermally and gravitationally unstable mantle. The surface output of heat in the hydrological discharge area (~2.0 HFU) is still lower than the inferred cumulative input of heat (~3.0 HFU), which implies temporary storage (accumulation) of the heat in the upper-middle crust. Actual surface heat flow data are from Sass and Lachebruch (1982). Assessment of the average heat flow is based on Figures 1-11 and 1-13.

a rational explanation. Although similar low heat flow occurs in some continental regions of the Earth, such as the cratonic shields and continental platforms, it is unreasonable to assume that these presently observed intensities represent the actual long-term average heat flow at Yucca Mountain.

Discrepancies between the conductive and the total (i.e., including the advective component) heat flows have often been observed, and Yucca Mountain is not unique in this regard. In most instances, these discrepancies are attributed to hydrothermal (advective) transport of the additional heat, which is not included in the traditional calculations of heat flow (e.g., Sclater et al., 1980; Ranalli, 1987).

Sass and Lachenbruch (1982) and Sass et al. (1983) considered the locally depressed surface heat flow at Yucca Mountain. The authors concluded that "*...the regional heat flow beneath the zone of hydrologic disturbance may be the same as that characteristic of the Great Basin in general (80 mWm^{-2}, or 2.0 HFU), or it could be as high as 100 mWm^{-2}, or 2.5 HFU.*" Later, Sass (1999) revisited the subject and argued that "*Yucca Mountain in particular is the site of a local heat sink, with local minimum (30 mWm^{-2}), coinciding with the proposed nuclear waste repository site*".

Although it is not clear what precisely their proposed explanation is, Sass and co-workers apparently propose that both a local aquifer recharge and then a lateral movement of shallow groundwater are jointly responsible for the apparent deficit. The resulting transport of heat, first downward and then laterally to the south away from Yucca Mountain into the discharge area, would have the effect of somewhat depressing the surface heat flow. Although the lateral transport undoubtedly is involved to some extent, this process alone cannot satisfactorily account for the totality of the inferred thermal deficit, as shown in Figure 1-24.

The figure shows a schematic cross-section of the distribution of heat flow across the hydrologic sub-system at Yucca Mountain, from the recharge area in Pahute Mesa to the discharge area in Amargosa Desert-Ash Meadows. It also shows that the integrated heat flux, over the entire groundwater sub-system,

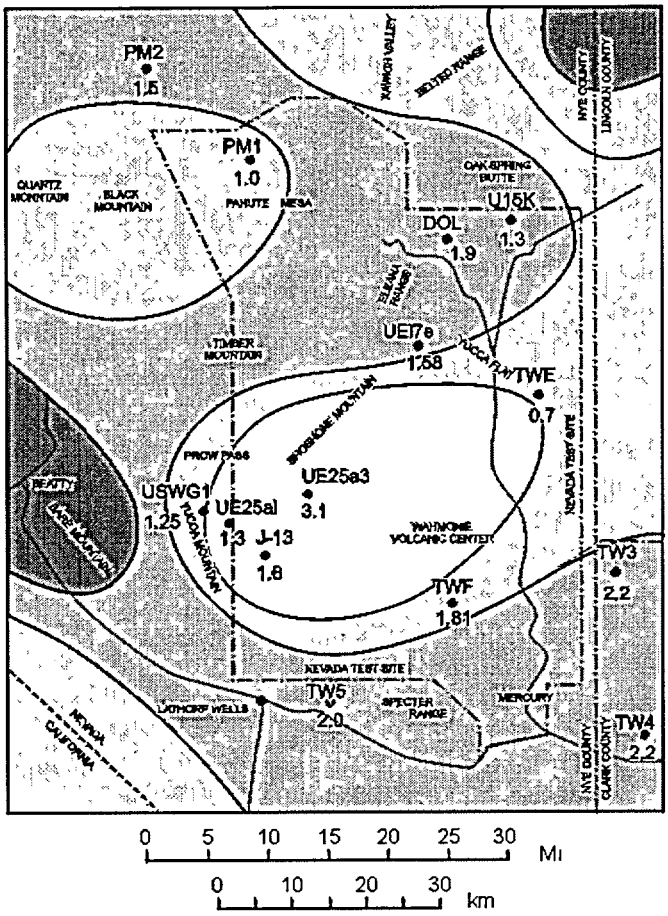

Well	Heat flow mWm^{-2}	HFU	Reference
PM2	63	1 5	Sass and others, 1971
PM1	42	1 0	Sass and others, 1971
DOL	80	1 9	Sass and others, 1971
U15K	56	1 3	USGS unpudlished
UE17e	66	1 58	USGS unpudlished
TWE	29	0 7	Sass and others, 1971
J-13	67	1 6	Sass and others, 1971
UE25a1	54	1 3	Sass and others, 1980
UE25b1	47	1 1	USGS unpudlished
UE25a3	130	3 1	Sass and others, 1980
USWG1*	52	1 25	Table 2, this paper
TWF	76	1 81	Sass and others, 1971
TW3	92	2 2	Sass and others, 1971
TW5	84	2 0	Sass and others, 1971
TW4	91	2 2	Sass and others, 1971

*Average heat flow in lowermost ~600 m

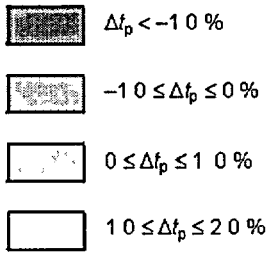

Figure 1-25. Surface conductive heat flow in comparison with the distribution of teleseismic *P*-wave velocity perturbations in the area of Yucca Mountain. Note that the distribution of surface conductive heat flow is highly heterogeneous. From Lachenbruch and Sass (1978).

from the mantle (about 2.5 to 3.0 HFU) and the radiogenic heat production in the crust (about 0.5 HFU) exceeds the surface output of heat into the atmosphere. The maximum intensity of this output is between 1.5 and 2.5 HFU, with the single exception being drill hole UE-25a3 (3.1 HFU, or 130 mWm^{-2}) in south central Nevada Test Site, as shown in Figure 1-25.

1.3.4. Inferred Long-Term Behavior

Even allowing for a lateral heat transport by groundwater, a deficit exists between the long-term average input of heat flux and the short-term conductive output of heat into the atmosphere. This problem vanishes, however, if the actual total heat flow fluctuates between a minimum, before the occurrence of hydro-tectonic events, and a maximum shortly thereafter. This implies a cyclic behavior of the groundwater system, as schematically illustrated in Figure 1-26.

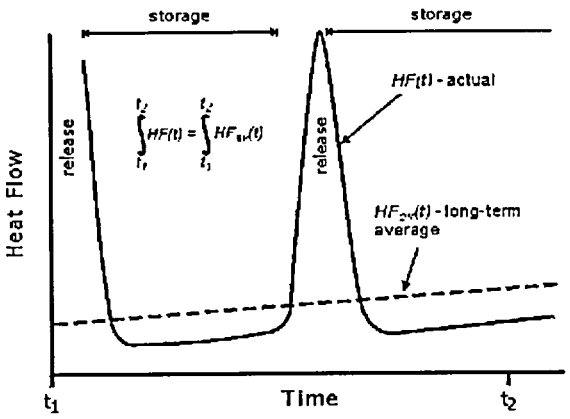

Figure 1-26. Inferred temporal distribution of the actual surface heat flow *HF(t)* compared to the long-term average $HF_{av}(t)$ heat flow at Yucca Mountain.

These cycles would consist of long periods of accumulation of the mantle-provided heat at mid-crust levels (at a depth of say 10-15 km), and of relatively brief periods of venting of the accumulated heat. The venting events would assume the form of hydrothermal or gaseous plumes, invading the vadose zone and discharging at the topographic surface.

The essence of this cyclic behavior, which is shown in Figure 1-26, is quite well summed up by the quotation from Ellis and Mahon (1977). The authors stated in this regard: "*... if it is considered that the water turnover time in a geothermal system is very long (of the order of 10^4-10^5 years), and the outflow intermittent, systems could then have long periods of conductive heating of water with little outflow, followed by comparatively brief periods (of order of 10^3-10^4 years) of high flow when new channels to the surface are formed This may be triggered by tectonic activity, or by hydrothermal explosions should the temperature cause steam pressures to exceed the lithostatic pressure. After a period of flow, the channelways may become sealed with deposits of silica and calcite.*" (emphasis added).

Interpretation of the long-term behavior of the surface heat flow must be made with the realization that the Yucca Mountain situation satisfies two important thermodynamic conditions.

First, the input of heat from the mantle is sufficiently large to produce a high vertical geothermal gradient in the crust. The observed properties (wavelength) of magnetic anomalies and the P_n velocities in the uppermost mantle (see Figures 1-11 and 1-13) jointly indicate that the long-term average value of this gradient exceeds 40 °C·km^{-1}.

Second, the observed lateral variations of the P_n velocity and of the depth of Curie isotherm (see Figures 1-11 and 1-13) jointly imply the presence of substantial lateral gradients of temperature. However, under the presence of lateral temperature gradients, the critical Rayleigh number (R_c), which expresses boundary conditions for a thermally stratified fluid, becomes very small ($R_c << 4\pi^2$).

In hydrodynamics, thermal stability of a fluid is assessed by the means of Rayleigh number (R_a). This dimensionless combination of parameters expresses a balance of forces that foster and hinder stability of a thermally stratified fluid. The instability sets in when the Rayleigh number (R_a) exceeds some critical value, or critical Rayleigh number (R_c). The R_a is a direct function of the geothermal

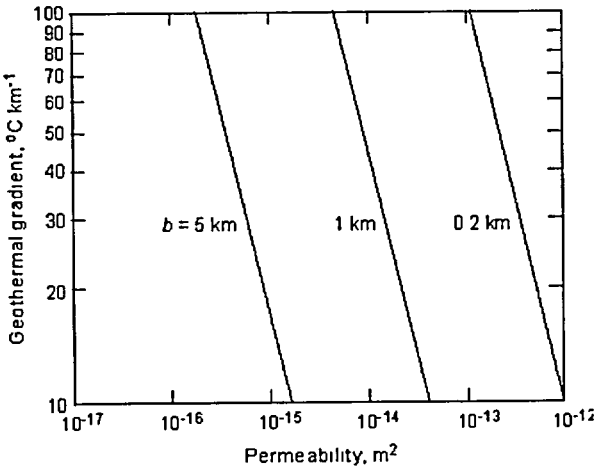

Figure 1-27. Values of geothermal gradient that is required for the onset of thermal convection of fluid in a porous medium as a function of the permeability and the thickness of the aquifer *b*. From Turcote and Schubert (1982).

gradient; so that, the high values of this gradient ensure that the Rayleigh number is large enough ($R_a > R_c = 4\pi^2$) to trigger the onset of thermal convection in most typical aquifers (i.e., those with a thickness between 0.2 and 5.0 km and a permeability between 10^{-12} and 10^{-15} m^2), as shown in Figure 1-27.

Stability of a thermally stratified fluid contained in a strongly heterogeneous fractured medium, such as the one at Yucca Mountain, is solely dependent on the actual *in situ* values of the critical Rayleigh number (R_c), which is unknown and is likely to remain such. This number is dependent on the availability of relatively wide permeability channels. The R_c is at a minimum if the slenderness (aspect ratio) of such a channel is between 0.5 and 3.0. It is also dependent on the "strength" of fluid-wall rock thermal interaction, with the R_c at a minimum if this interaction is adiabatic, as detailed by Murphy (1979) and in the text below.

The high density of wide fault zones at Yucca Mountain, the low thermal conductivity of the ash-fall tuffs (see Sass et al., 1987), and the substantial geothermal gradients all act in concert assuring that the R_c, and hence the $R_c - R_a$ difference, is relatively small. This means that at Yucca Mountain there is, and always has been, a high potential for the occurrence of hydrothermal circulation, whether continuous or intermittent, and for a resulting augmentation of the conductive heat flow. This also means that, at present, the hydrologic sub-system could be in a sub-critical state ($R_c - R_a \rightarrow 0$), in a neutral stability state ($R_c - R_a = 0$), see Murphy (1979), or it could contain heat dissipative structures in the form of Rayleigh-Bénard instabilities ($R_c - R_a < 0$).

It is important to recognize that potential heat dissipative structures, in the form of Rayleigh-Bénard instabilities (buoyant), may have already been observed at Yucca Mountain. In this regard, the results of geothermal studies by Sass et al. (1983) and Sass et al. (1987) infer the presence of two independent centers of hydrothermal circulation. These results are summarized in the form of a geothermal map, which is shown in Figure 1-28.

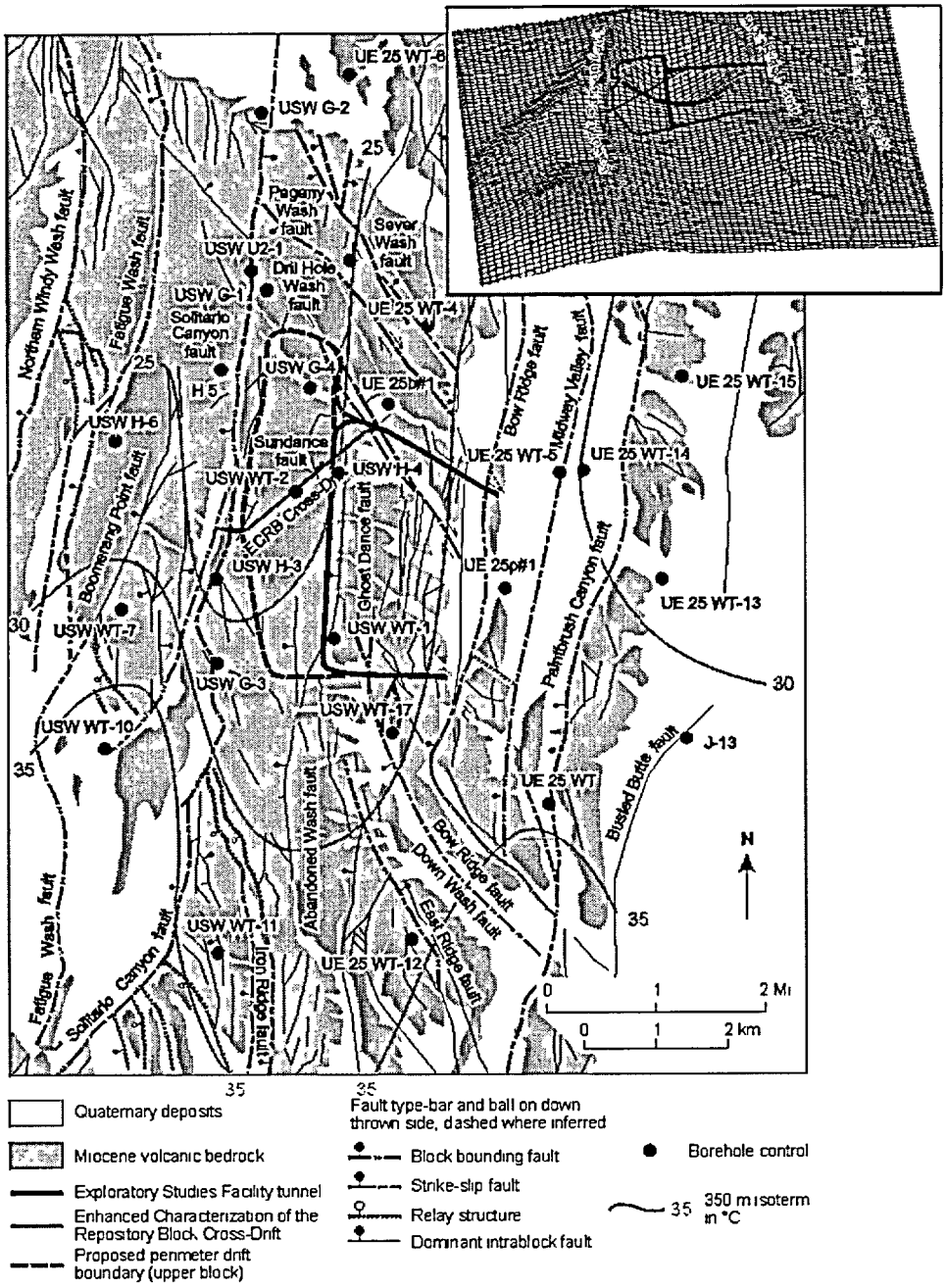

Figure 1-28. Mapped faults at Yucca Mountain and in the Yucca Mountain vicinity, and the 350 m-depth isotherm. Compiled from Sass et al. (1987) and Day et al. (1998). Note thermal highs that are centered on the horst bounding faults.

Inset· 3-D representation of the temperature at the water table. The lowest temperature (blue) is 22°C, the highest (red) is 38 °C. Approximate projection of the ESF, ECRB, and the outline of the proposed repository is shown in black. Based on the data of Sass et al. (1987) and Graves (1988).

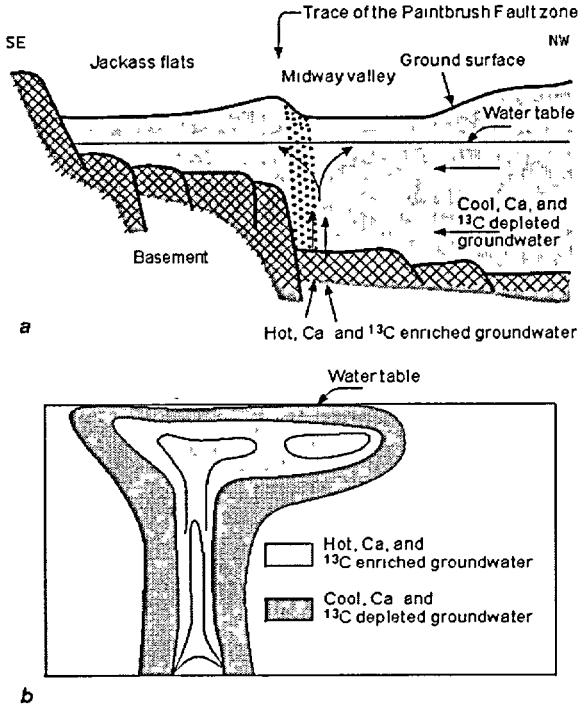

Figure 1-29. Conceptual diagram illustrating inferred origin of the geothermal anomalies at Yucca Mountain.

a – Schematic hydrologic cross secton across the eastern horst-bounding fault zone; *b* – Mushroom-shaped plume of hot and Ca-^{13}C enriched groundwater diffusing into cool and Ca-^{13}C depleted groundwater.

The figure shows that one of these potential centers may be present beneath the eastern edge of Yucca Mountain, where it would be hosted by the horst-bounding Paintbrush fault zone. It has been observed in well UE-25 p#1, at a depth of about 1.2 km. Referring to this particular geothermal anomaly, Sass et al. (1983) concluded: "*...in the Paleozoic rocks ... there is a complex hydrothermal circulation system*". (emphasis added).

In addition, the figure reveals the presence of a strong thermal high along the western flank of Yucca Mountain. This geothermal anomaly is centered along the horst-bounding Solitario Canyon fault zone, and it is very similar to the one surrounding the Paintbrush fault zone, as shown in Figure 1-28.

Both of these thermal highs imply the presence of an active upwelling of deep and hot aquifer fluids along the deeply penetrative horst-bounding fault zones, from the basement into the overlying tuffs. Short of complete understanding of the long-term behavior of these geothermal features, it is impossible to know whether the upwelling expresses a thermodynamically stable "forced convection", caused by non-buoyant forces, so that $R_a < R_c$. The only alternative is that this upwelling is produced by a thermodynamically unstable heat dissipative structure, so that $R_a > R_c$ or $R_a = R_c$. In either case, the upwelling would take the form similar to that schematically shown in Figure 1-29.

The picture shown in the figure has been confirmed, at least partly, by down hole measurements of piezometric head and *in situ* temperature in drill hole UE-25 p#1, results of which are given in Craig and Johnson (1984). This drill hole encountered the horst-bounding Paintbrush fault, which at this location forms a high-angle contact between the late Miocene tuffs and the early Paleozoic carbonates of the basement. Within and below this contact, the piezometric head is up to 20 m higher than that in the overlying tuffs. Furthermore, the UE-25 p#1 temperature profile revealed that at the fault contact the geothermal gradient becomes negative, as shown in Figure 1-30-*a*.

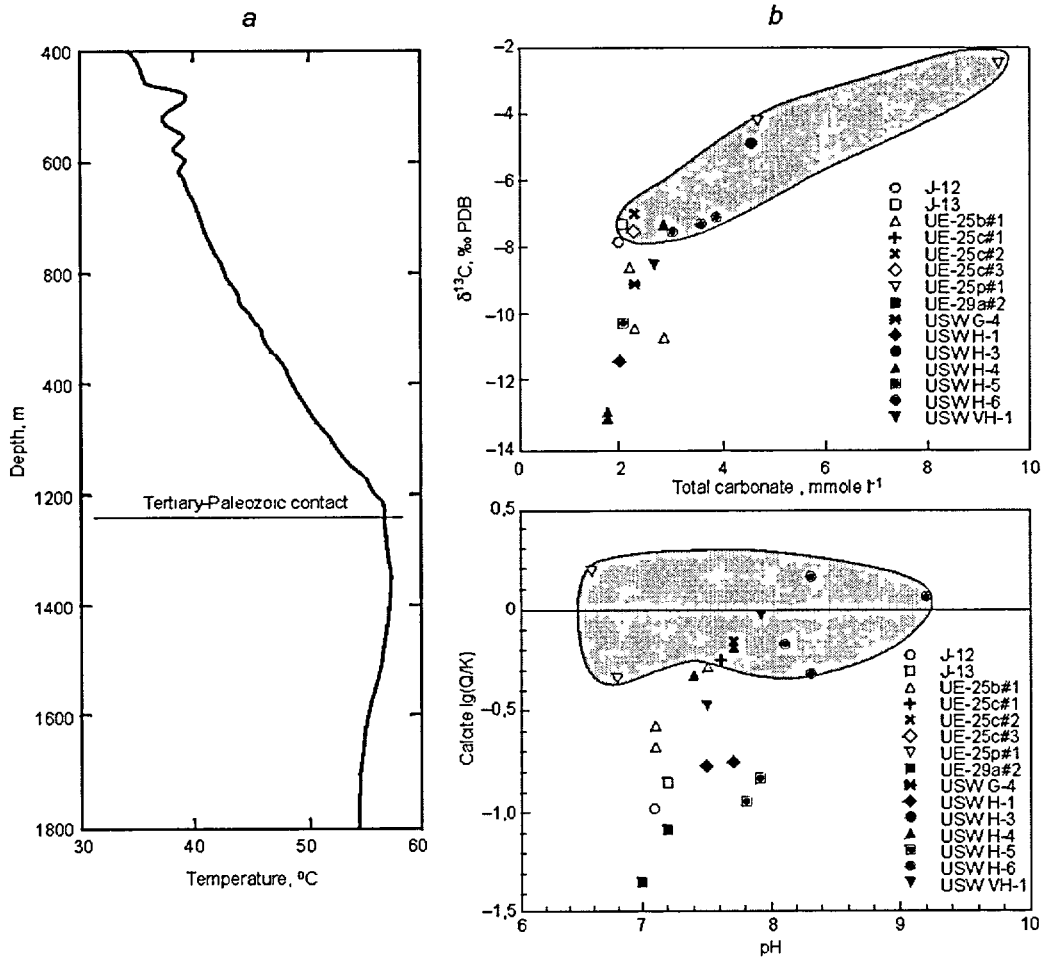

Figure 1-30. Chemical, isotope, and thermal bases for inferring the origin of the Paintbrish and Solitario Canyon geothermal anomalies.

a – Downhole temperature log from well UE-25p#1. From Craig and Johnson (1984). *b* – Chemical and carbon isotope composition of groundwater at Yucca Mountain. Shaded fields show samples that were collected from near and within Paintbrush and Solitario Canyon geothermal anomalies. From Kerrisk (1987).

The sharp reversal shown in the figure is a clear indicator of a hot fluid upwelling along an inclined fault contact. Location of this reversal coincides with the abrupt increase of the piezometric head.

The presence of such a fault-based upwelling, underneath both of the geothermal anomalies shown in Figure 1-28, is confirmed by the isotope and chemical composition of fluids from the phreatic zone. Samples of these fluids were collected from and around traces of the horst-bounding fault zones, as well as from the intervening block. As shown in Figure 1-30-*b*, the samples from near the geothermal anomalies yielded $\delta^{13}C$ and calcite saturation index [lg(*Q*/*K*)] values of which are consistently higher than those that represent the intervening block. Both the total carbonate abundance and the pH are also similarly increased.

Collectively, the higher $\delta^{13}C$, $\lg(Q/K)$, total carbonate abundance, and pH values indicate a localized input of fluid, which has been equilibrated with a calcium- and inorganic (reduced) carbon-bearing reservoir. At Yucca Mountain, such a reservoir underlies the late Miocene tuffs and consists of the early Paleozoic marine carbonate rocks of the basement.

It is clear therefore that the horst-bounding faults, specifically the Solitario Canyon and Paintbrush fault zones, both act as pathways for the ascent of ^{13}C- and Ca-enriched fluids from the carbonate aquifer into the overlying tuffs. These fluids ascend from a depth, which ranges between at least 1.2 to more than 3.5 km.

If the anomalies are expressing the presence of heat dissipative structures, in a neutral stability state ($R_c - R_a = 0$) or operating at a steady state ($R_c - R_a = \text{const} < 0$), then it follows that the total long-term output of heat is not constant. Instead, the total long-term output of heat into the atmosphere fluctuates between a maximum and a minimum. This is because a delicate balance exists between the opposing forces that foster and hinder buoyant instabilities, which occupy the fault-based conductivity channels. Any change of this balance either encourages (positive growth rate) or discourages (negative growth rate) these instabilities. With a changing growth rate, the total output of heat into the atmosphere must also be changing accordingly.

In a tectonic environment, such as that at Yucca Mountain, there are numerous processes that can stimulate a marginally stable heat dissipative structure, which prefers to operate at a steady state or to cease altogether. A change in hydraulic or thermal conductivity (by fault creep or mineral deposition), a change in the rate of upward flow of gas or fluid (by seismic displacements), etc., are examples of such processes. The reaction to such a variety of stimuli has the effect that the heat dissipative structures incessantly search for some sort of stability, where either $R_c - R_a > 0$ or $R_c - R_a = \text{const}$, so that, rather than the process being steady state in the long-term, instead, the intrinsically non-steady state nature of these structures must be presumed.

Chapter 1.4. Tectonic Environment and Structural Geology

1.4.1. Introduction

The region of the Great Basin, including the area around Yucca Mountain, is unique among the tectonically active regions of the Earth, and this region is clearly anomalous from a perspective of thermodynamics. What distinguishes it from almost any other tectonic environment of the present-day continents is an abnormally small thickness of the thermal lithosphere and its location immediately adjacent to an active transcurrent plate-tectonic juncture.

Figure 1-31 is a generalized map showing global distribution of thickness of the so-called thermal lithosphere, which is defined (following Ranalli (1987), and Pollak and Chapman (1987)) as a depth at which the temperature is equal to 85 % of the mantle solidus (T_m), so that $T = 0.85 \cdot T_m$.

The map shows that the thermal lithosphere in the southern Great Basin is exceptionally thin, with the average thickness ranging between 60 and 45 km. For the continents, the only other locations with the comparable thickness are the East African Rift and Mediterranean Sea. In both of these cases, the anomaly is a result of the isostatically uncompensated and thermally unstable sub-lithospheric mantle, which is corroding and invading the lithosphere. This process is thermodynamically analogous to "oceanization" of the continental crust, whether of the Atlantic type or the Mediterranean type, as described in Van Bemmelen (1972). Beloussov (1962) refers to this process as a "basification" of the continental sial. The form of this process and its geophysical expression are both illustrated in Figure 1-32.

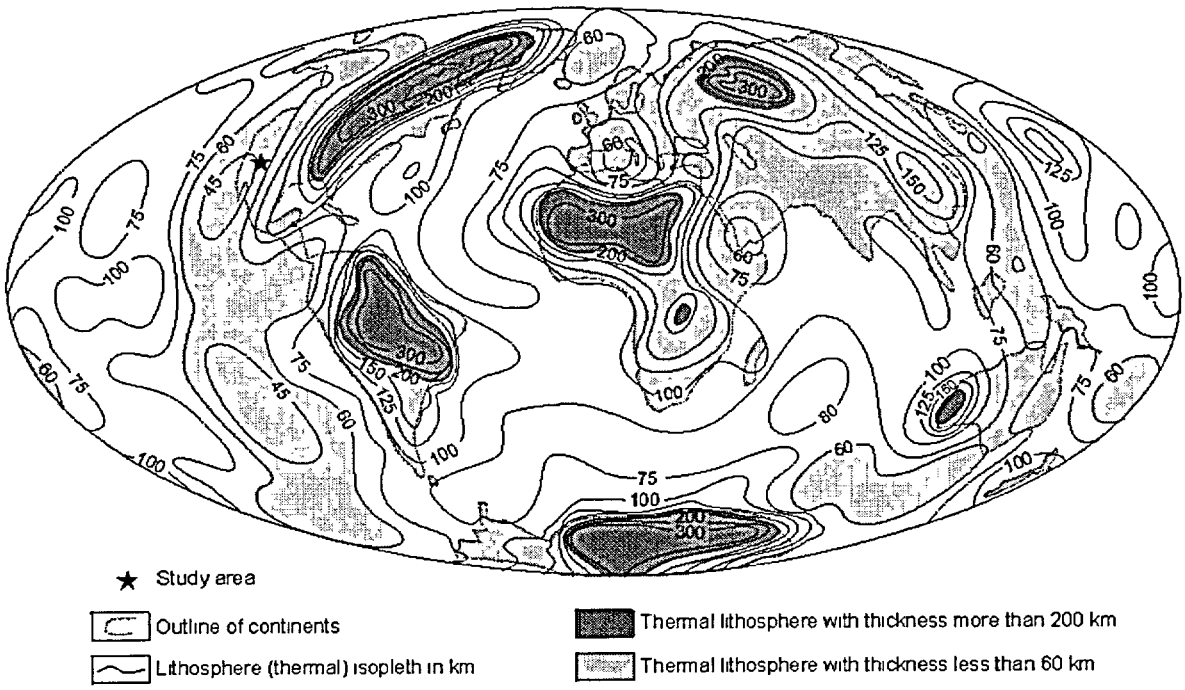

Figure 1-31. Thickness of the thermal lithosphere on the Earth. Modified from Pollak and Chapman (1977).

Thickness of the thermal lithosphere is the depth at which temperature $T = 0.8\ T_m$, where T_m is mantle solidus temperature. The Great Basin region is indicated by a star.

The figure shows that the process of "oceanization" is a result of a thermally and gravitationally unstable body in the sub-lithospheric mantle, which ascends under the influence of buoyancy forces. This cause-effect relationship is indicated by the deformed state of the lithosphere and by the abnormally low velocity of the *S*-wave.

In addition to being affected by the mantle diapirism, the tectonics of the Great Basin is also strongly affected by its proximity to the western margin of the North American continent. Now, this margin is developed in the form of a transcurrent plate-tectonic juncture. Such a juncture involves horizontal translations of one tectonic plate relative to the other. This plate-tectonic setting of the Great Basin is depicted in Figure 1-33.

Figure 1-33-*a* shows that the juncture involves the Pacific oceanic plate and the North American continental plate and, further that this juncture is along the San Andreas Fault of California. The oceanic plate slides to the northwest along this major wrench fault, relative to the continental plate. The fault trace is delineated by foci of frequent but shallow earthquakes, as shown in Figure 1-33-*b*, these having dextral strike-slip focal mechanisms.

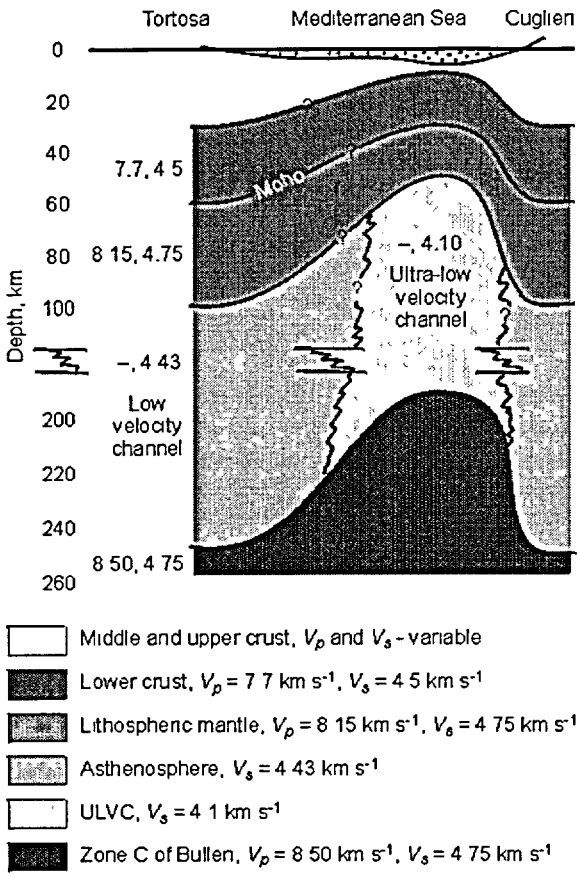

Figure 1-32. Diapiric rise of the astenosphere: Ultra-low velocity channel underneath western Mediterranean Sea. Modified from Berry and Knopoff (1967). Numbers indicate *P* and *S*-wave velocities (V_p and V_s).

The figures further show that the area of Yucca Mountain is located at a lateral distance of only a few hundred km to the east of the plate-tectonic juncture. In addition, this area is also in a close proximity to a major NW-SE trending plate-tectonic lineament. This lineament connects with the Juan de Fuca spreading center to the northwest and with the Gulf of California (Baja) spreading center to the southeast.

Both the San Andreas Fault and the lineament are sites of intense tectonic activity, which is a result of the most fundamental geodynamic processes involving various irreversible conversions of endogenic energy. Here, as is the case with any plate-tectonic juncture, significant amounts of potential gravitational and distortional strain energy accumulate and are converted into work. In addition, various phase transitions take place, large quantities of endogenic heat are released, and large quantities of entropy are produced and then lost as a result of various irreversible processes.

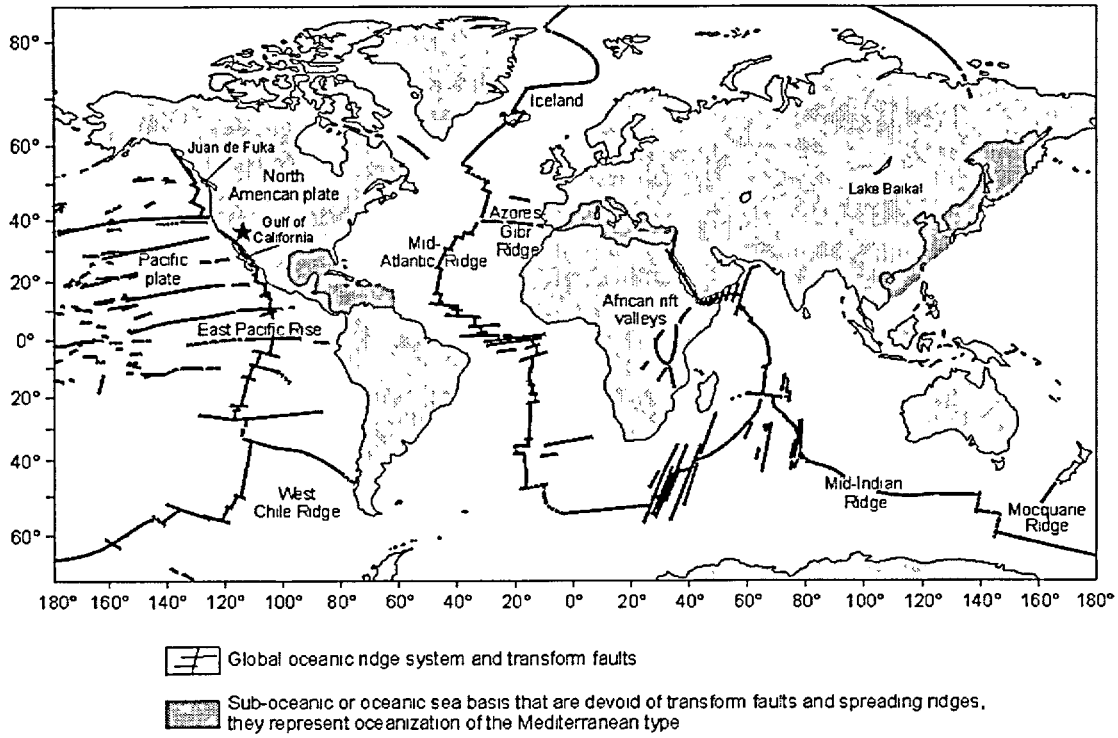

a

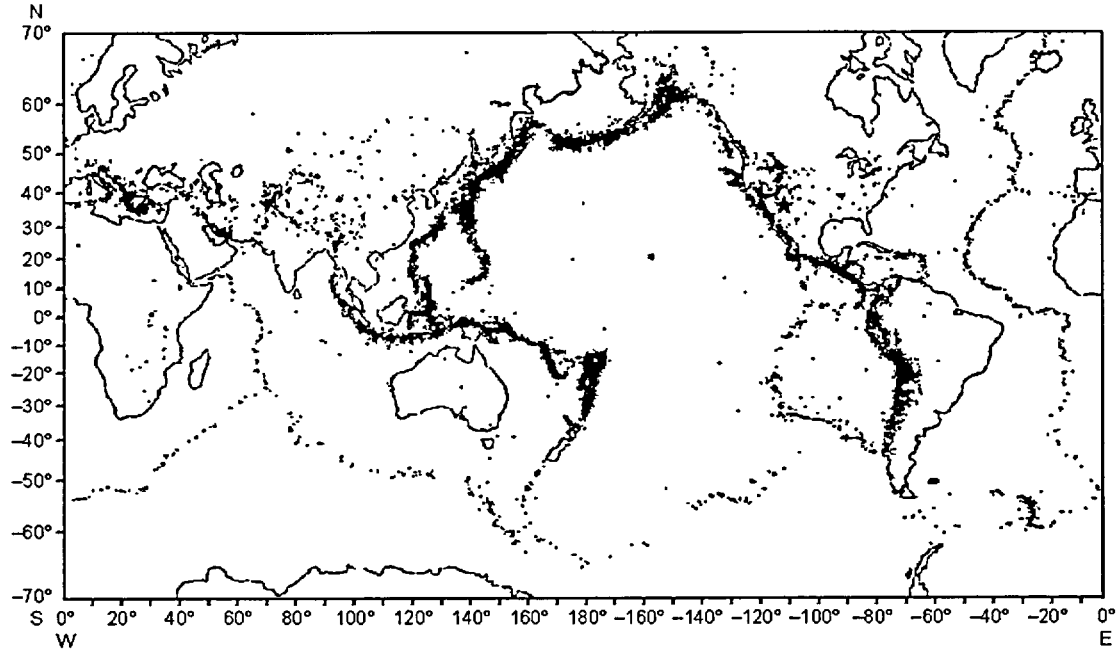

b

Figure 1-33. Global system of mid-oceanic ridges and transform faults (a) and global distribution of earthquake epicenters for period from 1961 and 1967. A star shows approximate location of Yucca Mountain.

a – From Sykes (1969); *b* – From Brazangi and Dorman (1969). Note strong correlation between density of earthquake epicenters and plate-tectonic boundaries. Also note that the convergent boundaries are associated with substantially greater density of epicenters, as compared to the divergent boundaries.

The mantle diapirism, or mantle upwelling, and plate-tectonic motions are processes, which, acting in concert with each other, have been controlling the tectonic evolution of the Yucca Mountain region over entire life span of this mountain. Both of these processes express a macroscopic order, which has been established by self-organization in response to strong flow of endogenic energy and matter. Each of the late Cenozoic structural elements (e.g., igneous bodies, uplifted mountain ranges, tectonic depressions, faults and fractures, ore bodies, etc.) is the consequence of the attaining and maintaining of such order. Each of these elements is a result of the outward flow of endogenic energy, and each represents work performed and entropy produced and lost as a result of various irreversible processes, which have accompanied this flow in the past.

Understanding of the coupled processes that were involved in the various conversions of endogenic energy into work and entropy is essential for comprehending the role that tectonics plays in long-term behavior of the hydrologic sub-system at Yucca Mountain. This behavior is crucial to the development of the appropriate release scenarios and then the assessments of anticipated releases of radioactivity from the proposed nuclear repository. In this regard, the accumulation and release of tectonic strain, in particular the resulting changes of physical conditions that foster and hinder non-Darcian flow processes, is one of the most important factors that must be considered.

1.4.2. Tectonic Strain

In a tectonic environment, such as the one in the region around Yucca Mountain, the flux of potential gravitational energy and distortional strain energy occurs across both the horizontal and vertical boundaries of the geologic system, which act as movable boundaries but not as fixed boundaries. This flux, of course, varies as a function of both time and space.

At the lower horizontal boundary, strain and potential energy is transferred from the mantle by shear and normal stresses acting at the base of the lithosphere, with variability in time and space, as Harper and Szymanski (1991) have suggested. These stresses are a result of the gravitationally unstable and therefore continually ascending body in the sub-lithospheric mantle. In addition, this body produces such effects as alteration of the temperature and viscosity fields, increase in the heat flow, and uplift of the Earth's surface, as shown in Figure 1-34.

Because of its ascent, the body introduces into the lithospheric mantle and into the overlying crust space- and time-dependent lateral gradients of the gravitational potential. In turn, these gradients give rise to a gravity deformation of the crust, as Ramberg (1967) has suggested. This deformation takes the form of a lateral spreading or extension of the crust and the underlying lithospheric mantle. The spreading motions are a result of downhill sliding away from the uplift center under the influence of gravity force, a process which is analogous to the sliding of a glacier, as Frank (1972) has suggested. As in the case of

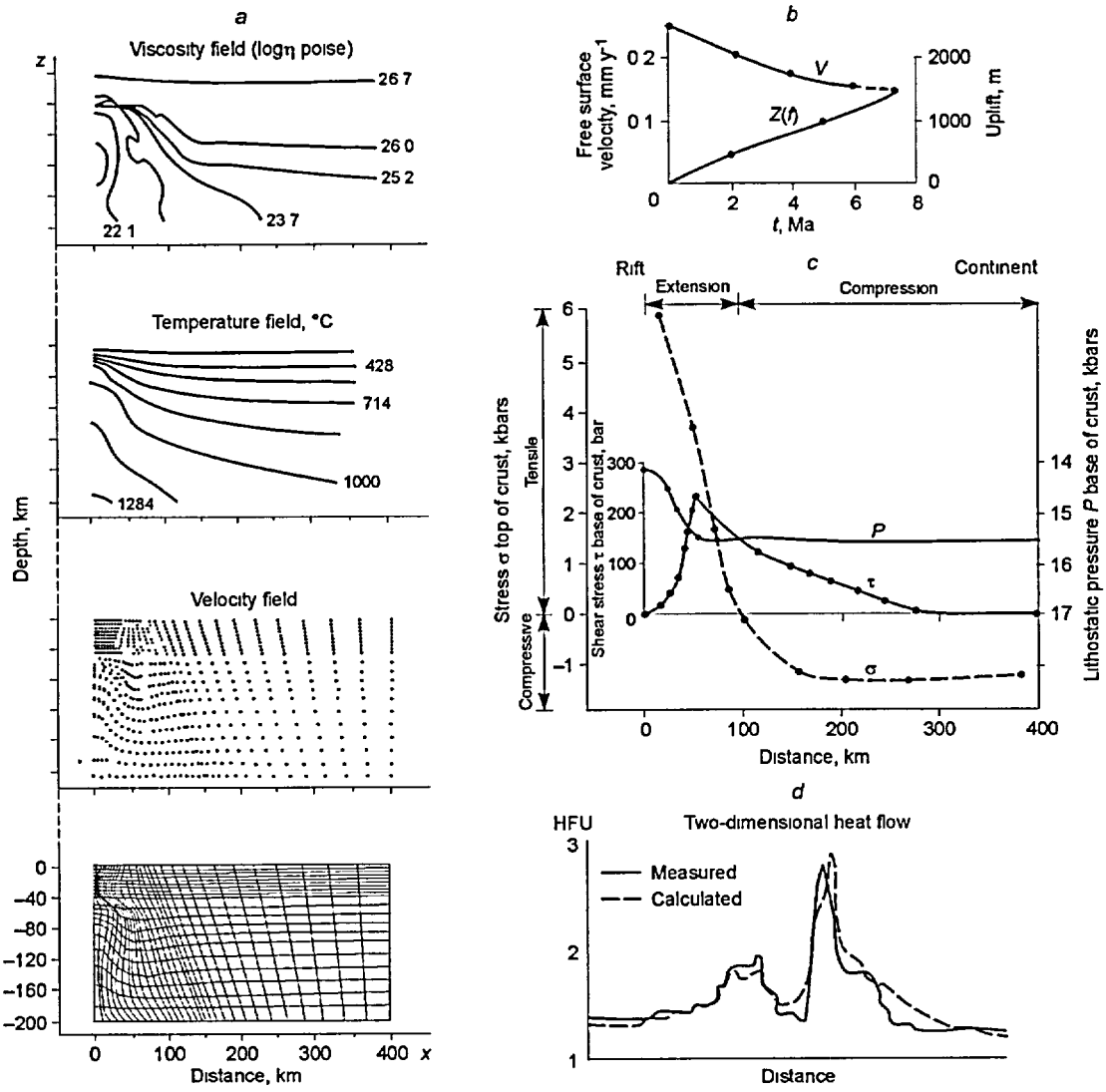

Figure 1-34. Some effects that a mantle diapir has on rheology, state of stress, and displacement in the crust. From Bridwell and Potzick (1981).

a – Results of numerical simulations expressed as changes in the fields of material viscosity (η), temperature, velocity, and deformations. *b* – Uplift velocity (V) and accumulated uplift (Z); *c* - continuum stress (σ and τ) and pressure (P) at the transition rift-continent. *d* - Surface heat flow.

glacier motion, "downhill" is to be interpreted with reference to the upper free surface, this is the ground surface.

The operability of space- and time-dependent lateral gradients of the gravitational potential has the effect of allowing the deformational system to have movable boundaries, in the manner of deformational boundaries in the case of a sliding glacier. In other words, the deformation of sliding masses involve dilatory failure mechanisms, in the form of progressing opening and sometime closing of fractures and cracks. These failure mechanisms are particularly important because they have the effect of allowing for

the progressing accumulation of heat and aqueous solutions, in addition to allowing for the progressing accumulation of strain energy. The most important effect of space- and time-dependent lateral gradients of the gravitational potential, from a perspective of non-linear thermodynamics, is that these gradients couple the long-term flows of endogenic heat, aqueous solutions, and strain energy.

The overall effect of the gravity tectonics, as expressed in the Great Basin geology, is that the western margin has been displacing to the west relative to the eastern margin over the late Cenozoic time span. The eastern margin corresponds to the Wasatch Front in central Utah, whereas the western margin lies along the Sierra Nevada Front.

The resultant stretching is commonly referred to as a generally east-to-west directed extension. This stretching has produced the characteristic topographic pattern consisting of tilted fault blocks separated by deep tectonic depressions. This topography is both a result and a surface expression of the deformation environment, which includes sub-horizontal detachment faults at mid-crust levels and listric normal faults. The latter extend upward from the detachment surfaces to the surface, where the deformation is expressed in the form of tilted tectonic horsts and adjacent tectonic depressions, which are bounded and separated by major normal faults usually at a high-angle.

A flux of distortional strain energy also occurs across vertical boundaries of the geologic system, including the hydrologic sub-system. This spatially and temporally variable flux coherently transports shear strain, which is being transferred from the plate-tectonic juncture by dextral and sinistral shear couples acting along the major synthetic and antithetic wrench faults, respectively. These shear couples are a result of the continental attenuation of the transcurrent plate-tectonic motions. They have the effect of continually displacing the western margin of the Great Basin to the northwest relative to the eastern margin.

The dextral wrench deformation is largely concentrated along a few northwest trending structural belts, such as the Sierra Nevada Front and the Death Valley-Furnace Creek fault zone. One of these structural belts is the Walker Lane wrench system and Yucca Mountain occurs within the southeastern portion of it, as shown in Figure 1-35.

The figure shows that the Walker Lane wrench system is a structural belt of continental dimension. This structure extends from Las Vegas to the northwest, parallel to the Nevada-California border, to Reno, Nevada, and then to the State of California. The deformation occurs in part as a dextral main shear, in part as a dextral bending, and in part as an antithetic wrench faulting along northeast and north-south trending faults.

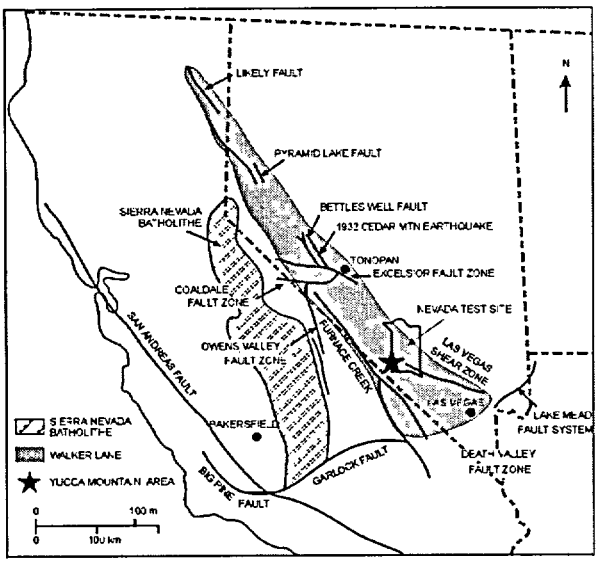

Figure 1-35. Location of Yucca Mountain within the Walker Lane shear belt. Modified from Stewart (1985).

The geologic record contains abundant evidence that the wrench deformations began in the late Oligocene and, further that this deformation has produced a total dextral dislocation in the range of 130-190 km, as given in Stewart (1968). Some of the Walker Lane fault structures are covered by undeformed formations of the late Miocene and Pliocene ages, whereas other fault structures displace the youngest late Quaternary deposits, indicating that the wrench deformation is still very active.

At and near Yucca Mountain, the volcanic and structural effects of the rising and melting body in the sub-lithospheric mantle overprint and effectively mask the Walker Lane wrench system. This does not mean, however, that the wrench deformation has ceased in this region. Rather, this deformation occurs concurrently with the gravity tectonics, producing an effect where the overall deformation involves rotations about vertical axes and a broad doming and tilting in addition to the listric and wrench faulting.

In this regard, paleo-magnetic studies of the late Miocene ash-flow tuffs by Scott and Rosenbaum (1986) revealed that these tuffs have been rotated up to 30^0 clockwise. These tuffs occur at and near Yucca Mountain and cover an area of about 25 km long and 6-7 km-wide. Thus, by any standard of geologic judgment, a very significant and rapid dextral shear distortion is evident.

Deformation involving broad doming is expressed in the form of a tilting of the western portions of the area of Yucca Mountain to the south and to the southwest, as noted in Carr (1984). This tilting has resulted in the ash-flow tuff units, which were erupted over the late Miocene, pinching out more rapidly to the southwest, as shown in Figures 1-3 and 1-4 in Chapter 1-2. This indicates that these units have been deposited on a topographic surface that sloped to the north and to the northwest. By contrast, the present topographic surface slopes generally to the south from a regional topographic high in central Nevada.

Carr (1984) has estimated that, over the past 3 Ma, the tilting has produced a shear strain of a magnitude ranging between 3.0 and 7.0 mkm^{-1}. The apparent tendency of the modern centers of playa deposition to keep shifting to the southwest provides evidence for the present-day continuation of this tilting and broad doming.

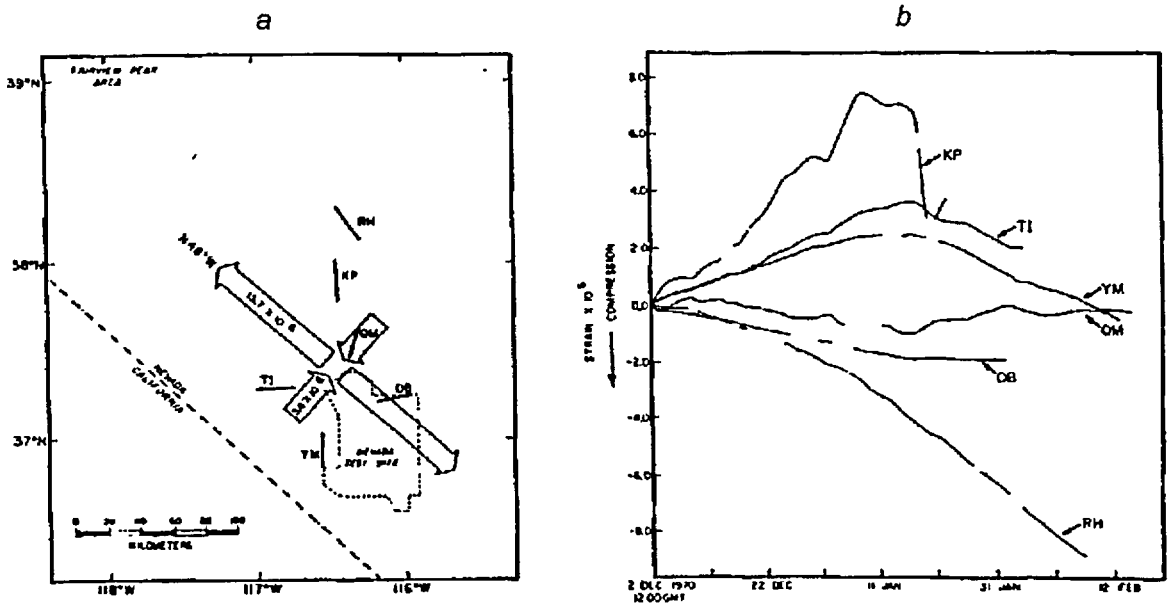

Figure 1-36. Strain changes in the vicinity of the Nevada Test Site during a two-month period. From Smith and Kind (1972).

a – Location of the strainmeter array. *b* – Strain record for December 1970-February 1971 period.

In 1970, tri-lateral geodetic survey networks were established in two areas of the Nevada Test Site, one in Yucca Flat and the other at Pahute Mesa. Repeated theodolite measurements were conducted by the USGS in 1972, 1973, and in 1983, and the results are given in SAIC (1985). The observations over a block 40 km long and 20 km wide, located in Yucca Flat, were statistically fitted by a uniform strain field. The results show that the strain rate is $-0.1 \cdot 10^{-6}$ per year (shortening) in a north south direction, and $+0.08 \cdot 10^{-6}$ (extension) per year in an east west direction.

Smith and Kind (1972) obtained a very important record of observations that reveals the state of the *in situ* strain (stress) field in the area around Yucca Mountain. This record is based on an array of as many as six strainmeters, which were deployed and operated at and near the Nevada Test Site. The locations of these instruments and some of the results are shown on Figure 1-36.

The record shows that synchronous perturbations in the strain field were observed at multiple sites on December 9, January 2, and January 18 of the observation period. The time variability and rapidity of the strain rates throughout the observation period is clearly remarkable. A peak regional change in the strain, calculated with the combined data from all instruments, was as much as 10^{-5} over only a two-month period. The surprised authors concluded: "*In the two-month interval analyzed, we detected a pulsating strain field that increased over a period of six weeks and decayed over a shorter interval of time. The*

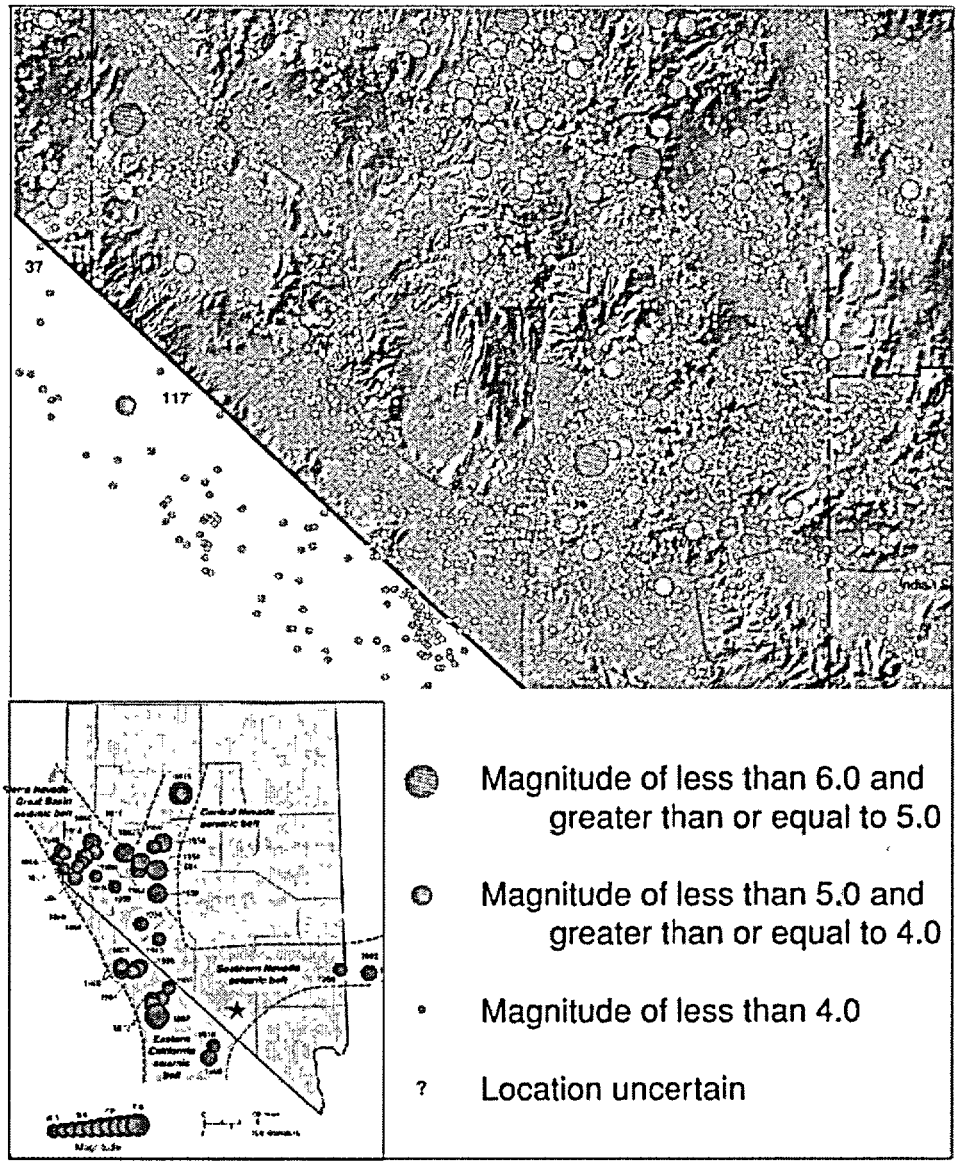

Figure 1-37. Fragment of map Earthquakes in Nevada 1852-1998 (DePolo and DePolo, 1999). Inset shows major earthquakes and seismic belts. Star shows approximate location of Yucca Mountain.

principal axes show northwest extension, and their directions remain fixed as the magnitude of the field varies." (emphasis added).

Thus, both the strain magnitude and the time history indicate that the *in situ* strain field is in a non-equilibrium state and that the evolution of this state involves strain fluctuations rather than monotonic accumulation. It is evident, therefore, that work is performed and entropy produced continually, although at fluctuating rates that vary in time and space.

Seismicity of the area that surrounds the hydrologic sub-system at Yucca Mountain is shown in Figure 1-37. The figure, reproduced from the map prepared by (DePolo and DePolo, 1999) shows that seismic activity in this area defines a pattern consisting of a widespread but diffuse background, generally corresponding to the east-west seismic belt of Greensfelder et al. (1980) or, Southern Nevada seismic belt. This diffuse background is punctuated by clusters of intense activity separated by larger nearly a seismic areas. The events are usually of a low magnitude, $1 < M_L < 3$, with focal depths ranging between less than 1.0 and about 17 km, as given in Rogers et al. (1987). The depth distribution has two broad peaks at between 0 and 2 km and between 5 and 8 km, as well as a distinct minimum at an average depth of about 3.5 km. However, the depth profiles show that, in the most active seismic pockets, the corresponding earthquake foci extend uninterruptedly from the ground surface all the way down to a depth of 10 km, or more.

Focal mechanism solutions, which were derived from radiation patterns generated by 29 events under the assumption of double-couple focal mechanisms, indicate that strike-slip faulting is the dominant mode of elastic stress release. The *B*-axis from most of the solutions, which represents a pole to the plane that contains the slip vector, plunges steeply. Only 6 or 7 solutions yield a *B*-axis whose plunge is less than 45°, which is typical of events having a normal-fault focal mechanism.

In summary, the preceding brief review indicates that Yucca Mountain is situated in an area that is experiencing a very active tectonic deformation. A large body of evidence reveals a complex displacement field in which the surface displacement strain rates far exceed those that could be accommodated by steady-state viscous or visco-elastic flows. Instead, it appears that the area contains a dense network of so-called "dissipative fault structures", which localize the strain accumulation, concentrate it and then suddenly and irreversibly release the accumulated strain.

1.4.3. Dissipative Fault Structures

We use the term dissipative fault structure to denote an active fault, including subsidiary faults that are structurally associated with it, which is evolving to a self-organized critical state of Bak et al., 1988. Such a structure therefore represents macroscopic order the establishment of which is a result of coherent energy flux through a non-equilibrium open system. This should not be confused with a relict or fossil dissipative structure, which is represented by an inactive fault whose role is limited to that of a structural boundary, a conductivity channel, or a host for an ore body.

The presence of discontinuous but coalescing over time "strain pockets" is the principal characteristic of dissipative fault structures. Within these pockets shear stress acting along the discontinuities, such as bedding planes and pre-existing fractures, exceeds the shear strength and/or the

tensile stress exceeds the tensile strength. One of such pockets is an ellipsoidal volume of fractured rock, clustered around the fault, which contains in its center hypocenter of a future large earthquake.

The establishment and growth of dissipative fault structures is a result of a strong flux of distortional strain energy and potential gravitational energy, with the latter facilitating the occurrence and accumulation of tensile or dilatory failures. The growth involves volumetric enlargement of the "strain pockets", increasing density of these pockets and of the unstable discontinuities that are contained within them, and the increasing displacement (both shear and dilatory) along these discontinuities.

Thus, the growing dissipative fault structure steadily accumulates distortional strain energy and/or potential gravitational energy. This structure is therefore a site of continuous performance of work, in the form of creep and brittle failures such as formation and dilation of micro cracks, dilation of pre-existing discontinuities, and shear displacement along them, some of which is reversible. In addition, the structure is a site of progressing accumulation of heat and potentially volatile phases (gas and aqueous solutions) inside the accumulating dilatory failures.

As the growth continues, eventually the combination of size of the "strain pockets", their density, and the overall displacement within them attains a fault specific limit, at which time the structure attains a self-organized critical state. This means that the growing structure became hypersensitive to small perturbations and responds unpredictably to these perturbations. Eventually, the response involves the rates of work performed and entropy produced that increase exponentially thus resulting in an "avalanche" of energy release, which manifests as the occurrence of the so-called characteristic earthquake.

What distinguishes a characteristic earthquake from the ones leading to it is that, this earthquake causes the overall energy content (i.e., the overall level of mechanical disequilibrium) to decrease, whereas the latter are causing this content to increase. The long-term accumulation of work performed and accumulated, in the form of structural and geologic framework, is principally a result of repeated occurrences of the characteristic earthquakes and various irreversible processes that accompany them, with the contribution of the leading ones being relatively minor.

Each of dissipative fault structures occupies its own semi autonomous deformational domain, which together with the bordering domains, is a part (small) of the overall deformational region (e.g., Great Basin). Each of these domains is a result of the breakage of an older and much larger deformational domain into two or more semi autonomously evolving ones, a process that is somewhat analogous to the development of a mature and large drainage system. The present-day structural and geologic framework, or the accumulated irreversible work performed, consists of two components. The first is the framework inherited from the precursor deformational domain. The second component is the work performed as a

result of the autonomous evolution, mainly in association with the repeated occurrences of the characteristic earthquake.

A number of factors distinguish an autonomously evolving deformational domain from the others. Among such factors is the size and return period for the characteristic earthquake, its focal and nucleation mechanisms, the hypocentral parameters such as depth and stress drop, the auxiliary or secondary effects, etc.

Over its entire semi autonomous life span, a deformational domain evolves via a series of evolutionary loops, or deformational cycles, which in terms of the duration and the auxiliary effects are specific to this particular domain. The occurrence of characteristic earthquake marks the end of the preceding deformational cycle and, at the same time, the onset of a succeeding one. Thus, over duration of a single deformational cycle, distortional strain energy and/or gravitational potential energy accumulates inside the dissipative structure, it concentrates within the growing and coalescing "strain pockets" (hypocentral region in particular), and then it is suddenly and irreversibly converted into work and heat.

1.4.4. Tectonic Setting and Structure of Yucca Mountain

Yucca Mountain is located near the center of a 35 km wide down-faulted block of the basement. The east-northeast trending and westward dipping Rock Valley bounds this block to the east. The north-south trending and eastward dipping Bare Mountain fault bounds it to the west. The block includes the central tectonic horst of Yucca Mountain as well as the adjacent tectonic depressions, Crater Flat to the west and Jackass Flats to the east. This general surface geology is illustrated in Figure 1-38.

Brocher et al. (1998) have determined the shallow subsurface structure for this area, based on regional gravity and seismic reflection data. This structure is shown in Figure 1-39.

The figure shows two northeast-to-southwest cross-sections, between Jackass Flats and Bare Mountain. Section 1-39-*a* shows the interpretation based on seismic reflection profiling, whereas section 1-39-*b* shows the rock density model constructed based on gravity data. Both of the sections show very significant down-faulting of the basement with the dislocation increasing to the southwest from about 1 km, in the western Jackass Flats, to 3.0 or 3.5 km in the eastern Crater Flat. Beneath Crater Flat, the down-faulted block is segmented by many eastward dipping normal faults. However, beneath Yucca Mountain and Jackass Flats, the segmentation is via a series of westward dipping normal faults.

The Tiva Canyon Member of the Paintbrush Tuff is a cap-rock of the horst, which is situated at the top of Yucca Mountain. This 13 Ma old ash-flow tuff is tilted to the east, so that it occurs at an altitude that decreases to the east, from 1500 to 1200 m above mean sea level (asl), over a lateral distance of only about 5 km. In addition, it is displaced across the horst-bounding faults, the Windy Wash-Solitario

Figure 1-38. Satellite image showing topography and general geology of the area of Yucca Mountain. Approximate projections of the underground excavations ESF and ECRB, as well as planed radioactive waste repository footprint are shown in white. Dashed blue line – boundary of the Nevada Test Site.

Canyon fault zone to the west and the Paintbrush-Stagecoach Road fault zone to the east, as shown in Figure 1-38.

Well J-13 revealed that the Tiva Canyon Member occurs, beneath western Jackass Flats, at an altitude of about 0.8 km above msl. Thus, the dip-slip component of the overall displacement, across the eastern horst-bounding fault zone, is at least 0.5 km. However, beneath central Crater Flat, this member was found, in drill hole USW VH-2, at an altitude of 0.36 km asl. The dip-slip component of displacement, across the western horst-bounding fault zone, is therefore as large as 1.25 km or more.

Both of these displacements are very large indeed, which suggests that the horst-bounding faults are discrete structures descending to the ductile crust, where detachment faults are present. They also indicate that about 50 percent of the basement down-faulting occurred over the past 13 Ma. The implied slip rates are very significant, rivaling those that are associated with the most active faults of the Great Basin.

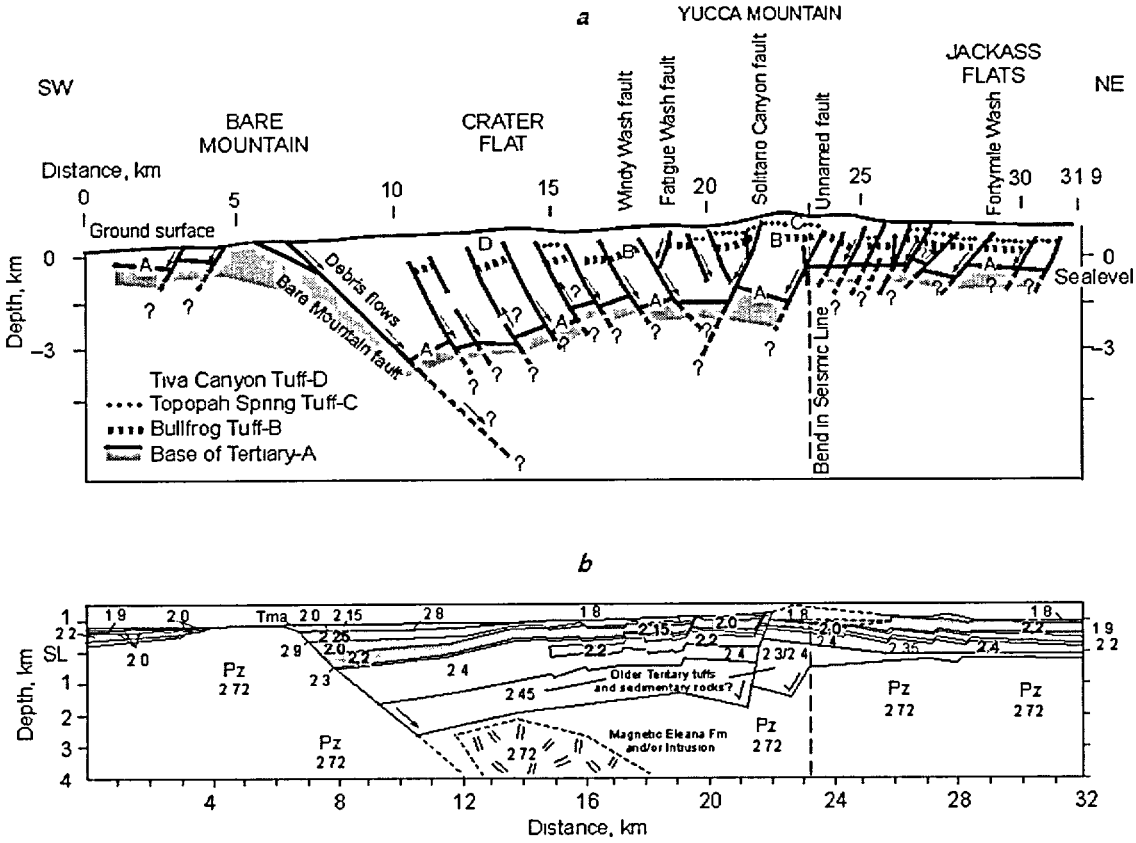

Figure 1-39. Sructural geology at and in the vicinity of Yucca Mountain. Conceptual structural cross-section from Bare Mountain to Jackass Flats. From Brocher et al. (1998).

a – Interpretation based on seismic reflection. *b* – Rock density model (values in $g \cdot cm^{-3}$; Pz – Paleozoic carbonates). Note important down-faulting of the basement and continuation of this process after the emplacement of the Paintbrush Tuff.

It is important to recognize that, over most of its short (about 13 Ma) life span, the Yucca Mountain horst did not behave as a rigid body. Instead, this horst was undergoing internal deformation. The resulting work performed, which has been accumulating over the past 13 Ma, is expressed in the form of a maze of variably-oriented wrench and normal faults, as shown in Figure 1-40.

The figure shows that, between the horst-bounding faults, i.e. Solitario Canyon fault zone in the west and Paintbrush Canyon fault zone in the east, Yucca Mountain contains many auxiliary faults with smaller dip-slip and strike-slip displacement. The overall structural pattern seems to be expressing the temporally increasing segmentation of the horst into smaller and smaller north-to-south trending structural domains. It seems that this segmentation has been contemporaneous with the wrench deformation, which most likely is related to the Walker Lane tectonics. This deformation is evident in the western part of the horst, where it is developed in the form of a few northwest trending faults with dextral slip, as shown in Figure 1-40.

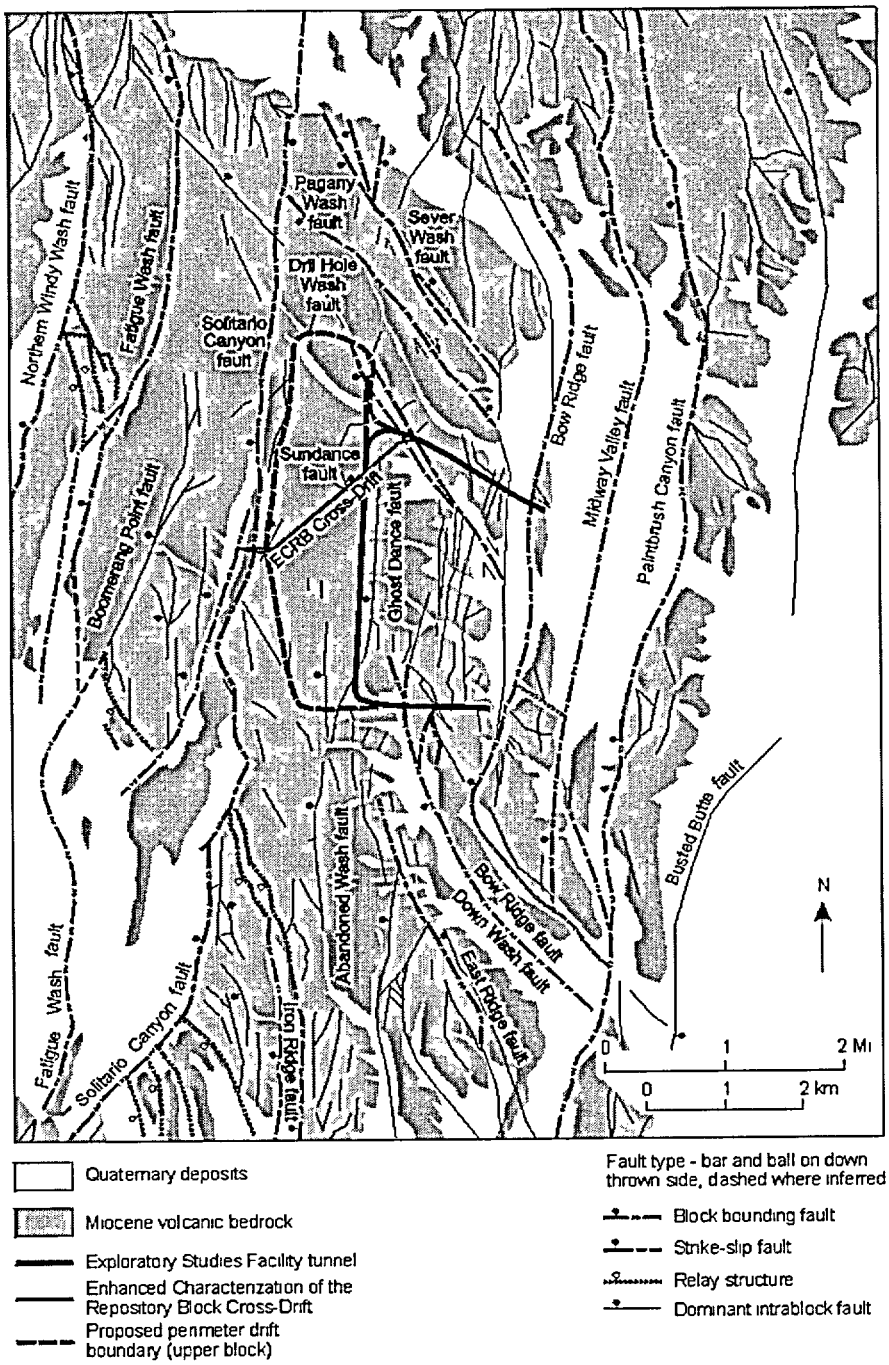

Figure 1-40. Structural geology map of Yucca Mountain. Note high density of variously trending fault structures. From Day et al. (1998).

The down-faulting of the basement and the internal deformation of the horst of Yucca Mountain are both contemporaneous with the volcanic activity in the southern Nevada volcanic field (see Chapter 1-2).

It is certain, therefore, that the deformation is a result, in part, of the gravitational instability of the upper mantle in this area.

Thus, in addition to providing a high flux of heat, this instability is also introducing distortional strain energy and potential gravitational energy, which results in the ongoing gravity deformation of this mountain. This aspect of the overall deformation scheme is very important because it implies that it is inappropriate to regard the deformational boundaries as fixed boundaries. Such would have the effect of eliminating the transient accumulations of heat and potentially volatile phases from the play.

The active deformation is particularly well displayed along the structural boundary between Yucca Mountain and Crater Flat. Detailed structural studies of this boundary revealed that the paleo-seismic events were typically associated with concurrent ruptures of multiple faults and with eruptions of basaltic ash. The evidence cited by Ramelli et al. (1991) includes "*...the high degree of fault interconnection, similarities in scarp morphology, similarities in ages and amounts of recent offset along multiple faults, and presence of basaltic ash within vertical fractures formed in fault-filling carbonate exposed in trenches across four faults.*"

Of the several active faults, which form the western structural boundary, the Windy Wash fault has the most detailed displacement chronology. The apparent dip-slip displacement of a 3.7 Ma old basalt flow is about 40 m (Ramelli et al., 1991). Four episodes of displacement over the past 0.27 Ma have also been documented. The youngest displaced stratum is eolian silt, which has been dated by thermo-luminescence as 3.0-6.5 Ka old (Whitney et al., 1986). Repeated ruptures of Quaternary age have also been documented along Solitario Canyon, Fatigue Wash, and Black Cone faults (Ramelli et al., 1991).

The distributed faulting along the Yucca Mountain-Crater Flat structural boundary has important implications in regard to inferring the size of past and future characteristic earthquakes. In this regard, DePalo et al. (1991) documented the configuration of surface ruptures caused by eleven historical earthquakes in the Basin and Range province. Without exception, the events had a Richter magnitude of 6.8 or larger, and the ground ruptures were very similar to those present at Yucca Mountain. This similarity suggests that earthquakes in the same magnitude range may have accompanied ground ruptures along the horst-bounding fault zones.

At present, a consensus has emerged as to the maximum magnitude of an earthquake, which can reasonably be expected to occur at and near Yucca Mountain. This magnitude is between 7.0 and 7.5, and its annual probability is about 10^{-4}, i.e. once every ten thousand years.

However, it would be a serious error in judgment to consider only those effects of a seismogenic fault rupture, which are a result of the vibratory ground motion, whilst assessing the long-term

performance of the proposed facility. What must also be considered is the influence that the rupture would exert on the short- and long-term behavior of the hydrologic sub-system. In view of the highly active geothermal and geodynamic setting of Yucca Mountain, this influence is a topic that demands serious attention.

As discussed earlier (Chapter 1-3), one of the most notable features of Yucca Mountain is the fact that both of the horst-bounding fault zones are associated with prominent geothermal anomalies. These anomalies are centered along these fault zones and are associated with substantially elevated temperatures, as shown in Figure 1-28 in Chapter 1-3.

As noted earlier, a number of independent lines of evidence confirm the presence of such thermal anomalies and allow for attributing them to upwelling of hot fluids from the Paleozoic carbonates into the overlying tuffs. In addition, Sass et al. (1983) and Szymanski (1989) have independently inferred that the upwelling expresses disequilibrium of the thermally stratified aquifer fluids, which occupy conductivity channels surrounding the horst-bounding fault zones.

It thus appears that, from a thermodynamics perspective, the horst-bounding fault zones act as concurrent strain energy and heat dissipative structures. This seemingly inescapable conclusion provides us with a radically new perspective from which to consider the suitability of Yucca Mountain for the construction of a nuclear waste repository. In particular, this conclusion implies that, in terms of non-linear dynamics, the mid-upper crust at Yucca Mountain acts as a non-equilibrium dissipative dynamical system evolving to a self-organized critical state.

The fluxes of strain energy and heat are both sufficiently strong for the crustal medium to self-organize into a macroscopically ordered state, which is characterized by the presence of concurrent strain energy and heat dissipative structures. In the case of the aquifer fluids, this self-organization takes the form of Rayleigh-Bénard instabilities. In the case of the faulted rocks, however, it takes the form of dissipative fault structures, which drift toward criticality and are the sites of future characteristic earthquakes, as Bak and Tang (1989) have suggested.

The geologic record at Yucca Mountain leaves us with little doubt that, over time spans measured in terms of 10^4 years, the rheological state of the mid-upper crust is characterized by the episodic presence of "strain pockets" in mechanical disequilibrium. This means that, in localized regions, the shear stress exceeds the shear strength and/or the tensile stress exceeds the tensile strength. The record further tells us that the flux of distortional strain energy and potential gravitational energy is sufficiently strong to repeatedly give rise to the occurrence of far-from-equilibrium states. Specifically, the flux is sufficiently strong to repeatedly cause the spatial enlargement of the "strain pockets", the enhancement of the "strain

pocket" density and intensity of the disequilibrium therein and, eventually, the occurrence of the characteristic earthquake.

On the other hand, the present-day thermal state of the crust at Yucca Mountain, as inferred based on geophysics, tells us that the conductive flux of heat is sufficiently strong to introduce a state of thermal disequilibrium into aquifer fluids. This means that locally the forces and boundary conditions that foster the buoyant instability exceed, by a certain margin, the forces and boundary conditions that hinder this instability. In other words, the Rayleigh number (R_a) exceeds or equals the critical Rayleigh number (R_c), so that $R_a > R_c$ or $R_a = R_c$.

Both of these disequilibria, from a hydrologic perspective, bear on the opening question, which is the one regarding the origin of calcite-silica deposits at Yucca Mountain. Our considerations of a heterogeneously evolving non-equilibrium state of the *in situ* stress field, in a deforming and dilating fractured medium, are designed to provide input to answering this question. A most important consideration in this regard is the influence that changes in the *in situ* stress field, produced by the characteristic earthquake, would exert on the present-day state of the hydrologic sub-system.

Chapter 1.5. Hydro-Tectonic Implications of the In Situ Stress Field

1.5.1. Introduction

Although there are substantial gaps in the database, we do know enough about the state of *in situ* stress field at Yucca Mountain, upon which a conceptual understanding of the potential hydro-tectonic implications can be based. In particular, we know that this field is in a state of heterogeneously evolving non-equilibrium, and that the evolution pertains to a system having movable boundaries. We also know that this state is a result of work performed in the form of partly recoverable strain over the current deformational cycle and, to a lesser extent, over the preceding cycles.

Thus, this field contains distortional strain energy and potential gravitational energy, which represent the potential for performing work and producing entropy in the form of future hydro-tectonic processes and events. As far as the proposed repository is concerned, these processes and events would constitute a hazard that cannot be mitigated and reduced to acceptable levels by engineered fixes.

The global observations of diastrophic processes involved in the evolution of the brittle crust imply that the influence, which tectonics exerts on long-term behavior of hydrologic sub-systems, ranges between two extreme possibilities. This influence is very small in stable intra-plate regions, such as cratonic shields and continental platforms, but very significant in volcanically and tectonically active regions, such as plate-tectonic junctures and continental rift systems.

1.5.2. Hydro-Tectonics in Stable Regions - an Expectation

In non-volcanic and non-geothermal regions, where the thickness of the lithosphere (i.e., the depth to the Low Velocity Zone) is appreciable and the rates of tectonic deformation are moderate to low, large earthquakes would nucleate with the involvement of double-couple focal mechanisms. Gravity tectonics would be inactive, or it would operate at sufficiently low rates, so that the involvement of dilatory straining, in the form of non-double couple (NDC) failures, would be minimal, if any. This means that the deformational system has fixed boundaries, and that the *in situ* stress field evolves (toward the self-organized critical states of Bak et al., 1988) with the spatially and temporally ubiquitous absence of "singular" and "negative isotropic points".

Under these conditions, the work performed, in the form of groundwater flow, would be a result of potential gravitational energy, which only indirectly relates to the outward flux of endogenic energy. This relationship would be through the topography, which is a factor that alone controls the spatial distribution of potentiometric heads that drive the groundwater flow. Apart from that, endogenic energy would not be involved, so that neither the accumulated heat nor the accumulated and accumulating distortional strain

energy and potential gravitational energy would play a role in inducing or otherwise influencing the groundwater flow.

Over the long-term, occasional tectonic events, of course, would locally induce the performance of work and the production of entropy in the form of a non-steady groundwater flow. However, the rates would always diminish rapidly, so that the exponential amplification of small perturbations and the resulting exponential increases of these rates would always be absent.

The deformation would amount to a build up of deviatoric stresses within the future hypocentral regions, which would amount to a steady increase of the accumulated distortional strain energy. Over time the accumulation would take the form of an increasing density of pockets, within which the *in situ* stress field is in a state of "limit equilibrium". In addition, this accumulation over time would also take the form of an increasing value of the mean stress around the "positive isotropic points". However, the density of the latter points would be decreasing, as the time of an earthquake approached. The accumulating strain energy would be converted into work (some of it recoverable), by gradually enlarging the strain pockets, including the future hypocentral region, and increasing the density of these pockets and the overall magnitude of the deviatoric stress.

Because the opening of fractures and cracks would be absent, the accumulation of heat and potentially volatile matter (fluids and gases) inside the strain pockets and future hypocentral region would also be absent. At a time when the deviatoric stresses reach levels approaching the shear strength in a sufficiently large volume of rock, a sudden slip would occur along a planar fault surface. Of course, before this slip could materialize the density of "positive isotropic points" would have to be reduced appropriately.

The slip would manifest itself as the characteristic earthquake, marking the end of a preceding deformational cycle and the onset of a succeeding one. During the slip, the accumulated strain energy would be converted into elastic waves and into work performed and entropy produced in the form of short-lived structural adjustments (such as aftershocks, minor uplift or subsidence, fluctuations of piezometric and potentiometric heads, and fault creep) and heat. The propagating elastic waves would define a radiation pattern, which, if it were interpreted in the form of a fault plane solution, would indicate a double couple focal mechanism.

It thus appears that a large double couple earthquake would influence the hydrologic system in the manner, which is short-lived and with a magnitude, which ranges from small to practically inconsequential. After the earthquake occurrence, both the intensity of heat flow and the heat transport mechanism would remain as they were before the occurrence. The rates of work performed and entropy produced and lost as the result of various irreversible diastrophic processes would substantially increase

over the period immediately before and after the occurrence of the characteristic earthquake. However, the rates of work performed and entropy produced in the form of a non-equilibrium groundwater flow would remain essentially zero so that the hydrologic effects would be limited to three phenomena.

First, the vibratory ground motion would induce some fluctuations of the potentiometric and piezometric heads. These fluctuations, however, would be short-lived in accordance with the duration of the vibratory motion and relatively small in amplitude.

Second, a fault rupture and the resulting vibratory ground motion could jointly induce some permanent alteration of the hydraulic conductivity structure. This alteration would be in the form of auxiliary fracturing and fissuring of surface rocks, displacements of the aquifers relative to the aquitards, and "weakening" or "strengthening" of the permeability barriers. The hydrologic response would involve some alteration of the flow rates and paths but the overall properties of the hydrologic system would not change dramatically.

Third, a fault rupture and the vibratory ground motion could jointly induce some permanent alterations of the potentiometric and piezometric heads in addition to those resulting from the minor alterations of the hydraulic conductivity structure. These alterations would largely be the result of a minor uplift of aquifer recharge areas relative to the discharge areas, or vice versa, and the result of compaction of weakly consolidated aquifers. They would be measured in terms of meters, which is not enough to substantially disrupt the hydrologic regime.

The above picture is what the Yucca Mountain Project hydrologists have considered in their evaluations of the suitability of Yucca Mountain. However, these hydrologists do not seem to recognize that this picture is generally applicable only to tectonically stable regions such as cratonic shields and continental platforms. By any stretch of the imagination, the Yucca Mountain site is not a part of such a setting. On the contrary, the region of Yucca Mountain has obviously experienced intense tectonic activity, including volcanism, in the recent geologic past, which has continued into the present-day, and which will continue long into the foreseeable future.

1.5.3. Hydro-Tectonics in Active Regions - an Expectation

By way of contrast, in volcanically and tectonically active regions the thickness of the lithosphere is decreasing over geologic time and the rates of tectonic deformation range between moderate to very high depending upon the lithospheric thickness. In these regions, the nucleation of characteristic earthquakes could occur with the involvement of non-double couple (NDC) focal mechanisms, particularly in those regions where the lithospheric thinning and corrosion is at very advanced stages. Here, gravity tectonics

are active, and operate at sufficiently high rates, so that the deformational system has movable boundaries and the involvement of dilatory straining is at a maximum.

The evolution of the *in situ* stress fields, toward the eventual self-organized critical state, would therefore be accompanied, partly, by the spatially and temporally increasing presence of "singular" and "negative isotropic points". Under these conditions, the work performed and entropy produced, in the form of groundwater flow, would be the combined result of topography-related potential energy and endogenic energy, which flows at elevated rates in these cases. The latter would play a major role in controlling the spatio-temporal distribution of potentiometric and piezometric heads, which drive the groundwater flow. Both the *in situ* temperature field and the *in situ* stress field would be evolving over the duration of the deformational cycles, so that their potentials and gradients would be changing over the long term. These evolving fields would significantly influence the groundwater flow, particularly by controlling the timing and mode of non-steady state discharges of the accumulated energy and matter.

The deformation would involve the build up of deviatoric stresses within the growing and coalescing pockets, including future hypocentral regions, and a steady increase of the accumulated distortional strain energy and potential gravitational energy. However, the accumulation would now take the form of increasing (over time) density of "singular" and "negative isotropic points", in addition to the increasing density of "limit equilibrium points". The accumulation would also take the form of the increasing (over time) value of the mean stress around the "positive isotropic points", although the density of these points would be decreasing as the time the characteristic earthquake approaches. The strain energy would be stored in the form of partly recoverable work (strain), and its accumulation would have the effect of increasing the density of "singular" and "negative isotropic points" and the overall magnitude of deviatoric stress.

The increasing density of "singular" and "negative isotropic points" would have the effect of opening fractures and cracks, increasing density of these openings, and enlarging their apertures. Thus, the deformation would have the effect of facilitating the progressive accumulation of heat and potentially volatile matter inside these openings. At a time when a combination of the deviatoric stress and the density of "singular" and "negative isotropic points" had reached a certain level in a sufficient volume of the strained rock, the collapse of the dilated hypocentral region would suddenly occur. This collapse would again manifest itself as a characteristic earthquake, marking the end of the preceding deformational cycle and the onset of a succeeding one.

The collapse would take the form of a combination of slip along a planar fault surface and a uniform outward motion in a plane of this fault. The accumulated distortional strain energy and potential gravitational energy would be converted into work performed and entropy produced in the form of seismic

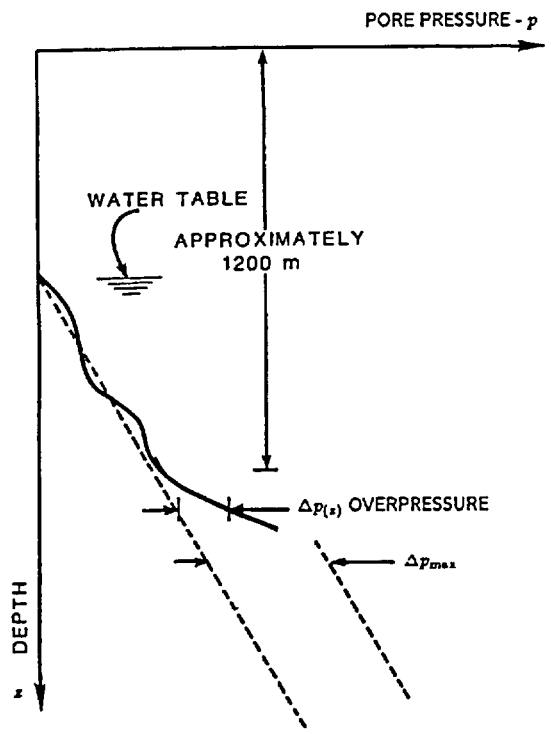

Figure 1-41. Idealized changes of pore pressure with depth at Yucca Mountain. Based on data from Robinson (1984).

Data for boreholes: UE-25p#1 $\Delta p_{(z)}$ = 20 m, Z = 1300 m; USW H-1 $\Delta p_{(z)}$ = 53 m, Z = 1123-1733 m; and USW H-3 $\Delta p_{(z)}$ = 22 m, Z = 1200 m.

waves, auxiliary structural adjustments, non-equilibrium fluid flow, and heat. Furthermore, the accumulated fluids would be ejected from the collapsed region, in the form of a plume. The propagating waves would define a pattern, which if it were interpreted in the form of a fault plane solution would indicate a non-double couple mechanism with a compensated linear vector dipole (CLVD) character.

The preceding general remarks imply that there are major differences in the conceptual expectations regarding hydro-tectonic phenomena, which are appropriate for the respective diastrophic environments. In addition, these remarks allow for identifying what connects the tectonics and the long-term behavior of the corresponding hydrologic systems. Clearly, the connection involves the *in situ* stress and temperature fields, which operate in a deformational system having movable boundaries.

It thus appears that the evolving *in situ* stress and temperature fields, which have been previously inferred to operate at Yucca Mountain, have major hydro-tectonic implications. In particular, the presence of these fields implies operability of as many as three inter-related hydro-tectonic phenomena. These are long-term and short-term instabilities of the potentiometric surface, seismic pumping phenomena, and Rayleigh-Bénard instabilities of fluids residing in the horst-bounding Paintbrush and Solitario Canyon fault zones.

In the remainder of this chapter, we will focus our attention on the above three hydro-tectonic phenomena. The reader may find it helpful to consult Part Two of this report, or Murphy (1979), regarding the balance of forces and boundary conditions that foster and hinder buoyant instability of thermally stratified fluids in faults and fractures.

1.5.4. Long-Term and Short-Term Stability of the Potentiometric Surface at Yucca Mountain

One of the most intriguing characteristics of the field of hydraulic potentials, which operates at Yucca Mountain, is the presence of a depth stratification of piezometric head. The piezometric head, at a

depth of about 1.2-km and below, exceed the potentiometric heads, so that hydraulic "over-pressure" conditions exist at depth as shown in Figure 1-41.

Figure 1-41 shows that the minimum value of the "over-pressure" (Δp_z), at Yucca Mountain, ranges between 20 and 22 m, in wells UE-25 p#1 and USW H-3, and it is 55 m in well USW H-1, as given in Robison (1984). However, the actual maximum value is unknown.

Although it is certain that the "over-pressure" conditions manifest the presence of a very substantial decrease of the hydraulic conductivity with increasing depth, important questions, nevertheless, remain. What is the cause of the conductivity gradient, and in particular, is it permanent or is it related to the state of *in situ* stress and, thus, reversible?

It is important to recognize that the "over-pressure" conditions are developed only in select parts of the overall hydrologic sub-system. One of such parts is located to the north of Yucca Mountain, in the area of western Pahute Mesa, as described in Blankenegel and Weir (1973). The other is situated in the central (wells UE-25 p#1 and USW H-3) and the north-central (well USW H-1) sectors of Yucca Mountain, where the potentiometric head is at a constant elevation of about 730 m asl.

The *in situ* stress data, specifically the depth distribution of σ_c and/or σ_3, are not available for the area of Pahute Mesa. Thus, it is not possible to know whether these "over-pressure" conditions are developed in an area where the closure pressure (σ_c) is substantially less than the Poisson's effect adjusted overburden load, so that $\sigma_c < \mu\rho h$.

The situation is quite different at Yucca Mountain, where we know that the "over-pressure" conditions correspond to an area where $\sigma_c < \mu\rho h$. In addition, the Yucca Mountain "over-pressure" conditions are developed in an area to the south and east of the steep potentiometric gradient (see Figure 1-53), where the potentiometric surface is conspicuously flat. Thus, this "over-pressure" zone corresponds to an area where the hydraulic conductivity is very high and a result of the *in situ* stress enhancement. The closure pressure (σ_c) in this area is substantially less than the Poisson's effect adjusted overburden load, so that $\sigma_c << \mu\rho h$.

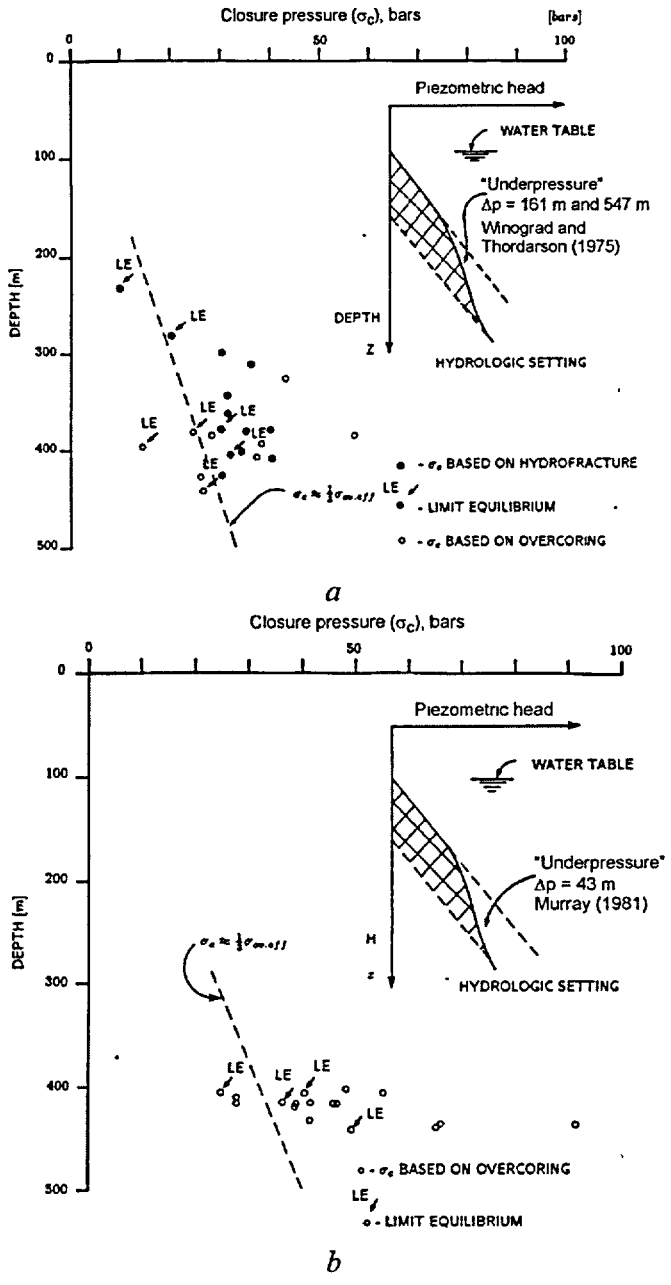

Figure 1-42. State of *in situ* stress – summary. *a* – Rainier Mesa and Aqueduct Mesa, Nevada Test Site; *b* – Climax Stock, Nevada Test Site. Based on the data of Ellis and Magner (1980 and 1982).

However, in those parts of the overall hydrologic sub-system where the Poisson's effect adjusted overburden load exceeds the closure pressure (σ_c), so that $\sigma_c > \mu ph$, the opposite relationship between the potentiometric and piezometric heads is sometimes observed. Two examples of such relationship are known from the Nevada Test Site, one from the Climax Stock and the other from the Rainier-Aqueduct Mesa. A schematic representation of the piezometric head *vs.* depth relationship and the actual $\sigma_c = \sigma_3$ *vs.* μph relationship for both of these areas is shown in Figure 1-42.

Figure 1-42 shows that, if $\sigma_c > \mu ph$, the "over-pressure" is absent and a very large "under- pressure" is developed instead. In other words, the piezometric head, at some depth below the water table, is lower than the corresponding potentiometric head. The difference may be as large as 161 and 547 m, as shown in the figure.

Based on the above correlations and the preceding theoretical considerations, a reasonable hypothesis may be constructed, namely that in those areas where the "under-pressure" conditions are developed deformational cycles are at early stages. Consequently, "singular" and "negative isotropic points" are absent below the potentiometric surface, so that the fractures have a residual aperture. The effect of this is that the hydraulic conductivity is a result of interstitial permeability only, which is very low and, hence,

restricts the downward flow preventing bodies of semi-perched water to drain from the tuffs into the underlying and highly conductive older rocks.

By contrast, in areas where the "over-pressure" conditions are developed, Yucca Mountain in particular, the deformational cycle is advanced, and "singular" and "negative isotropic points" are present hundreds of meters below the potentiometric surface. However, the underlying tuffs do not contain them and, therefore, these tuffs are associated with very low hydraulic conductivity, which reflects a residual aperture of fractures and interstitial permeability of these zeolitic tuffs. They restrict the upward flow, thus allowing the vertical piezometric gradient to persist, which manifests the observed "overpressure" conditions.

It thus appears that, at least the Yucca Mountain "overpressure" conditions are artifacts of the enhanced hydraulic conductivity of the shallow tuffs, which expresses a heterogeneously evolving non-equilibrium state of the *in situ* stress field. This implies that the water table was higher and the slope of the potentiometric surface steeper at early stages of the current deformational cycle, when "singular" and "negative isotropic points" were absent. However, when the density of these points became sufficient, the "overpressure" conditions began developing close to the Earth's surface. The increasing density and depth extent of these points, both of which keep pace with the advancing cycle, have the effect of allowing the "over-pressure" to be preserved but only at greater depths, which keeps increasing with time.

In addition, the enhancing *in situ* stress gradients and the resulting hydraulic conductivity gradients have the effect of causing the potentiometric surface to eventually become unstable, which manifests short-lived and local fluctuations of the potentiometric head. This is because the uppermost tuffs, which occur between the ground surface and the increasing distances below the potentiometric surface, contain "singular" and "negative isotropic" points. Around these points, the hydraulic properties, specifically conductivity and storativity, and the fluid pressure are coupled through the principle of effective normal stress. This means that very small increases of fluid pressure, or very small decreases of the normal stress, have the effect of enlarging the apertures of some fractures, thus causing these properties to increase.

Responding either to the fluid influx (from the "over-pressure" zone) or to very small local changes of the σ_1-σ_3 difference, which are induced by external perturbations and control the value of the normal stress, the potentiometric head incessantly attempts to rise by forming a hydraulic mound. The ensuing mound, however, has the effect of locally increasing the fluid pressure, which furthers the opening of fractures, thus causing their conductivity and storativity to increase. The increased values of these properties have the effect of continuously restraining the formation of a hydraulic mound, which manifests itself as short-lived fluctuations of the potentiometric head.

Initially, the advancing straining and the resulting increasing density and depth of "singular" and "negative isotropic points" could be accommodated by a steady decline of the potentiometric gradient. Eventually, the potentiometric surface becomes virtually flat but only in those areas, which are affected by the straining. Thereafter, further increases in the density and depth of "singular" and "negative isotropic points" would have to be accommodated by steadily increasing the amount of fluid contained (stored) in the phreatic zone.

Thus, one way for an advanced deformational cycle to manifest itself is through a characteristic configuration of the potentiometric surface, which is flat in an area where $\sigma_c < \mu\rho h$ and $\sigma_c \rightarrow 0$ but very steep outside this area. Such joint configurations are observed at Yucca Mountain, as shown in Figure 1-43.

Figure 1-43 shows that the water table at Yucca Mountain consists of two parts, which are associated with sharply different values of the piezometric gradients and heads. The gradient is very steep and the piezometric head high to the north, where $\sigma_c > \mu\rho h$ and "singular points" are absent. Whereas to the south, where $\sigma_c < \mu\rho h$ and "singular points" are present, the gradient is practically zero and the piezometric head is up to 400 m lower. This configuration, as well as the far-from-equilibrium state of the *in situ* stress field which is responsible for it, cannot possibly be stable in the long-term. Both are subject to change at a time when the current deformational cycle ends and the characteristic earthquake occurs.

1.5.5. Seismic Pumping as a Dissipative Process

A conceptual model for the nucleation of an NDC characteristic earthquake is based on a presumption that this event is preceded by a nucleation period. Over the nucleation period, the strain energy concentrates and its amount increases steadily within the future hypocentral region and other *in situ* stress pockets. The non-linear processes, which the accumulating strain energy activates within the hypocentral region or nucleation zone, would occur in three stages. First, in some parts of this zone episodes of accelerating creep would set-in, eventually leading to the development of "singular" and "negative isotropic points" along grain and crystal boundaries. Second, responding to the steadily increasing straining, these isotropic points would coalesce, leading to a steady increase of the dilatancy through the opening of increasingly larger cracks and micro-fractures. Third, the increasing straining would lead to a steady growth in the size (volume) of the rock mass affected by this dilatancy.

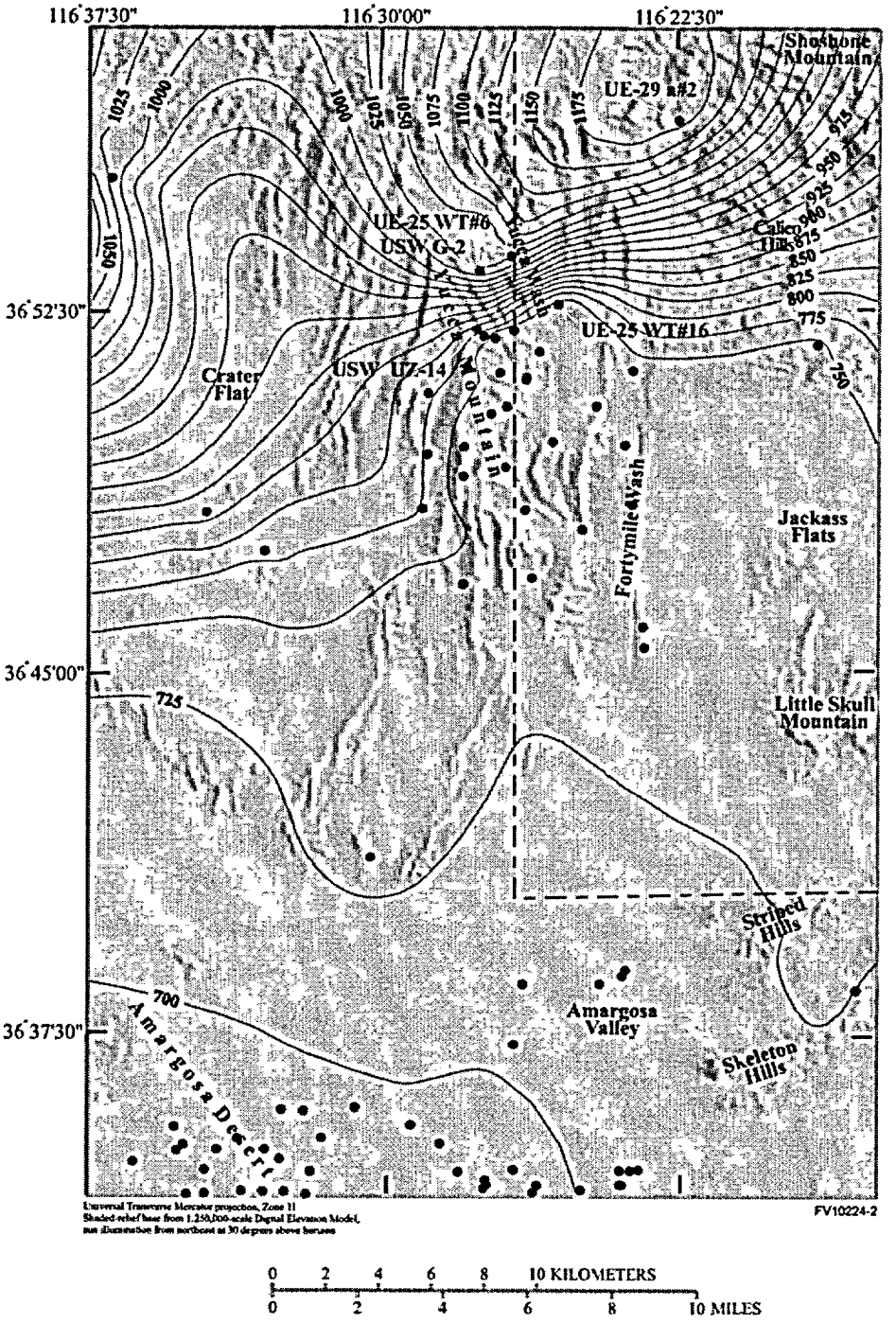

Figure 1-43. Potentiometric surface (water table elevation) in the Yucca Mountain region. From U.S. DOE (1998).

Thus, the nucleation of a non-double couple (NDC) earthquake would have the effect of steadily increasing the hydraulic conductivity and storativity of the rock mass, which comprises the growing hypocentral region. This increase, therefore, would present an opportunity for fluids, which reside in the surrounding rock to infiltrate into this region and for some fraction of them to become trapped inside. Enlargement of the dilating region would have the effect of increasing (over time) the volume of the entrapped fluids. Furthermore, the entrapment would expose the accumulating fluids to an influx of heat and potentially volatile matter, such as carbonic fluids and gases flowing from the Earth's interior into the atmosphere. The accumulating fluids would heat up and dissolve some fraction of the in-flowing matter. Thus, the hypocentral region of a non-double couple earthquake would store, in this manner, heat and potentially volatile matter, in addition to storing large quantities of distortional strain energy and potential gravitational energy.

At a time when the inevitable characteristic earthquake occurs, the strain levels in the hypocentral region would rapidly diminish. Many of the openings would close, so that the previously enhanced conductivity and storativity would diminish rapidly. The resulting sudden increase in pressure, acting on the entrapped fluids and gases, would produce fluid flow through the fracture network, and the gas-charged hot fluids would rush upward to the surface in the form of a plume.

Both the temperature and the pressure of the plume-forming fluid would keep dropping over the duration of the ascent. If the ascent velocity were sufficiently large then, near the ground surface, the temperature would exceed the boiling point of water. If the plume was sufficiently voluminous and the temperature remained sufficiently high, the vaporescence would be rapid enough to cause the steam pressure to exceed the lithostatic pressure, which would produce a hydrothermal explosion.

Similar effects could result from the effervescence of CO_2 dissolved in an ascending plume. In this regard, calculations by Malinin (1979) have demonstrated that, as a CO_2-charged hot water (200-300°C) ascends, the solubility of carbon dioxide decreases in a non-linear manner. Because the solubility of calcite ($CaCO_3$) in a thermal and CO_2-saturated aqueous fluid is controlled by the content of CO_2 dissolved in the fluid, the $CaCO_3$ solubility may be regarded as a proxy for the latter. The solubility of $CaCO_3$ in a CO_2 dominated hydrothermal system is shown in Figure 1-44 as a function of depth (pressure) and temperature change.

Figure 1-44 shows that the $CaCO_3$ solubility attains a maximum at a pressure equivalent to a depth ranging between 1-2 km to as little as about 250 meters or less. With further ascension, the solubility reverses, and thereafter it keeps dropping at a very rapid rate, so that the plume releases the dissolved CO_2 at an accelerating rate. The pressure, or depth, at which the solubility reversal takes place, varies as a function of the initial temperature, the degree of cooling, and the ionic strength of the solution, as shown

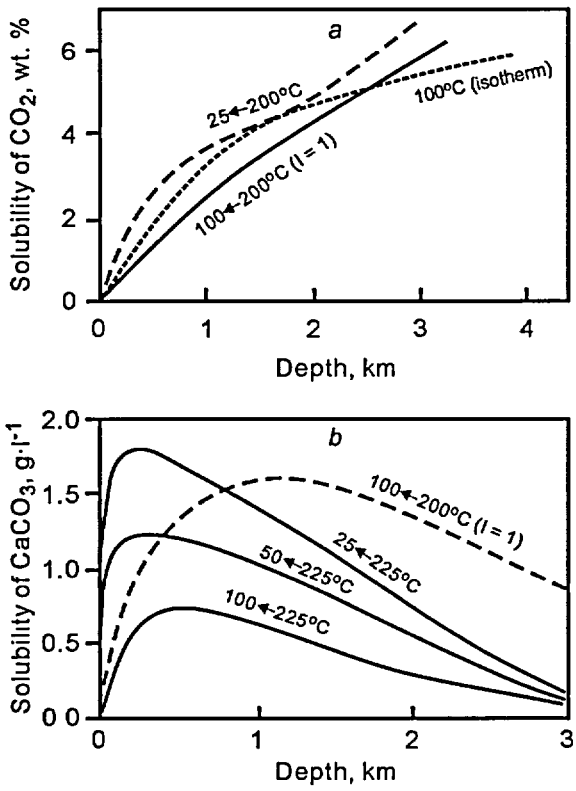

Figure 1-44. *a* - Solubility of CO_2 in upwelling water (hydrostatic pressure, different temperature regimes) and *b* – solubility of $CaCO_3$ in a CO_2-dominated upwelling water. *I* denotes ionic strength. From Malinin (1979).

in Figure 1-44. In the case of a slowly cooling plume, for which the temperature has dropped from an initial 200°C to 100°C, the solubility reversal occurs at a depth of about 1200 meters. However, for a rapidly cooling plume, from 225 to 25 °C, this depth is less than 250 meters and the effervescence rate could be very high.

At a time when the CO_2 effervescence sets-in, the generation of CO_2 bubbles begins, which has the effect of reducing the density of the fluid that overlies the ascending and gas-charged plume. This reduction in density augments the pressure drop, which independently accompanies the ascent, and thus has the effect of generating yet more of the bubbles. Henceforth, the CO_2 effervescence proceeds with positive feedback or as a run-away process. The rates of work performed and entropy produced both increase in an exponential manner and the effervescence takes the form of a gaseous explosion. At or near the ground surface, such an explosion would have the effect of causing explosive fragmentation of the bedrock and very rapid precipitation of SiO_2 and $CaCO_3$ in the form of micritic siliceous and calcareous sinters and veins. It is in such a manner that calcite-silica deposits would be formed, at least in part, at the topographic surface and within the vadose zone.

The fact that the nucleation of some earthquakes, those in volcanic and geothermal regions in particular, sometime involves the opening of cracks and fractures at a substantial depth in the crust is perhaps best demonstrated by the fact that these events are sometimes accompanied by seismic pumping phenomenon. This phenomenon involves a massive outflow of fluids from the crust, which follows the seismogenic rupture of a fault. Numerous examples of such events have been observed and documented, for example by Berberian and Tchalenko, 1976; Sibson et al., 1975; Muir-Wood and King, 1993; and Hickman et al., 1994. Several examples are given below.

The Salmas earthquake of 1930 in northwest Azerbaijan, Iran had a Richter magnitude of about 7.0. This event was followed by renewed activity of warm and mineral springs, some of which were extinct at

the time but showed evidence for the prior activity (Berberian and Tchalenko, 1976). Particularly important is the fact that the earthquake produced an alignment of springs parallel to the ruptured fault, including the Zelele Bolaghi (literally, the Earthquake Spring), some of which deposited sinters for many decades.

The Kern County, California, earthquake of 1952 had a Richter magnitude of about 7.7, and this event was followed by numerous discharges of warm water directly from a granite batholith (Sibson et al., 1975). In this case, the ejection of warm water constitutes direct evidence for the flow from a considerable depth, which implies the opening and then closing of deep fractures.

The Hebgen Lake, Montana, earthquake of August 17, 1957 had a Richter magnitude of about 7.0, and this event produced spectacular outflows of groundwater and pressure increases in the adjacent aquifers. Muir-Wood and King (1993) estimated that the total outflow was measured in the order of $5 \cdot 10^8$ m^3.

Similarly, the Borax Peak, Idaho, earthquake of November 1983 with a Richter magnitude of 7.3 was followed by increased rates of discharge from many springs in an area immediately adjacent to the epicenter. In addition, violent fluid discharges occurred near the epicenter (Wood, 1991). Muir-Wood and King (1993) inferred that the total area affected by this event produced a fluid outflow with a volume of about 10^8 m^3, over a period of about 6 months.

The Matsushiro earthquake swarm in Japan, as described in Sibson et al. (1975), was energetically equivalent to a single event with a Richter magnitude of about 6.3. This earthquake swarm produced a total fluid outflow of about $5 \cdot 10^6$ m^3. Sibson et al. (1975) have estimated that the average dilatory strain ($\Delta V/V$) was about 10^{-5}, and that the affected rock had a volume (V) of about 10^{11}-10^{12} m^3.

It thus appears that the hydro-tectonic effects of a large NDC earthquake at Yucca Mountain could vastly exceed those, which would be produced by a double couple event with comparable magnitude. This is because the former could be accompanied by seismic pumping phenomenon and the resulting eruption of a hydrothermal or gaseous plume. Such an eruption could produce a wide range of deleterious effects in shallow parts of the hydrologic sub-system.

First, the plume would introduce large amounts of heat and potentially volatile matter directly into the vadose zone and at the ground surface. Second, the resulting pressurization of shallow faults and fractures would have the effect of inducing auxiliary shear and tensile failures along these faults and fractures. Third, the induced failures would have the effect of drastically reducing the density of "singular" and "negative isotropic points", or eliminating them all together. That would allow for the renewed presence of steep potentiometric gradients in the wall rock of the ruptured faults. Finally, the

ascending plume could undergo run-away effervescence or vaporescence, which would lead to further pressurization of the shallow rocks possibly causing explosive fragmentation of these rocks.

1.5.6. Rayleigh-Bénard Instabilities as a Heat Dissipative Process

The established facts support the past and present existence, at Yucca Mountain, of the *in situ* stress field, which is in a heterogeneously evolving non-equilibrium state. This conclusion is not open to serious challenge, in our opinion. In addition, it is certain that the strain accumulation has been occurring over the entire life span of the mountain, and further that this accumulation has led to repeated occurrences of fault ruptures and large earthquakes.

In addition, it is highly probable that the horst-bounding Paintbrush and Solitario Canyon fault zones contain Rayleigh-Bénard instabilities (see Chapter 1-3), which presently operate at a low level of thermal disequilibrium. Thus, considering these points, a need arises to explore means by which a seismogenic fault rupture could alter the disequilibrium state of the co-existing Rayleigh-Bénard instability and, to this end, the following pages are devoted.

In this regard, a specific question of major conceptual importance is: By what mechanisms and by which processes could a surface rupture along the horst-bounding fault zones affect the stability of the coexisting Rayleigh-Bénard instabilities? Central to answering this question, the issue is whether there is a potential for a significant lowering of the difference between the critical Rayleigh number (R_c) and the actual Rayleigh number (R_a) by the rupture.

The critical Rayleigh number (R_c) expresses boundary conditions for a potential Rayleigh-Bénard instability. These conditions pertain mainly to heat losses from this instability into its wall rock as represented by the so-called heat transfer grouping and pertain also to the geometry of the available conductivity channel as represented by the height to width ratio (h/w) of the channel. The Rayleigh number (R_a) expresses a balance between forces that foster and hinder the instability, mainly the geothermal gradient and the permeability of the conductivity channel.

Figure 1-45 shows that R_c attains a minimum value, which is equal $4\pi^2$, for the adiabatic boundary conditions (i.e., the heat transfer grouping equals unity) and for the slenderness ratio of about unity, so that $h/w \rightarrow 1$. The increasing heat transfer from the fluid into the wall rock and the greater or smaller than unity value of the slenderness ratio have the effect of increasing R_c, which stabilizes a thermally stratified fluid.

The R_c - R_a difference expresses stability of a thermally stratified fluid. The R_c - $R_a = 0$ relationship has the effect of allowing for exponential amplification of small perturbations, which involve fluid density, velocity, pressure, and temperature. The ensuing amplifications are means by which a dormant and/or dampened Rayleigh-Bénard instability tends to reduce the thermal energy that fuels the instability.

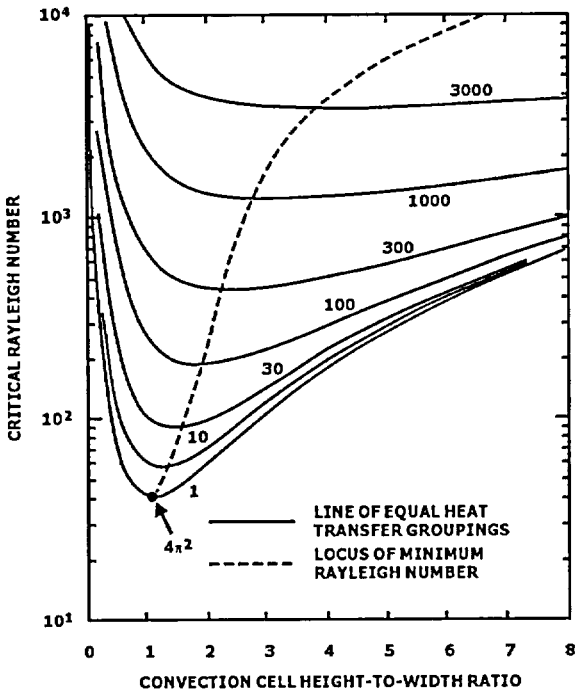

Figure 1-45. Critical Rayleigh number (R_c) for vertical fault and fractures as a function of the aspect ratio (h/w) and heat transfer grouping ($2\lambda_f h^2\phi/\lambda_m a$). See Murphy (1979) for details.

Heat losses from the incubating instability into the wall rock prevent the incubation of a steady state (mature) Rayleigh-Bénard instability, one for which the growth rate is zero.

As discussed earlier in Chapter 1-3, there are strong grounds to believe that, at Yucca Mountain, each of the horst-bounding faults contains dampened or dormant Rayleigh-Bénard instabilities. It thus becomes particularly appropriate to consider the influence that a heterogeneously evolving non-equilibrium state of the *in situ* stress field exerts on the stability of thermally stratified aquifer fluids, which occupy both of the horst-bounding faults.

Before the characteristic earthquake, but at a time when the deformational cycle is advanced, the wall rock hosts the *in situ* stress field, within which the density of "singular" and "negative isotropic points" is high and increasing over time. The evidence indicates, we believe, that such is presently is the case at Yucca Mountain. These conditions have the effect of causing heat transfer, from the incubating (amplifying) instability into the wall rock, to be very efficient. This means that the critical Rayleigh number is relatively large, so that $R_c >> 4\pi^2$. In addition, the fault-based conductivity channel is relatively slender (with a relatively high h/w ratio), which has the effect of further increasing R_c, on one hand, and decreasing the amplification factor, on the other. The relationship between the amplification factor, the aspect ratio (h/w), and the Rayleigh number (R_a) is shown in Figure 1-46.

Figure 1-46 shows that the amplification factor, which expresses the potential size of the mature Rayleigh-Bénard instability, is strongly dependent upon the balance of forces, expressed by the Rayleigh number (R_a) that fosters and hinders the instability. In addition, this factor is dependent upon the slenderness ratio (h/w). The amplification factor attains a maximum for $h/w \rightarrow 1$ and becomes increasingly greater as R_a increases.

However, before the characteristic earthquake, the conductivity channel is undilated and contains various minerals and sediments deposited after the preceding deformational cycle, so that the hydraulic conductivity is relatively low. This low conductivity has the effect of further lowering R_a and thus

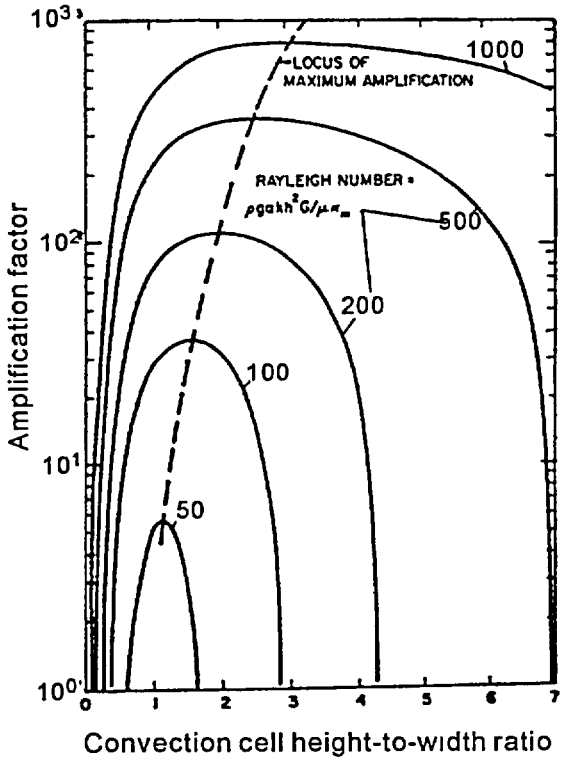

Figure 1-46. Dependence of the amplification factor ($\omega h^2/k_m+2\lambda$, $h^2\phi/\lambda_m a^2$) upon the *in situ* Rayleigh number and the aspect ratio. From Murphy (1979).

lowering both the amplification factor and the growth rate. The dependence between the growth rate and the Rayleigh number (R_a) is shown in Figure 1-47.

Figure 1-47 shows that the growth rate, which expresses the potential velocity of attaining a mature size, is strongly dependent on R_a. This rate increases with the increasing R_a, so that rapid growth requires large values of R_a.

The above relationships have the effect that, at a time when the tectonic cycle is at advanced stages, the R_c - $R_a \rightarrow 0$ difference cannot decrease appreciably, so that both the amplification factor and the growth rate remain low. Under these conditions, the amplification of small perturbations involves low-level dynamics, which means that the time and space integrals of the work performed and entropy produced have relatively low values. It is in this way that the *in situ* stress field keeps the incubating Rayleigh-Bénard instabilities at bay.

However, the restraint comes at the price of not releasing thermal energy, which fuels the instability, and thus, of not relaxing the potential for performing work and producing entropy at an exponentially increasing rate. This potential therefore remains unabated, and could be readily mobilized in response to appropriate modifications of the *in situ* stress field.

After the characteristic earthquake, but at a time when the deformational cycle is at an early stage, the wall rock hosts the *in situ* stress field, within which the density of "singular" and "negative isotropic points" is greatly reduced. Under these conditions, the incubation of a mature Rayleigh-Bénard instability takes a drastically different path.

The absence of "singular" and "negative isotropic" points has the effect of restricting the diffusion of fluids, from the incubating instability into the wall rock, and through that of reducing the heat losses. The reduced heat losses, in turn, have the effect of allowing the critical Rayleigh number (R_c) to attain some smaller values. In addition, seismic pumping has the effect of increasing the width (w) of the

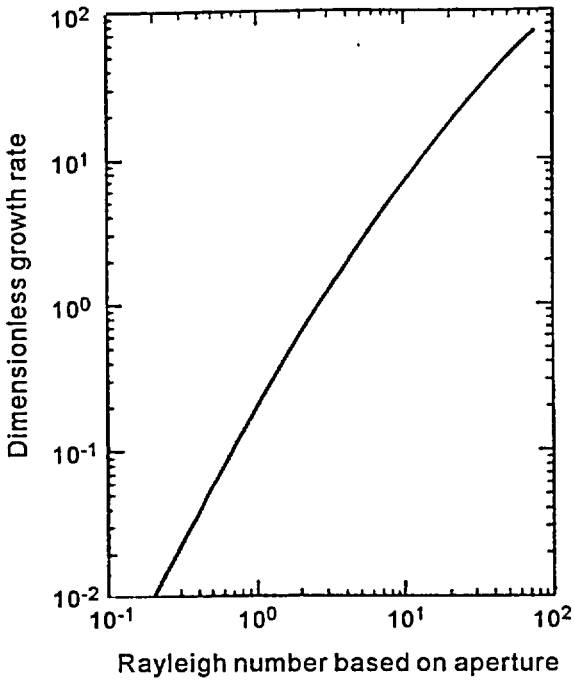

Figure 1-47. Dependence of the perturbation growth rate ($\omega h^2/k_m$) upon the *in situ* Rayleigh number. From Murphy (1979).

conductivity channel to some extent through the fracturing and fragmentation of the bedrock, so that the slenderness ratio (h/w) attains a smaller but still greater than unity value. The increased slenderness has the effect of not only further reducing the critical Rayleigh number (R_c) but also of increasing the amplification factor.

The seismic pumping causes dilation, fracturing, and fragmentation of the conductivity channel, which has the effect of increasing R_a by increasing the hydraulic conductivity. Therefore, the Rayleigh number (R_a), the amplification factor, and the growth rate all increase, as implied by the relationships shown in Figures 1-46 and 1-47.

The most important effect of the seismic pumping induced restructuring of the factors controlling R_a and R_c is that, when a deformational cycle sets-in, the R_c-R_a difference could attain a strongly negative value. In addition, potential values of both the amplification factor and the growth rate are high, provided the Rayleigh number (R_a) is sufficiently high. Under these conditions, the amplification of small perturbations potentially involves high-level dynamics. This means that the time and space integrals of the work performed and entropy produced, in the form of the flow of the buoyantly unstable fluid, may attain very high values.

The flow of the buoyantly unstable fluid materializes some time after the fault rupture and after cessation of the seismic pumping induced flow. This flow occurs when fluids, which before were mobilized by the seismic pumping, cool sufficiently to restore an adequate geothermal gradient (dT/dz), on one hand, and the ensuing amplifications produce a sufficient thickness of thermal skin in the wall rock, on the other.

The performance of work and production of entropy at exponentially increasing rates, in the form of the flow of the buoyantly unstable fluid, has the effect of locally raising the potentiometric head and thus forming a hydraulic mound. This mound is mainly the result of thermal expansion of the buoyantly unstable fluid. For example, if the resulting temperature differential of say $\Delta T = 100°C$ were maintained over a depth of 5 km then, the geothermal component of the total increase of the piezometric head would

be as large as about 350 meters. This temperature differential would require a near-surface temperature of about 50°C and a geothermal gradient of about 20°C·km^{-1}. The rise having a minimum magnitude of about 350 m would be sufficient to inundate a vadose zone, even one of a few hundred meters thick such as that at Yucca Mountain, and to discharge at the topographic surface.

The main point to be emphasized in summing up this chapter is that the through-flow of heat and strain energy in the crust, which deforms with the involvement of NDC failure mechanisms, is not a steady state process. Rather, this through-flow process fluctuates, attaining a maximum at the end of deformational cycles, and a minimum over advanced stages of these cycles. The effect of the co-existence of the heat dissipative structures and dissipative fault structures, which deform with the involvement of the NDC failure mechanisms, is that neither separate dissipative processes nor separate phases operate in isolation from each other. Instead, they interact with each other forming a complexly coupled and evolving non-equilibrium dynamical system.

References

Suitability of the Yucca Mountain Site to Accommodate a permanent Repository for High-Level Radioactive Waste and Spent Nuclear Fuel: an Independent Assessment

By
J.S. Szymanski,
Y.V. Dublyansky,
T.R. Harper,
S.Z. Smirnov,
S.E. Pashenko,
and
G.P. Palianova

References

A

Aliev (1966) — Aliev R. 1966 Ontogenetic studies of calcite crystals from Dashkesan iron-ore deposit. In: D.P. Grigoriev, ed., *Origin of mineral individuals and aggregates.* Moscow, Nauka pp. 181-200.

Allmendinger et al (1987) — Allmendinger, R. W., Hauge, T. A., Hauser, E.C., Potter, S. L., Klemperer, K. D., Nelson, K D , Kneupfer, P, and Oliver, J. 1987 Overview of the COCORP 40 °N Transect, Western United States: The Fabric of an Orogenic Belt. *Geological Society of America Bulletin*, **98**.

Amundson et al. (1988) — Amundson, R. G., Chadwick, O. A., Sowers, J. M , and Doner, H. E. 1988 Relationship between Climate and Vegetation and the Stable Carbon Isotope Chemistry of Soils in the Eastern Mojave Desert, Nevada. *Quaternary Research,* **29**, pp. 245-254.

Archambeau and Price (1991) — Archambeau C B. and Price, N.J. 1991 An assessment of J.S Szymanski's Conceptual Hydro-Tectonic Model and Its Relevance to Hydrologic and Geologic Processes at the Proposed Yucca Mountain Nuclear Waste Repository. *Minority Report of the Special DOE Review Panel.* pp. 98-112.

Atkinson (1977) — Atkinson, T.C. 1977 Carbon dioxide in the atmosphere of the unsaturated zone: an important control of ground water hardness in limestones. *J. Hydrol.*, 35, pp. 111-123.

Atkinson et al. (1983) — Atkinson, T.C., Smart, P.L., and Wigley, T.M.L. 1983 Climate and natural radon levels in Castleguard Cave, Columbia Icefields, Alberta, Canada *Arctic and Alpine Research*, **15**, 4, pp. 487-502.

B

Bak (1996) — Bak, P. 1996 How nature works. New York: Copernicus 212 p.

Bak and Tang (1989) — Bak, P. and Tang, C. 1989 Earthquakes as a Self-Organized Critical Phenomenon *Journal of Geophysical Research*, **94** , B11, pp. 15635-15637.

Barnes et al. (1996) — Barnes, C.M., James, J.M. and Whittlestone, S. 1996 Radon and its decay products in caves *Helictite,* 34(2). pp. 33-37.

Barsukov and Borisov (1989) — Barsukov, V.L. and Borisov, M.V. 1989 Inversion of solution acidity during the self-rebuilding of hydrothermal flow structure. *In*: V.A. Zharikov, *Ed* Physico-chemical analysis of mineral-forming processes Moscow, Nauka, pp. 168-175. (*In Russian*)

Bender (1981) — Bender, M.M. 1971 Variations in the $^{13}C/^{12}C$ ratios of plants in relation to the pathway of photosynthetic carbon dioxide fixation *Phytochemistry* **10**, pp. 1239-1244.

Benning et al , 2000 — Benning L G., Wilkin R.T., and Barnes H.L. 2000 Solubility and Stability of Zeolites in Aqueous Solutions: II. Calcic Clinoptilolite and Mordenite, *American Mineralogist*. **85**. pp. 495-508.

Benson and McKinley (1985) — Benson, L. V. and McKinley, P. W. 1985 Chemical composition of ground water in the Yucca Mountain area, Nevada, 1971-84. *USGS, Open-file report, 85-484*

Bergna (1994) — Bergna, E. 1994 The colloid chemistry of silica - an overview. *In*: The colloid chemistry of silica *Ed* E. Bergna. Washington, D.C., American Chemical Society, pp 4-47.

Bish (1989) — Bish, D.L. 1989 Evaluation of past and future alterations in tuff at Yucca Mountain, Nevada based on clay mineralogy of drill cores USW G1, G2, and G3. *Los Alamos Natl. Lab Report LA-10667-MS*. 41 p

Bish and Aronson (1993) — Bish, D.L. and Aronson, J.L 1993 Paleogeothermal and Paleohydrologic Conditions in Silicic Tuff from Yucca Mountain Nevada *Clays and Clay Minerals*. **41**, 2, pp 148-161.

Bish and Chipera (1989) — Bish, D.L. and Chipera, S.J. 1989 Revised Mineralogical summary on Yucca Mountain, Nevada. *Los Alamos Natl Lab Report 11497-MS.*

Bish and Vaniman (1984) — Bish, D.L. and Vaniman, D T. 1985 Mineralogic Summary of Yucca Mountain, Nevada. *Los Alamos Natl Lab. Rept. LA-10543-MS* 55 p.

Blakely (1988) — Blakely, R. J. 1988 Curie Temperature Isotherm Analysis and Tectonic Implications of Aeromagnetic Data from Nevada. *Journal of Geophysical Research*, **93**

Blankenegel and Weir (1973) — Blankenegel, R K and Weir, J.E. 1973 Geohydrology of the Eastern Part of Pahute Mesa, Nevada Test Site, Nye County, Nevada. *USGS Professional Paper 712-B*, Washington, DC.

Blyth et al. (1998) — Blyth, A R , Frape, S.K., Blomqvist, R., and Nissinen, P. 1998 Combining fluid inclusion studies with isotopic investigations of fracture calcite to assess the past thermal and fluid history of the Olkiluoto research site, Finland. *GSA Abstracts with*

Program. Toronto, Canada. A-88.

Bodvarsson et al (1997) — Bodvarsson, G S., Bandurraga, T. M., and Wu, Y.S. 1997 The Site-Scale Unsaturated Zone Model of Yucca Mountain, Nevada, for the Viability Assessment. *LBNL-40376 #UC-814*, Berkeley, California: Lawrence Berkeley National Laboratory, MOL 19971014 0232.

Boles (1972) — Boles, J. R. 1972. Composition, optical properties, cell dimensions and termal stability of some heulandite group zeolites *Am. Miner.* **57**, pp. 1463-1493.

Bottrell (1991) — Bottrell, S. 1991 Radon production and release from cave sediments. *Cave Science* (UK) **18**, 2, pp. 79-82.

Bottynga (1969) — Bottynga, Y. 1969 Calculated fractionation factors for carbon and hydrogen isotope exchange in the system calcite-carbon dioxide-graphite-methane-hydrogen-water vapor. *Geochim et Cosmochim Acta*, **33**, pp. 49-64.

Boughton (1986) — Boughton, C. 1986 Integrated Geochemical and Hydraulic Analysis of the Nevada Test Site Groundwater Systems. *M. S Thesis, University of Nevada-Reno, Reno*, Nevada.

Bredehoeft (1997) — Bredehoeft, J.D. 1997 Fault permeability near Yucca Mountain. *Water Resources Research.* **33**, 11. pp 2459-2463.

Brock ... (2000) — Brock Biology of Microorganisms. Ninth Edition Eds : M Mdigan, J Martineo, and J. Parker. Prentice Hall. Upper Saddle River, NJ, 2000.

Broxton et al (1987) — Broxton, D.E., Bish, D.L , and Warren, R G. 1987 Distribution and chemistry of diagenetic minerals at Yucca Mountain, Nye County, Nevada. *Clay and Clay Minerals*, **35**, 2, pp. 89-110.

Bryxina and Sheplev (1997) — Bryxina N. A and Sheplev V. S. 1997 Oscillatory zoning in calcite growing from an aqueous solution. *Mathematical Modeling*, **9**, pp 32–38. (*In Russian*)

Bryxina et al. (2000) — Bryxina N.A., Dublyansky Y.V., Halden N.M., Campbell D.L and Tysdale V.D 2000 Statistic characteristics of rhytmic zonation of cave calcite - Hungarian popcorn. *Doklady RAS*, **372**, pp. 514-517. (*In Russian*)

Bukata et al. (1998) — Bukata, A.R , Kotzer, T., and Cornett, R.J. 1998 Fracture-infilling calcite as a proxy for the paleohydrogeology of a fractured granitic gneiss, an integration of stable isotopes, fluid inclusions and U-series dating. *GSA Abstracts with Program.* Toronto, Canada A-225.

Burke (2001) — Burke E. 2001 Raman microspectrometry of fluid inclusions. *Lithos*, **55**, pp. 139-158.

C

Cahn (1967) — Cahn, J.W. (1967) On the morphological stability of growing crystals *In:* Crystal Growth, H. S. Peiser (Ed) Pergamon Press, Oxford

Caporuscio et al. (1982) — Caporuscio, F., Vaniman, D T., Bish, D L., Broxton, D.E., Arney, D. Heiken, G., Byers, F.M., and Gooley, R. 1982 Petrographic studies of drill cores USW-G2 and UE25b-1H, Yucca Mountain, Nevada. *Los Alamos Natl. Lab Report LA-9255-MS.* 114 p

Carbon... (1978) — Carbon and its compounds in endogene processes of mineral formation (Based on the results of fluid inclusion studies in minerals) (G N. Dolenko, G.M. Gigashvili, V.A. Kaliuzhniy, and A S. Schiritsa *Eds*) Kiev, Naukova Dumka PH. 171 p. (*In Russian*)

Carlos (1987) — Carlos, B. A. 1987 Minerals in Fractures of the Saturated Zone from Drill Core USW G-4, Yucca Mountain, Nye County, Nevada. *Los Alamos National Laboratory Report LA-10927* Los Alamos, New Mexico

Carlos et al. (1993) — Carlos, B.A., Chipera, S J., Bish, D.L., and Craven, S J. 1993 Fracture-Lining Manganese Oxide Minerals in Silicic Tuff, Yucca Mountain, Nevada, USA *Chemical Geology.* **107,** 1-2, pp 47-69.

Carlos et al. (1995-a) — Carlos B.A , Chipera S.J., and Bish D.L. 1995-a Distribution and Chemistry of Fracture-Lining Materials at Yucca Mountain, Nevada. *Los Alamos Natl. Lab Report LA-12977-MS,* 92 p.

Carlos et al (1995-b) — Carlos, B , Chipera, S.J., and Snow, M G. 1995-b Multiple episodes of zeolite deposition in fractured silicic tuff. *A.A.Balkema Publishers. 8th International Symposium on Water-Rock Interaction* Vladivostok, Russia, August 13-28, 1995.

Carr and Parish (1984) — Carr, W.J. and Parish, L.D. 1984 Geology of Drill Hole USW VH-2, and Structure of Crater Flat, Southwestern Nevada *USGS Open File Report 85-475,* Denver, CO.

Carr et al. (1986) — Carr, M. D , Waddell, S. J., Vick, G. S., Stock, J. M., Monsen, S. A., Harris, A. G., Cork, B W., and Byers, F.M 1986 A Test Hole into Pre-Tertiary Rocks Near Yucca Mountain, Southern Nevada *USGS Open File Report 86-175,* Menlo Park, CA.

Castor et al. (1989) — Castor, S. B , Feldman, S. C , and Tingley, J V. 1989 Mineral Evaluation of the Yucca Mountain Addition, Nye County, Nevada Nevada Bureau of Mines and Geology - Desert Research Institute, Reno, Nevada.

Castor et al. (1999) — Castor, S B , Garside, L J., Tingley, J.V., LaPointe, D.D , Desilets, M.O., Hsu, L C., Goldstrand, P.M , Lugaski, T.P., and Ross, H.P. 1999 Assessment of metallic and

mined energy resources in the Yucca Mountain Controlled Area, Nye County, Nevada *Nevada Bureau of Mines and Geology Open-file Report 99-12*. 204 p

Cathlineau et al. (1999) Cathlineau, M., Freiberger, R., Boiron, M.-C., Ayt Ougougdal, M., Cuney, M., Coulibaly, Y., Banks, D., Aranyossy, J.F., Virlogeux, D. and Leuth, Y. 1999 Reconstruction of paleofluid percolation in the Vienne granites: Evidence of fluid circulation restricted to major geodynamic events (abs.); in Luders, V.; Schmidt-Mumm, A.; and Thomas, R (eds.) *Abstracts of ECROFI XV Conference*. Potsdam, June 21-24, 1999, pp. 63-65.

Cerling (1984) Cerling, T.E. 1984 The stable isotopic composition of soil carbonate and its relationship to climate. *Earth and Planetary Science Letters* **71**, pp 229-240.

Chafetz and Lawrence (1994) Chafetz, H. and Lawrence, R. 1994 Stable Isotopic Variability within Modern Travertines *Geographie physique et Quaternaire*. **48**, 3, pp. 257-273.

Chatterjee et al (1975) Chatterjee, A., Kerker, M., and Cooke, D.D. 1975 Brownian coagulation of Aerosols in the Transition Regime. *J. Coll. and Inter. Science* **53**, 1, pp. 71-78

Chebotarev (1955) Chebotarev, I I. 1955 Metamorphism of Natural Waters in the Crust of Weathering. *Geochimica at Cosmochimica Acta*, **8**.

Chepizhko and Dublyansky (1995) Chepizhko, A. and Dublyansky , Y. 1995 Accessory minerals from bedrock tuffs, mosaic breccias and calcite/opal veins at Yucca Mountain (Feasibility Study) *Report submitted to the Nuclear waste project office State of Nevada*, 139 p.

Chepizhko et al (1998) Chepizhko, A. Dublyansky, Y., and Lapin, B., 1998 Ontogenetic studies of accessory minerals at Yucca Mountain, Nevada, and the ascending vs. descending water controversy. *GSA Abstracts with Program*, Toronto, Canada.

Cherdintsev (1969) Cherdintsev, V.V. 1969 Uranium-234. Moscow, Atomizdat. (*In Russian*)

Chernov et al (1980) Chernov, A.A , Givargizov, E.I., Bagdasarov, Kh. S , Kuznetsov, V.A , Demyanets, L.N., and Lobachev, A.N. 1980 Modern crystallography. Moscow, Nauka. 407 p.

Chesnokov (1966) Chesnokov, B. V. 1966 Morphological method for determination of relative age of minerals. *In*: The genesis of mineral individuals and aggregates (ontogeny of minerals), *Ed*: D.P. Grigoryev, Moscow, Nauka, pp. 9–24.

Chipera and Bish (1997) Chipera, S J. and Bish, D. L. 1997 Thermodynamic Modeling of Zeolite Stability. 11th International Clay Conference, Ottawa, Ontario, Canada , June 15-21, 1997.

Choquette (1968) Choquette, P.W. 1968 Marine Diagenesis of shallow marine lime-mud sediments· Insights from O^{18} and C^{13} data *Science*, **161**, pp. 1130-1132.

Chrustschoff (1887) — Chrustschoff, K. 1887 Über gelungene Versuche zur Darstellung des Quarzes auf nassem und des Tridymit auf trockenem Wege. *N. Jb Mın* I.

Chukhrov (1955) — Chukhrov, F.V. 1955 Colloids ın the Earth crust. Moscow, Academy of Sciences of the USSR Press. 672 p.

Clouds ... (1989) — Clouds and cloudy atmosphere. Reference book. 1989 I.P. Mazin, A.Kh Khrgian, *Eds* Gıdrometeoızdat, Leningrad. (*In Russian*)

Cohon (1998) — Cohon, J.L. 1998 Letter of the Chairman of the U S. NWTRB J.L. Cohon to Acting Director of the U.S DOE Office of Civilian Radioactive Waste Management Lake Barrett. July 24, 1998, p. 2

Coplen et al. (1994) — Coplen, T. B., Wınograd, I. J., Landwehr, J. M., and Riggs, A. C. 1994 500,000-Year Stable Carbon Isotopic Record from Devils Hole, Nevada. *Science*, **263**. pp 361-365

Craig (1953) — Craig, H. 1953 The Geochemistry of the stable carbon isotopes. *Geochım et Cosmochim. Acta*, **3**. pp. 53-92

Cunnıngham and LaRock (1991) — Cunningham, K.I. and LaRock, E.J 1991 Recognition of microclimate zones through radon mapping, Lechuguilla Cave, Carlsbad Caverns National Park, New Mexico. *Health Physics*, **61**, 4, pp. 493-500.

D

Daniel and Gillespie (1981) — Daniel, T. and Gillespie, A 1981 A stochastic analysis of the homogeneous nucleation of vapor condensation *J Chem Phys*. **74**, 1, pp. 661-678.

Davıes and Archambeau (1997) — Davies, J B ; Archambeau, C. B 1997 Geohydrological models and earthquake effects at Yucca Mountain, Nevada. *Environmental Geology*, 32(1) pp. 23-25.

Davis and De Wiest (1966) — Davis, S.N. and De Wıest, J.M. 1966 Hydrogeology. John Wiley and Sons, Inc. New York-London-Sydney.

Deines (1980) — Deines, P. 1980 The isotopic composition of reduced organic carbon *In*: P. Frıtz and J.Ch. Fontes (Eds) Handbook of Environmental Isotope Geochemistry, 1. The Terrestrial Environment, A. Elsevier, Amsterdam, pp 329-406.

Denniston et al. (1997) — Denniston, R.F., Shearer, C.K., Layne, G.D , and Vaniman, D.T. 1997 SIMS analyses of minor and trace element distribution in fracture calcite from Yucca Mountain, Nevada, USA. *Geochim et Cosmochim Acta*. **61**, 9, pp. 1803-1818

Devison (1951) — Devison, B. 1951 Influence of a black sphere and of black cylınder upon the neutron density in an infinity non capturing medium *Proc Phys Soc* A **64** pp 881 902

density in an infinity non-capturing medium *Proc. Phys. Soc.* A. **64**, pp. 881-902

Dolidze at al. (1975) — Dolidze, N.I., Zverev, V.Y., Spiridonov, A I. et al. 1975 Notes of the Academy of Sciences of Georgia. **78**, 2, p. 385.

Donaldson (1979) — Donaldson, C.H. 1979 An experimental investigation of the delay in nucleation of Olivine in mafic magmas. *Contrib. Mineral. Petrol* , **69**, 21-32.

Donovan et al. (1974) — Donovan, T.J., Friedman, I., Gleason, J.D. 1974 Recognition of petroleum-bearing traps by unusual isotopic compositions of carbonate-cemented surface rocks *Geology*, **2**, pp 351-354.

Dublyansky (1994-a) — Dublyansky Y. V. 1994-a Paleotemperature Environment at Yucca Mountain, Nevada (Status Report) Annual Report-Nevada, Submitted to the Nuclear Waste Project Office of the State of Nevada

Dublyansky (1994-b) — Dublyansky, Y.V. 1994-b Dialogs by Yuri V. Dublyansky regarding "Fluid Inclusion Studies of Calcite Veins From Yucca Mountain, Nevada, Tuffs: Environment of Formation". *TRAC Special Report No 15* submitted to the Nuclear Waste Project Office State of Nevada, July, 1994, 61 pp.

Dublyansky (1998-a) — Dublyansky, Y. 1998-a Fluid inclusion studies of samples from the Exploratory Studies Facility, Yucca Mountain, Nevada. *Institute for Energy and Environmental Research*, Dec. 1998, 49 p + Appendices

Dublyansky (1998-b) — Dublyansky, Y. 1998-b Traces of epigenetic hydrothermal activity in the Yucca Mountain volcanic tuffs: Fluid inclusion and gas chemistry evidence. *Abst 7th PACROFI Meeting*, Las Vegas, Nevada, 1-4 June, 1998 (no pages)

Dublyansky (1999) — Dublyansky, Y. 1999 Fluid Inclusions in Calcite from the ESF, Yucca Mountain, Nevada· Evidence of Saturated Environments and Elevated Temperatures *Supplement to EOS*, April 27, 1999. p. S4.

Dublyansky (2001-a) — Dublyansky, Y.V. 2001 Environment of deposition suggested by all-gas inclusions and stable isotopes in secondary minerals from Yucca Mountain, Nevada, USA in· F. Noronha and A. Guedes, Eds. XVI ECROFI Faculdade de Ciencias do Porto, Departamento de Geologia, Memoria no. 7, pp 131-134.

Dublyansky (2001-b) — Dublyansky Y.V. 2001 Paleohydrology at Yucca Mountain by coupled stable isotopic and fluid inclusion studies of secondary minerals. Report Submitted to the Agency for Nuclear Projects, State of Nevada, May 2001. Part II. 80 p + Appendices

Dublyansky (2001-c) — Dublyansky Y.V. 2001 Stable Isotope and Chemistry Data on the Carbonate-Opal Surface Deposits in the Solitario Canyon Yucca Mountain Nevada Report

Surface Deposits in the Solitario Canyon, Yucca Mountain, Nevada. Report Submitted to the Agency for Nuclear Projects, State of Nevada, June 2001. 36 p + Appendices

Dublyansky (2002) — Dublyansky Y.V. 2002 Extreme crystal-scale variability of $\delta^{13}C$ in hydrothermal calcite from Yucca Mountain, Nevada. *2002 International Goldschmidt Conference on Geochemistry*. Zurich, 14-25 August 2002.

Dublyansky and Lapin (1996) — Dublyansky, Y. V. and Lapin, B.N 1996 Bedrock Tuffs, Mosaic Breccias, and Young Volcanic Rocks at Yucca Mountain: Field Observations, Petrography, and Chemistry. *In* TRAC-NA Final Report, Research Conducted During FY' 92 through FY' 95, Submitted to the Nuclear Waste Project Office of the State of Nevada

Dublyansky and Mazurova (2000) — Dublyansky, Y. and Mazurova, S 2000 Stable isotopes and fluid inclusions in calcite-opal-fluorite crusts from Yucca Mountain, Nevada, USA. *GSA Abstracts with Program*. **32**, 7. p. A-259

Dublyansky and Reutsky (1995) — Dublyansky, Y. and Reutsky, V. 1995 Preliminary Data on Fluid Inclusions in Epigenetic Minerals from Tunnel Excavated under Yucca Mountain. *TRAC Report to the Nuclear Waste Project Office, State of Nevada*. 78 pp.

Dublyansky and Reutsky (1998) — Dublyansky, Y. and Reutsky, V. 1998 Epigenetic Quartz-Opal-Calcite Crusts in the Yucca Mountain Subsurface: Fluid Inclusion and Stable Isotopic Evidence of Hydrothermal Origin. *GSA Abstracts with Program*, Toronto, Canada

Dublyansky and Smirnov (1999) — Dublyansky, Y. and Smirnov, S. 1999 Ontogenetic Observations on the Scepter-like Calcite and Hyalite Opal from the ESF, Yucca Mountain, Nevada: Evidence of Depositional Environment. *Supplement to EOS*, April 27, 1999. p S8.

Dublyansky et al (1996-a) — Dublyansky, Y., Reutsky, V., and Shugurova, N. 1996-a Fluid Inclusions in Calcite from the Yucca Mountain Exploratory Tunnel. *In:* Brown, P. E.; Hageman, S G., (eds.), Proceedings of the VI PACROFI Conference. Madison, Wisconsin, USA. pp. 38-39.

Dublyansky et al. (1996-b) — Dublyansky, Y., Shugurova, N , and Reutsky, V. 1996-b Preliminary Data on Gases Trapped in Fluid Inclusions in Calcite from the Yucca Mountain Exploratory Tunnel. *GSA Abstracts with Program*, Denver, Colorado, USA. **28**, 7. p. A-522.

Dublyansky et al. (1998) — Dublyansky, Y., Szymanski, J., Chepizhko, A., Lapin, B., and Reutsky, V. 1998 Geological History of Yucca Mountain (Nevada) and the Problem of a High-Level Nuclear Waste Repository. *In*· M.J. Stenhouse and V.I Kirko (Eds) Defence Nuclear Waste Disposal in Russia NATO ASI Series Kluwer Academic Publishers,

The Netherlands. pp. 279-292.

Dublyansky et al. (1999) Dublyansky, Y., Szymanski, J , Chepizhko, A., Lapin, B., and Reutsky, V. 1999 Paleohydrology of Yucca Mountain (Nevada, USA): A key to the assessment of the suitability of the proposed radioactive waste disposal site *Geoecology.* **1,** pp 77-87. (*In Russian*)

Dublyansky et al. (2001) Dublyansky, Y., Ford, D., and Reutski, V. 2001 Traces of epigenetic hydrothermal activity at Yucca Mountain, Nevada· preliminary data on the fluid inclusion and stable isotope evidence. *Chemical Geology.* **173,** pp. 125-149

Dudley et al. (1971) Dudley, W.W., Wollitz, L E., Baldwin, D.A., and Claassen, H.C. 1971 Geologic and Hydrologic Effects of the Handley Event, Pahute Mesa, Nevada Test Site (Effects on Wells and Aquifers). *USGS Open File Report, 95-474,* Denver, CO.

E

Ebinger (1992) Ebinger, M.H. 1992 Water-rock interactions and the pH stability of groundwaters from Yucca Mountain, Nevada, USA. *Water-Rock Interaction* Kharaka & Maest (eds). Balkema, Rotterdam pp. 783-786.

Ebler (1911) Ebler, E 1911 Über die Adsorption radioactiver Stoffe durch kolloide Kieselsäure. *Kolloidzs.,* **9.**

Eckert and Drake (1959) Eckert, E. and Drake, R. 1959 Introduction to the transfer of heat and mass.

Ellis and Mahon (1977) Ellis, A.J. and Mahon, W.A.J. 1977 Chemistry and Geothermal Systems Academic Press, New York, San Francisco, London.

Else et al. (1999) Else, T.A L., Pantle, C., Amy, P.S., Dublyansky, Y., Southam, G., and Mielke, R. 1999 Moderately Thermophilic, Calcium-Precipitating Bacteria Found in Calcite Deposits at Yucca Mountain *American Society of Microbiology 99th General Meeting.* Chicago, IL, May 31, 1999. p. 448.

Ermolaev et al (1965) Ermolaev, N.P., Zhidkova, A.P., Zarinski, V.A 1965 Transport of uranium in aqueous solutions in the form of complex silicate ions *Geochemistry International,* **2,** pp. 629-640.

F

Fabryka-Martin et al. (2000) Fabryka-Martin, J. Meijer, A., Marshall, B , Neymark, L., Paces, J., Whelan, J , and Yang, A. 2000 Analysis of Geochemical Data from the Unsaturated Zone. *ANL-*

NBS-HS-000017, Rev 00. 156 p.

Faiia et al. (2000). Faiia, A.M., Aronson, J.L., Feng, X., and WoldeGabriel, G. 2000 K/Ar in Clinoptilolite: K variability and rock permeability. *GSA Abstracts with Program*, **32**, 7.

Faure (1986) Faure, G. 1986 Principles of Isotope Geology. Second Edition. John Wiley & Sons. New York. 589 p.

Fauver (1987) Fauver, D N. 1987 Survey of Radon and Radon Daughter Concentrations in Selected Rainier Mesa Tunnels *DOE/NV 10327-31.*

Feng et al, 1999 Feng, X., Faiia, A , WoldeGabriel, G., Aronson, J.L., Poage, M.A., Chamberlain, C.P. 1999 Oxygen isotope studies of illite/smectite and clinoptilolite from Yucca mountain: implication for paleohydrologic conditions. *Earth and Planetary Science Letters*, **171**, 95-106

Fhrohlich (1994) Fhrohlich, C. 1994 Earthquakes with Non-Double Couple Mechanisms. *Science*, **264**.

Fleischer (1988) Fleischer, R.L. 1988 Alpha-recoil damage: Relation to isotopic disequilibrium and leaching of radionuclides *Geochim. et cosmochim Acta* **52**, 6, pp. 1458-1466.

Fontes (1980) Fontes, J.Ch. 1980 Environmental isotopes in groundwater hydrology. In: P. Fritz and J Ch. Fontes, Eds *Handbook of Environmental Isotope Geochemistry, 1. The Terrestrial Environment, A.* Elsevier, Amsterdam, pp 75-140

Forester et al (1998) Forester, R M., Bradbury, J P., Carter, C., Elvidge-Tuma, A.B., Hemphill, M.L., Lundstrom, S C., Mahan, S.A , Marshall, B.D., Neymark, L.A., Paces, J.B , Sharpe, S.E , Whelan, J.F., and Wigand, P.E 1998 The Climatic and Hydrologic History of Southern Nevada During the Quaternary. *USGS Open File Report, 98-635*, Denver, CO.

Frenkel (1975) Frenkel, J I 1975 Kinetic theory of liquids Nauka, Leningrad (*In Russian*)

Fridrich et al. (1994) Fridrich, C.J., Dudley, W.W., and Stuckless, J.S. 1994 Hydrogeologic analysis of the saturated-zone ground-water system *J. Hydrol.* **154**, pp 133-168.

Friedman (1970) Friedman, I. 1970 Some Investigations of the Deposition of Travertine from Hot Springs. – I. The isotopic chemistry of a travertine-depositing spring *Geochim et Cosmochim Acta.* **34**. pp. 1303-1315.

Friedman and O'Neil (1977) Friedman, I. and O'Neil, J.R. 1977 Compilation of stable isotope fractionation factors of geochemical interest *In:* M Fleischer, ed , Data of Geochemistry, sixth ed , Chapter KK, U.S Geol. Survey Prof. Paper 440-KK, 12 pp. and 49 figures

Fritz (1965) Fritz, P. 1965 Composizione isotopica dellóssigeno e del carbonio nei travertini della Toscana. *Boll. Geofis Teor. Applic.* **7**, 25.

Frolov (1976) Frolov, N.M 1976 Hydrogeothermia Nedra, Moscow. 280 p. (*In Russian*)

Fuex (1977) Fuex, A N. 1977 The use of stable isotopes in hydrocarbon exploration. *J. Geochem. Exploration.* **7**, 2, pp. 155-188.

G

Garrels and Christ (1965) Garrels, R. M. and Christ, C. L. 1965 Solutions, Minerals, and Equilibria Harper and Row, New York, N.Y.

Garside (1994) Garside, L.J. 1994 Nevada Low-Temperature Geothermal Resource Assessment: 1994. *Final Report Nevada Bureau of Mines and Geology OF 94-2*. 118 p.

Gascoyne (1992) Gascoyne, M. 1992 Geochemistry of actinides and their daughters. *In*: Ivanovich, M., and Harmon, R.S. (Eds) Uranium-series disequilibrium: Applications to Earth, Marine and Environmental Sciences, Second ed., Clarendon Press, Oxford, UK. p. 34-61.

Gilbert (1875) Gilbert, G.K. 1875 Report on the geology of portions of Nevada, Utah, California, and Arizona. *U S Geol. Surveys W. 100th Mer.*, **3**, pp. 17-178.

Glikin and Petrov (1966) Glikin A.E. and Petrov T.G. 1966 Experimental investigation of growth forms of fluorite in hydrothermal conditions. *Mineralogical digest of Lvov University*. **20**, 3, pp. 443 - 446. (*In Russian*)

Glossary of Geology (1972) Glossary of Geology 1972 M. Gary, R. McAfee (J), and C.L Wolf (Eds) American Geological Institute, Washington, D.C.

Godovikov et al. (1987) Godovikov, A. A., Rippinen, O. I. and Motorin, S G. 1987. *Agates*. Moscow, Nedra, 368 p.

Goldstein (2001) Goldstein, R.H. 2001 Fluid inclusions in sedimentary and diagenetic systems. *Lithos* **55**, pp. 159-193.

Goldstein and Reynolds (1994) Goldstein, R. and Reynolds, J. 1994 Systematics of fluid inclusions in diagenetic minerals *SEPM Short Course*, **31**. 199. p

Gonfiantini et al. (1968) Gonfiantini, R , Panici, C., and Tongiorgi, E. 1968 Isotopic Disequilibrium in Travertine Deposition *Earth and Planetary Science Letters* **5**. pp. 55-58.

Gorrell (1958) Gorrell, H.A. 1958 Classification of Formation Waters Based on Sodium Chloride Content *Bull Amer. Assoc. Petrol Geologists*, **42**

Gottardı and Galli (1985) — Gottardı, G. and Gallı, E 1985. Natural zeolites. Berlin, Heidelberg, New-York, Tokyo, Springer-Verlag, 409 p

Graetsch (1994) — Gratesch H 1994 Structural characteristics of opaline and microcristalline silica minerals In: P.J. Heaney, C.T. Prewitt, G.V. Gibbs, Eds. *Silıca. Physical behavior, geochemistry and material applications* Reviews in Mıneralogy, **29**, pp. 209-232.

Graton (1933) — Graton, L C. 1933 The depth zones in ore deposition. *Econ Geol.* **28**, pp. 513–555.

Graves (1998) — Graves, R.P., 1998 Water levels in the Yucca Mountain area, Nevada, 1996. *U.S Geol. Survey Open-File Report 98-169.*

Green (1959) — Green, J 1959 Geochemical table of elements for 1959. *Geol Soc Amer. Bull.* **70** pp. 1127-1184.

Grigoriev (1961) — Grigoriev D P. 1961 Ontogenesis of minerals Lvov, Lvov University Press. 315 p (*In Russian*)

Grigoriev and Zhabin (1975) — Grigoriev, D P., and Zhabın, A.G. 1975 *Ontogenesıs of minerals*. Moscow, Nauka. 337 p (*In Russian*)

Grow et al. (1994) — Grow, J., Barker, C., and Harris, H 1994 Oil and gas exploration near Yucca Mountain, Southern Nevada *High-Level Radioactive Waste Management.* Proc. Int. Con , Amer. Nucl. Soc., La Grande Park, Illinois pp. 1298-1315.

Gunn, et al (1990) — Gunn, J., Fletcher, S., and Prime, D. 1990 Research on radon in British limestone caves and mines, 1970-1990. *Cave Science* (UK), **18**, 2, pp. 63-65.

Guthrie et al. (1995) — Guthrie, G D. (Jr), Raymond, R. (Jr), and Chipera, S. 1995 Eolian-deposited minerals around drill hole USW SD-9, Yucca Mountain, Nevada *Proc. Int. Con., Amer. Nucl. Soc* "High-Level Radioactive Waste Management". La Grande Park, Illınois. pp 135-136

H

Halden (1996) — Halden N. M 1996 Determination of Lyapunov exponents to characterize the oscillatory dıstrıbutıon of trace elements in minerals. *Can. Mıneral* **34**, pp. 1127–1135.

Halden and Hawthorne (1993) — Halden N. M. and Hawthorne F. C. 1993 The fractal geometry of oscillatory zoning in crystals: Application to zircon. *Am. Mineral.* **78**, pp 1113–1116

Hanks et al. (1999) — Hanks, T.S., Winograd, I.J., Anderson, E.R., Reilly, T.E., and Weeks, E.P. 1999 Yucca Mountain as a Radioactive-Waste Repository. A Report to the Director, U.S.

Geological Survey. *Circular 1184*. 19 p.

Hanson et al. (1987) — Hanson, G. N., Baker, V.R , Bethke, P.M., Hudleston, P.J., and Roquemore, G.R. 1987 Report of the Peer Review Panel on the Proposed Program of Studies of the Calcite and Opaline-Silica Deposits in the Yucca Mountain Area, Nevada U.S Department of Energy, Las Vegas, Nevada.

Harmon (1993) — Harmon, R. S. 1993 Isotopic and Fluid Inclusion Study of Yucca Mountain Samples. TRAC-NA Quarterly Report No.6. Submitted to the Nuclear Waste Project Office of the State of Nevada.

Haskell and McKeever (1994) — Haskell, E. H. and McKeever, S.W.S 1994 Determination of Historical Thermal Gradients and Dates of Calcite Formation Using Thermoluminescence, Optically Stimulated Luminescence and Electron Spin Resonance Analysis of Minerals Removed from Excavated and Cored Samples at Yucca Mountain: *Interim Progress Report*, Submitted to the Nuclear Waste Project Office of the State of Nevada

Haukwa et al. (1998) — Haukwa, C., Wu, Y.S , Hinds, J.J., Zhang, W., Ritcey, A.C., Pan, L.H., Simmons, A.M., and Bodvarsson, G S. 1998 Results of Sensitivity Studies of Thermo-Hydrologic Behavior Conducted on Hydrologic Parameter Sets. *Yucca Mountain Project Level 4 Milestone Report SP3CK5M4* Lawrence Berkeley National Laboratory, Berkeley, CA.

Hay (1978) — Hay, R. L. 1978 Geologic occurrences of zeolites. In Natural zeolites. Ed· L. B Sand and F. A Mumpton Oxford, Pergamon Press, 135-144.

Hay et al. (1986) — Hay, R.L., Pexon, R.E., Teague, T.T., and Kyser, T.K. 1986 Spring-Related Carbonate Rocks, Mg Clays, and Associated Minerals in Pliocene Deposits of the Amargosa Desert, Nevada and California *Geological Society of American Bulletin*, **97**. pp 1488-1503

Hearn et al. (1990) — Hearn, T., Beghoul, N., and Barazangi, M. 1990 First Tomographic Study of Western U S - Completed Transactions *EOS*, American Geophysical Union, **71**, 36

Heiken et al (1996) — Heiken, G., Woldegabriel, G , Morley, R., Plannerer, H., and Rowley, J. 1996 Disposition of Excess Weapon Plutonium in Deep Boreholes. Site Selection Handbook. *LA-13168-MS*. 48 p.

Helz and Holland (1969) — Helz, G.R. and Holland, H.D. 1969 The solubility and geologic occurrence of strontianite. *Geochim et Cosmochim Acta*, **29**, pp 1303-1315.

Henish (1970) — Henish H.K. 1970 Crystal growth in gels The Pennsylvania State University Press, University Park and London // 1973 Russian translation Moscow Mir 112 p

University Park and London // 1973 Russian translation, Moscow, Mir, 112 p.

Hickman et al. (1994) — Hickman, S., Sibson, S , and R. Brune 1994 Proceedings of Workshop LXIII, the Mechanical Involvement of Fluids in Faulting. *USGS Open-File Report 94-228*, Menlo Park, CA.

Hill and Dublyansky (1999) — Hill, C.A. and Dublyansky, Y.V. 1999 Response to Stuckless and others (1998) on "Overview of calcite/opal deposits at or near the proposed high-level nuclear waste site, Yucca Mountain, Nevada, USA: Pedogenic, hypogene, or both?" *Environmental Geology.* **38**, 1, pp. 77-81.

Hill and Forti (1997-a) — Hill C. and Forti P. 1997 (Eds) *Cave minerals of the World* National Speleological Society.

Hill and Forti (1997-b) — Hill, C.A and Forti, P. 1997 Monocrystalline and macrocrystalline speleothems In C. Hill and P. Forti, Eds. *Cave minerals of the world.* Second edition. National speleological society. p 463.

Hill and Livingston (1993) — Hill C.A. and Livingston D E. 1993 Chemical analyses of rocks, minerals and detritus, Yucca Mountains—Preliminary report. *TRAC Special Report No 11* Submitted to the State of Nevada Nuclear Waste Project Office.

Hill et al (1995) — Hill, C.A , Dublyansky, Y.V., Harmon, R., Schluter, C. 1995 Overview of calcite/opal deposits at or near the proposed high-level nuclear waste site, Yucca Mountain, Nevada pedogenic, hypogene, or both? *Environmental Geology*, **26**, 1, pp. 69-88.

Hoefs (1980) — Hoefs, J. 1980 Stable Isotope Geochemistry. Second, Completely Revised and Updated Edition Springer-Verlag Berlin Heidelberg New York.

Hoefs (1987) — Hoefs, J. 1987 Stable Isotope Geochemistry. Springer-Verlag, Berlin, Heidelberg, New York, London, Paris, Tokyo.

Holloway et al. (1989) — Holloway, R W, Carilli, J.T., Faller, S.H., Chung-King Liu, and Kuroda, P.R. 1989 Thorium-230 Dating of Thermal Waters in the Vicinity of the Nevada Test Site. *Journal of Radioanalytical and Nuclear Chemistry*, **131**, 2.

Holmes (1928) — Holmes, A. 1928 The nomenclature of petrology. N.Y., D. Van Nostrand Co., Inc 284 p.

Holten et al. (2000) — Holten, T., Jamtveit, B., and Meakin, P. 2000 Noise and oscillatory zoning of minerals *Geochim et Cosmochim. Acta* **64**, 11, pp 1893–1904

Hower and Altaner (1983) — Hower, J. and Altaner, S. P. 1983 The petrologic significance of illite/smectite. In *Program, Abstracts*, 20th Annual Meeting of Clay Minerals Society, Buffalo, NY,

I

Ikornikova (1975) — Ikornikova N. 1975 Hydrothermal crystal synthesis in chloride systems. Moscow, Nauka. 224 p. (*In Russian*)

Iler (1955) — Iler, R K. 1955 The colloid chemistry of silica and silicates Ithaka, New York, Cornel University Press. 323 p.

J

Johannesson et al (2000) — Johannesson, K. H., Xiaoping, Z., Ciaxia, G., Stetzenbach, K J. and Hodge, V. F. 2000. Origin of rare earth element signatures in groundwaters of circumneutral pH from southern Nevada and eastern California, USA *Chemical Geology.* **164,** 239-257.

K

Kachurin (1973) — Kachurin, L.G. 1973 Physical bases of the influence on atmospheric processes Moscow, Gidrometeoizdat.

Kalb (1929) — Kalb G 1929 Bemerkungen zu den minerogenetischen Kristalltrachtstypen des Kalkspates. *Zbl. Mineral.*, Abt. A, 4. ss. 137-138.

Kalinin et al (1998) — Kalinin D.V., Vosel, S V., and Sedobintseva, V.V. 1998 New interpretation of the structure of the precious opal and energetic analysis of the interaction of the spherical particles of silica during its formation. *Russian Geology and Geophysics,* **39,** 7, pp 1013-1016.

Keilis-Borok (1990) — Keilis-Borok, V.I. 1990 The Lithosphere of the Earth as a Non-Linear System with Implications for Earthquake Prediction *Review of Geophysics,* **28**

Keith and Padden (1963) — Keith, H D. and Padden, F.J. 1963 A phenomenological theory of spherulitic crystallization *Journal of applied physics.* **34,** 8, pp. 2409-2421.

Keller (1960) — Keller, G.V. 1960 Physical Properties of the Oak Spring Formation, Nevada *USGS Professional Paper 400-B,* Denver, CO

Keller (1962) — Keller, G.V. 1962 Electrical Resistivity of Rocks in the Area 12 Tunnels, Nevada Test Site, Nye County, Nevada *Geophysics,* **27,** 2.

Kendall and Broughton — Kendall, A C. and Broughton, P.L. 1978 Origin of fabric in speleothems composed

(1978) of columnar calcite crystals. *Jour. Sed Petrol* **48**, 2, 519-538.

Khimcheva et al (1991) Khimcheva, N.V., Plusnina, I.I., and Isirikian, F.F. 1991 Sorptive properties of minerals from the sequece opal-quartz *Newsletters of the Moscow University,* Series 4, Geology. 1. pp. 33-44. (*In Russian*)

Khmelnitsky (1988) Khmelnitsky, R.A. 1988 Physical and colloidal chemistry. Moscow, Vishaya Shkola 400 p (*In Russian*)

King et al. (2000) King, C.-Y., Azuma, S , Asaai, Y., He, P., Kitigawa, Y., Igarashi, G., Wakita, H. 2000 In search of earthquake precursors in the water-level data of 16 closely clustered wells at Tono, Japan. *Geophysical Journal International*, **143**, p. 469-477.

Kinsman (1969) Kinsman, J.J. 1969 Interpretation of Sr concentrations in carbonate minerals and rocks. *Journal of Sedimentary Petrology*, **39**, pp 486-508.

Kipp (1987) Kipp, K.L. Jr. 1987 Effect of Topography on Gas Flow in Unsaturated Fractured Rock: Numerical Simulation. *In:* D.D. Evans and T.J. Nicholson, (Eds) Flow and Transport Through Unsaturated Fractured Rock. American Geophysical Union. pp. 171-176.

Kirkpatric (1975) Kirkpatrik, R J. 1975 Crystal growth from the melt: A overview. *Amer. Mineral.* **60**, 798 – 814.

Klimchuk and Nasedkin (1992) Klimchuk, A.B. and Nasedkin, V.M. 1992 Radon in caves of the FSU. *Svet*, **4**, (6) pp. 21-35. (*In Russian*)

Kodenev (1984) Kodenev, G.G. 1984 Formation of fluctuating nuclei in supersaturated vapor. Institute of Geology and Geophysics, Preprint 3, Novosibirsk, A. of Sci. USSR. 11 p. (*In Russian*)

Kondratiev et al. (1982) Kondratiev, K.Y., Moskalenko, N I., Pozdniakov, D.V. 1982 Atmospheric aerosol. Gidrometeoizdat, Leningrad. (*In Russian*)

Krasnova and Petrov (1997) Krasnova, N. I and Petrov, T. G. 1997. Genesis of mineral individuals and aggregates. St Petersburg, Nevsky kuryer, 228 p. (*In Russian*)

Kreshkov (1976) Kreshkov, A.P. 1976 Fundamentals of the analytical chemistry. Chemistry. Moscow. 401 p (*In Russian*)

Kuznetsov and Ust-Kachkintsev (1976) Kuznetsov, V.V. and Ust-Kachkintsev, V.F. 1976 Physical and colloidal chemistry. Visshaya Shkola. Moscow. (*In Russian*)

L

Lachenbruch and Sass (1978) — Lachenbruch, A.H., and Sass, J.H. 1978 Models of an Extending Lithosphere and Heat Flow in the Basin and Range Province. *In*: Cenozoic Tectonics and Regional Geophysics of the Western Cordillera, *Geological Society of America Memoir*, **152**.

Langmuir (1978) — Langmuir, D. 1978 Uranium solution-mineral equilibria at low temperature with applications to sedimentary ore deposits *Geochim et Cosmochim Acta* **43**, pp. 547-569.

Langmuir and Herman (1980) — Langmuir, D. and Herman, J.S. 1980 The mobility of thorium in natural waters at low temperatures. *Geochim et Cosmochim Acta.* **44**, pp. 1753-1766.

Lebedev (1975) — Lebedev, L M. 1975 Modern ore-forming hydrotherms Moscow, Nedra. 261 p. (*In Russian*)

Lebedev (1979) — Lebedev, L.M. 1979 Minerals of modern hydrotherms Moscow, Nauka, 200 p. (*In Russian*)

Lee and Morse (1999) — Lee, Y-J, Morse, J. W. 1999 Calcite precipitation in synthetic veins: implications for the time and fluid volume necessary for vein filling. *Chemical Geology*, **156**, pp. 151-170.

Lehman and Brown (1995) — Lehman, L.L. and Brown, T.P. 1995 Compartmentalized saturated flow at Yucca Mountain *High-Level Radioactive Waste Management.* Proc. Int Con., Amer. Nucl. Soc., La Grande Park, Illinois. pp. 206-208.

Levy (1984) — Levy, S S. 1984 Studies of altered vitrophyre for prediction of nuclear waste repository-induced thermal alteration at Yucca Mountain, Nevada Materials Research Society Symposium Proceedings, v. 26959-966

Levy (1992) — Levy, S.S. 1992 Natural gels in the Yucca Mountain area, Nevada, USA. *Applied Clay Science*, **7**, pp. 79-85.

Levy and Naeser (1991) — Levy, S. and Naeser, C. 1991 Bedrock Breccias Along Fault Zones Near Yucca Mountain, Nevada. Paper Submitted to United States Geological Survey Bulletin

Levy et al. (1995) — Levy, S., Chipera, S , and Norman, D. 1995 Alteration History Studies in the Exploratory Studies Facility, Yucca Mountain, Nevada, USA. *Scientific Basis for Nuclear Waste Management XIX, Proceedings Materials Research Society Symposium* V, Boston, 27 November- 1 December 1995.

Lifshitz and Landau (1979) — Lifshitz, E.M. and Landau, L.P. 1979 Physical kinetics. Nauka Moscow. (*In Russian*)

Lindgren (1933) — Lindgren, W. 1933 Mineral Deposits. 4th edn. McGraw-Hill, New York.

Liu et al. (1995) — Liu, N., Sorensen, C.D , Tung, C.-H., and Orchard, C.R. 1995 Continuous, environmental radon monitoring program at the Yucca Mountain Site Characterization Project. *High-Level Radioactive Waste Management.* Proc. Int. Con., Amer. Nucl. Soc., La Grande Park, Illinois pp.

Livingston (1993) — Livingston, D. E 1993 A review of the major element geochemistry of Yucca mountain, Nye county, Nevada. TRAC Technology and resource Assessment Corporation, Special Report No. 4, 46p. + Appendix

Lorens (1981) — Lorens, R.B 1981 Sr, Cd, Mn and Co distribution coefficients in calcite as a function of calcite precipitation rate. *Geochim et Cosmochim Acta*, **45**, pp. 553-561.

Lovering (1954) — Lovering, T.G. 1954 Radioactive Deposits of Nevada A contribution to the geology of uranium *Geological Survey Bulletin 1009-C.* U.S Government Printing Office, Washington. 106 p

Lushnikov (1978) — Lushnikov, A A. 1978 Some new aspects of the theory of coagulation. *Newsletters of the A of Sci USSR.* Ser FAO, **14**, 10, pp. 1048-1055. (*In Russian*)

M

Machette (1985) — Machette, M N. 1985 Calcic soils of the southwestern United States *GSA Special Paper* 203 21 p

Marcus (1968) — Marcus, A H 1968 Stochastic coalescence *Technomitriecs* **10**, 1, pp. 133-148

Marshall and Futa (2001) — Marshall, B D. and Futa, K. 2001 Strontium Isotope Evolution of Pore Water and Calcite in the Topopah Spring Tuff, Yucca Mountain, Nevada. *Proc Int Con , Amer. Nucl Soc.* "High-Level Radioactive Waste Management". La Grande Park, Illinois.

Marshall and Mahan (1994) — Marshall, B.D. and Mahan, S.A 1994 Strontium isotope geochemistry of soil and playa deposits near Yucca Mountain, Nevada *Proc. Int Con , Amer. Nucl. Soc* "High-Level Radioactive Waste Management". La Grande Park, Illinois. pp 2685-2691.

Marshall and Whelan (2000) — Marshall, B and Whelan, J 2000 Isotope geochemistry of calcite coatings and the thermal history of the unsaturated zone at Yucca Mountain, Nevada *GSA Abstracts with Program.* **32**, 7. p. A-259.

Marshall et al. (1990) — Marshall, B.D., Peterman, Z E. Futa, K , Stuckless, J. S. Mahan, S. A., Downey, J. S., and Gutentag, E. D. 1990 Origin of Carbonate Deposits in the Vicinity of Yucca Mountain, Nevada· Preliminary Results of Strontium-Isotope Analyses. . *Proc. Int. Con , Amer. Nucl Soc.* "High-Level Radioactive Waste Management". La Grande Park, Illinois.

Marshall et al. (1993) — Marshall, B.D., Peterman, Z.E, and Stuckless, J.S., 1993 Strontium isotopic evidence for a higher water table at Yucca Mountain. *Proc. Int. Con , Amer. Nucl. Soc.* "High-Level Radioactive Waste Management". La Grande Park, Illinois. pp 1948-1952.

Marshall et al. (1995) — Marshall, B. D., Kyser, K.T., and Peterman Z.E. 1995 Oxygen Isotopes and Trace Elements in the Tiva Canyon Tuff, Yucca Mountain and Vicinity, Nye County, Nevada *U S Geological Survey Open-File Report 95-431.* 49 p

Marshall et al (1998) — Marshall, B.D., Paces, J.B., Peterman, Z.E., Neymark, L.A., Whelan, J.F., and Futa, K. 1998 Isotopic evidence for the origin of low-temperature calcite and opal exposed in an underground laboratory at Yucca Mountain, Nevada *GSA Abstracts with Program* Toronto, Canada. p A-363.

McConnaughey (1989) — McConnaughey, T. 1989 ^{13}C and ^{18}O isotopic disequilibrium in biological carbonates 1. Patterns *Geochim. et Cosmochim Acta*, **53**, pp 163-171.

McConnaughey et al. (1994) — McConnaughey, T.A., Whelan, J.F., Wickland, K.P., and Moscati, R.J. 1994 Isotopic Studies of Yucca Mountain Soil Fluids and Carbonate Pedogenesis. *Proc. Int. Con , Amer. Nucl Soc.* "High-Level Radioactive Waste Management". La Grande Park, Illinois pp. 2584-2589.

Michaelis et al (1985) — Michaelis, J , Usdowski, E., and Menschel, G. 1985 Partitioning of ^{13}C and ^{12}C on the degassing of CO_2 and the precipitation of calcite – Rayleigh-Type fractionation and a kinetic model. *Amer. J. of Sci.* **285**, pp. 318-327.

Michard and Albarede (1986) — Michard, A. and Albarede, F. 1986 The REE Content of Some Hydrothermal Fluids. *Chemical Geology*, **55**.

Michard et al. (1987) — Michard, A.C., Beaucaire, C., and Michard, D. 1987 Uranium and Rare Earth Elements in CO_2-Rich Waters from Vals-Les-Bains (France). *Geochimica at Cosmochimica Acta*, **51**.

Mineev and Rozenkova (1962) — Mineev, D. A and Rozenkova, N. I. 1962 On the zonation of Vyshnevogorsky pyrochlore. *ZVMO.* **91**, 1, pp. 89 - 93. (*In Russian*)

Moore et al. (2001) — Moore, J.N., Norman, D.I., and Kennedy, B M 2001 Fluid inclusion gas compositions from an active magmatic hydrothermal system· a case study of The

compositions from an active magmatic–hydrothermal system a case study of The Geysers geothermal field, USA. *Chemical Geology* **173** pp 3–30.

Morey and Niggli (1913) — Morey, G W. and Niggli, P. 1913 The hydrothermal formation of silicates, a review. *Jour. Am Chem Soc.* **35**, pp. 1086-1130.

Morse (1983) — Morse, J.W. 1983 The kinetics of calcium carbonate dissolution and precipitation In: Reeder, R.J. (Ed.), *Carbonates· Mineralogy and Chemistry*. Mineral. Soc. Am. pp. 227-264.

Mozgova, 1963 — Mozgova, N.N. 1963 Mineralized cavities in the Tetiukhe Skarns. *Zapiski Vsesoyuznogo Mineralogicheskogo Obschestva (Notes of the All-Union Mineral Soc)*, **6**, 42, pp 645-663 *(In Russian)*

Mucci and Morse (1983) — Mucci, A. and Morse, J.W. 1983 The incorporation of Mg^{2+} and Sr^{2+} into calcite overgrowths: Influence of growth rate and solution composition *Geochim Cosmochim Acta*, **47**, pp. 217 - 233.

Muir-Wood and King (1993) — Muir-Wood, R. and King, G C.P. 1993 Hydrological Signatures of Earthquake Strain *Journal of Geophysical Research*, **98**

Mukherjee (1986) — Mukherjee A.L 1986 Fluorite mineralisation in Garampani thermal spring area, Palamau district, Bihar. *J. Geol Soc. Indian*, **28**, 6, pp 442-448.

Murphy (1979) — Murphy, H D. 1979 Convective Instabilities in Vertical Fractures and Faults *Journal of Geophysical Research*, **84**.

N

NAS/NRC (1992) — NAS/NRC 1992 Ground Water at Yucca Mountain: How High Can It Rise? *Final Report of the Panel on Coupled Hydrologic/Tectonic/ Hydrothermal Systems at Yucca Mountain*. National Research Council. National Academy Press. Washington D.C. 231 p.

NBMG/UNR 1999 — NBMG/UNR 1999 Geochemical Anomalies at Yucca Mountain and Implications for Metallic Mineral Potential. Report by Nevada Bureau of Mines and Geology, University of Nevada Reno to TRW Environmental Safety Systems Inc *TDR-NBS-GS-000001* REV. 00. 34 pp. + Appendices.

NC NWRPO (2000) — NC NWRPO (Nye County Nuclear Waste Repository Project Office) 2000 Summary Annual Report, Grant DE-FG08-96NV 12027, May 1999 - April 2000

NEA/IAEA (2001) — NEA/IAEA 2001 Joint NEA-IAEA International Peer Review of the Yucca Mountain Site Characterisation Project's Total System Performance Assessment

Supporting the Site Recommendation Process, *Final Report.* December 2001

Nelson and Giles (1985) — Nelson, C. E., and Giles, D. L. 1985 Hydrothermal Eruption Mechanisms and Hot Spring Gold Deposits. *Economic Geology*, **80**.

Newman et al (1996) — Newman, B D., Norman, D.I., Gundimeda, N., and Levy, S.S. 1996 Understanding the genesis of nonmarine calcite deposits through quadrupole mass spectrometric analysis of fluid inclusion gases. *Chemical Geology*, **132**. pp. 205-213.

Newman et al. (1997) — Newman, B.D., Campbell, A.R., Norman, D.I , and Ringelberg, D B. 1997 A model for microbially induced precipitation of vadose-zone calcites in fractures at Los Alamos, New Mexico, USA *Geochim. et Cosmochim Acta* **61**, 9, pp. 1783-1792.

Neymark and Paces (2000) — Neymark, L A. and Paces, J.B. 2000 Consequences for Slow Growth for ^{230}Th/U Dating of Quaternary Opals, Yucca Mountain, Nevada, USA. *Chemical Geology*, **164**.

Neymark et al. (1998-a) — Neymark L. A., Paces J. B., and Amelin Y. V 1998-a Neogene to Quaternary U–Th–Pb geochronology using opal, Yucca Mountain, Nevada, USA. *Mineral Mag.* **62A**, pp. 1077–1078.

Neymark et al (1998-b) — Neymark, L.A , Amelin, Y.V., Paces, J.B , and Peterman, Z E. 1998-b U-Pb age evidence for long-term stability of the unsaturated zone at Yucca Mountain. *Proc. Int. Con , Amer Nucl. Soc.* "High-Level Radioactive Waste Management". La Grande Park, Illinois pp. 85-87.

Neymark et al. (2000) — Neymark A.L. Amelin, Y.V., and Paces, J.B. 2000 ^{206}Pb-^{230}Th-^{234}U-^{238}U and ^{207}Pb-^{235}U geochronology of Quaternary opal, Yucca Mountain, Nevada. *Geochemica et Cosmochemica Acta*, **64**, 17, pp. 2913-2928.

Neymark et al. (2002) — Neymark, L A , Amelin, Y., Paces, J.B and Peterman, Z.E. 2002 U-Pb ages of secondary silica at Yucca Mountain, Nevada: Implications for the paleohydrology of the unsaturated zone. *Applied Geochemistry* (*In press*)

Nicolis and Prigogine (1977) — Nicolis, G. and Prigogine, I. 1977 Self-organization in nonequilibrium systems From dissipative structures to order through fluctuations. John Wiley and Sons 491 p.

Nillson and Sternberg (1999) — Nilsson, O. and Sternberg, J. 1999 A mechanistic model for calcite crystal growth using surface speciation *Geochim. et Cosmochim Acta*, **63**, pp. 217-225.

Noble et al (1991) — Noble, D.C., Weiss, S.I., and McKee, E.H. 1991 Magmatic and hydrothermal activity, caldera geology, and regional extension in the western part of the southwestern Nevada volcanic field *In:* G.L. Raines, R.E. Lisle, R.W. Shafer, and W.W. Wilkinson, *Eds* Geology and Ore Deposits of the Great Basin. Reno, Geol.

Soc. of Nevada. pp. 913-934

Norman and Moore (1999) — Norman, D.I. and Moore, J.N. 1999 Methane and excess N_2 and Ar in geothermal fluid inclusions *Proc. 24th Workshop Geotherm. Reservoir Eng.*, Stanford Univ., pp 196–202.

Nur (1972) — Nur, A. 1972 Dilatancy, Pore Fluids and Premonitory Variations of Vs/Vp Travel Times. *Seismological Society of America Bulletin*, **62**.

O

O'Neil and Silberman (1974) — O'Neil, J.R. and Silberman, M.L 1974 Stable Isotope Relations in Epithermal Au-Ag Deposits. *Econ. Geol.* **69**. pp. 902-909.

Ohmoto (1972) — Ohmoto, H. 1972 Systematics of sulfur and carbon isotopes in hydrothermal ore deposits *Econ Geol.* **67**, 551-578.

Ohmoto (1986) — Ohmoto, H. 1986 Stable Isotope Geochemistry of Ore Deposits. *In*: Valley, J., Taylor, H and O'Neil. J., *Eds. Stable Isotopes in High-Temperature Geological Processes*. Reviews in Mineralogy, **16**. pp. 491-559.

Ohmoto and Rye (1979) — Ohmoto, H. and Rye, R.O 1979 Isotopes of sulfur and carbon *In:* H L Barnes, ed , Geochemistry of Hydrothermal Ore Deposits, second ed , pp. 509-567. John Wiley, New York, 798 p

Okamoto et al. (1963) — Okamoto, G., Okura, T., and Goto, K 1963 Silica properties in water. *In*· Geochemistry of lithogenesis. Moscow, Inostrannaya Literatura. pp. 196-208 (*In Russian*)

Onac (1997) — Onac B.P. 1997 Crystallography of Speleothems. *In*· Hill C., Forti P., Eds. Cave minerals of the World National Speleological Society. pp. 230-236.

Osmond and Cowart (1982) — Osmond, J.K. and Cowart, J.W. 1982 Ground Water. *In*: Uranium Series Disequilibrium· Applications to Environmental Problems. Clarendon Press, Oxford

P

Paces and Whelan (2001) — Paces, J.B. and Whelan, J.F. 2001 Water-Table Fluctuations in the Amargosa Desert, Nevada *Proc. Int Con , Amer. Nucl. Soc* "High-Level Radioactive Waste Management". La Grande Park, Illinois

Paces et al. (1993) — Paces, J.B., Taylor, E.M., and Bush, Ch., 1993 Late Quaternary History and Uranium Isotopic Compositions of Ground Water Discharge Deposits, Crater Flat,

Nevada *Proc Int. Con., Amer. Nucl. Soc.* "High-Level Radioactive Waste Management". La Grande Park, Illinois. pp 1573-1580.

Paces et al. (1996) — Paces, J., Neymark, L A , Marshall, B.D , Whelan, J.F., and Peterman, Z.E 1996 Ages and origins of subsurface secondary minerals in the Exploratory Studies Facility (ESF) *USGS Milestone Report 3GQH450M* 55 p.

Paces et al. (1998) — Paces, J., Neymark, L.A., Marshall, B.D., Whelan, J.F., and Peterman, Z.E. 1998 Inferences for Yucca Mountain unsaturated zone hydrology from secondary minerals. *High-Level Radioactive Waste Management.* Proc. Int Con., Amer. Nucl. Soc., La Grande Park, Illinois pp. 36-39

Paces et al. (2000) — Paces, J B., Whelan, J. F., Peterman, Z. E., Marshall, B. D., and Neymark, L. A. 2000 Formation of calcite and silica from percolation in a hydrologically unsaturated setting, Yucca Mountain, Nevada *GSA Abstracts with Program*, **32**, 7, p. A-259.

Palyanova et al (2002) — Palyanova, G., Smirnov, S., and Dublyansky, Y. 2002 Thermodynamic modeling of the rhyolite-water interaction and the mineralogy of secondary assemblages at Yucca Mountain, Nevada *Russian Geology and Geophysics* (in press)

Panichi and Tongiorgi (1975) — Panichi, C. and Tongiorgi, E 1975 Carbon isotopic composition of CO_2 from springs, fumaroles, mofettes and travertines of central and southern Italy: a preliminary prospection method of geothermal area *Proc. 2nd Symp. Development and Use of Geothermal Resources, Sam Francisco, Calif.* Pp. 815-825.

Parker et al. (1983) — Parker, L.W., Miller, J., Steinberger, Y., and Whitford, W.G. 1983 Soil respiration in a Chihuahuan desert rangeland *Soil Biology and Biochemistry* **15**, pp. 303-309.

Pashenko and Dublyansky (2002-a) — Pashenko, S E. and Dublyansky, Y.V. 2002-a The role of radon and colloids in distorting the U-Pb age dates of geologically young minerals deposited in open cavities 2002 International Goldschmidt Conference on Geochemistry. Zurich, 14-25 August 2002.

Pashenko and Dublyansky (2002-b) — Pashenko, S.E and Dublyansky, Y.V. 2002-b Theoretical investigation of production, migration in fluid and incorporation in growing minerals of the Rn-derived Pb isotopes Internal Report of the Institute of Mineralogy and Petrography, Russian Academy of Sciences, Siberian Branch, Novosibirsk, June 2002 110 p.

Pashenko and Sabelfeld (1992) — Pashenko S.E. and Sabelfeld, K.K. 1992 Atmospheric and technogene aerosol: kinetic, microprobe and numerical methods of studies *Acta of Institute of Chemical Kinetics and Combustion*, Russian Academy of Sciences, Novosibirsk. 310 p. (*In Russian*)

Pashenko et al. (1980) — Pashenko, S E , Kutsenogy, K.P., Pashenko, A.E., Ankilov, A.I., and Baklanov, A.M. 1980 Experimental studies of the kinetics of the non-steady-state nucleation in gaseous phase *Letters to Journal of Theoretical and Experimental Physics*, **6**, 22, pp 1380-1383. (*In Russian*)

Pashenko et al (1996) — Pashenko, S , Vlasenko, A , Ankilov, A , Baklanov, A , Eremenko, S., Korolev, V., Shirokov, Y., Wyers, G.P, Ten Brink, H.M, Khlystov, A., Waijers-Ypelaan, A. 1996 A study of emission sources at Novosibirsk. *J. Aerosol Sci.* **27**, Suppl.1, pp. S129-130

Penrose (1991) — Penrose, R. 1991 The Emperor's new mind. Penguin Group. 466 p

Peterman et al (1992) — Peterman, Z E., Stuckless, J.S., Marshall, B D , Mahan, S.A., and Futa, K. 1992 Strontium isotope geochemistry of calcite fracture fillings in deep core, Yucca Mountain, Nevada – A progress report. *Proc. Int Con , Amer. Nucl Soc* "High-Level Radioactive Waste Management". La Grande Park, Illinois pp. 1582-1586.

Peterman et al. (1993) — Peterman, Z.E., Spengler, R W., Singer, F.R., and Dickerson, R.P., 1993 Isotopic and trace element variability in altered and unaltered tuffs at Yucca Mountain, Nevada. *Proc Int Con., Amer. Nucl Soc.* "High-Level Radioactive Waste Management". La Grande Park, Illinois pp. 1940-1947.

Peterman et al. (1994) — Peterman, Z E., Widmann, B. L., Marshall, B. D., Aleinikoff, J. N., Futa, K. and Mahan, S. A. 1994 Isotopic tracers of gold deposition in Paleozoic limestones, Southern Nevada *Proc. Int. Con , Amer. Nucl. Soc* "High-Level Radioactive Waste Management". La Grande Park, Illinois pp. 1316-1323.

Petrov (1982) — Petrov, Y.I 1982 Physics of small particles. Nauka, Moscow. (*In Russian*)

Pokrovsky (1989) — Pokrovsky, V. A 1989 Theoretical prediction of differential mobility of components in hydrothermal systems on the basis of phase diagrams *In*. Physico-chemical analysis of mineral forming processes. *Ed* V. A Zharikiov. Moscow, Nauka, pp. 212-245.

Pollack and Chapman (1977) — Pollack, H N. and Chapman, D S 1977 On the Regional Variation of Heat Flow, Geotherms, and Lithospheric Thickness. *Tectonophysics*, **38**

Principles of Hydrogeology... (1982) — Principles of Hydrogeology. Geological activity and history of water in the Earth's interiors. (E.V. Pinneker, *Ed.*) Novosibirsk, Nauka PH 1982. 239 p. (*In Russian*)

Q

Quade (1994) — Quade, J. 1994 Spring Deposits and Late Pleistocene Ground Water Levels in Southern Nevada *Proc Int Con Amer Nucl Soc* "High Level Radioactive Waste

Southern Nevada *Proc. Int Con , Amer. Nucl Soc* "High-Level Radioactive Waste Management". La Grande Park, Illinois

Quade and Cerling (1990) — Quade, J., Cerling, T.E. 1990 Stable isotopic evidence for a pedogenic origin of carbonates in trench 14 near Yucca Mountain, Nevada *Science*, **250**, pp. 1549-1552.

Quade et al (1988) — Quade, J, Cerling, T. E , and Bowman, J. R. 1988 Systematic Variations in $\delta^{13}C$ and $\delta^{18}O$ of Soil Carbonate Along Elevation Transects in the Southern Great Basin, USA. Update Report: The Paleohydrology and Paleoenvironments in the Vicinity of the Proposed Yucca Mountain Nuclear Waste Repository. W. G. Spaulding, ed Submitted to the Nuclear Waste Project Office of the State of Nevada

Quade et al. (1989) — Quade, J., Cerling, T.E., and Bowman, J.R. 1989 Systematic variations in the carbon and oxygen isotopic composition of pedogenic carbonate along elevation transects in the southern Great Basin. *Geol Soc Amer. Bull.* **101**, p 464-475.

Quinke (1902) — Quinke, J. 1902 Die oberflächenspannung an der Grenze wassriger Kolloidlösungen von verschiedener Contentration. *Ann. Physik* , **9**, 13.

R

Ranalli (1987) — Ranalli, G 1987 Rheology of the Earth Allen and Urwin, Boston, Mass.

Reheis et al. (1992) — Reheis, M C , Sowers, J.M., Taylor, E M , McFadden, L.D., and Harden, J.W. 1992 Morphology and Genesis of Carbonate Soils on the Kyle Canyon Fan, Nevada, USA *Geoderma*, **52**, pp. 302-342.

Rhiele (1973) — Rhiele, J.R 1973 Calculated Compaction Profiles of rhyolitic ash-flow tuffs. *Geol. Soc. Amer. Bull* **84**, pp 2193-2216.

Rimstidt et al. (1998) — Rimstidt, J.D., Balog, A., and Webb, J. 1998 Distribution of trace elements between carbonates and aqueous fluids *Geochim et Cosmochim Acta*, **62**, pp. 1851-1863

Robie and Hemingway (1995) — Robie R.A and Hemingway B.S. 1995 Thermodynamic properties of minerals and related substances at 298 15 and 1 bar (10^5 Pascals) pressure and at higher temperatures *Geol. Surv Bull.* **2131**. 461 p.

Robison (1984) — Robison, J. H. 1984 Ground-Water Level Data and Preliminary Potentiometric-Surface Maps, Yucca Mountain and Vicinity, Nye County, Nevada *United States Geological Survey, Water Resources Investigations Report, USGS-WRI-84-4197.*

Roedder (1984) — Roedder, E. 1984 Fluid Inclusions Review in Mineralogy. v. 12. Min Soc. Amer. 644 p.

Roedder and Whelan (1998) — Roedder, E and Whelan, J.F. 1998 Ascending or descending water flow through Yucca Mountain tuffs? – Fluid Inclusion Evidence. *Abst. 7th PACROFI Meeting*, Las Vegas, Nevada, 1-4 June, 1998, p. 56.

Roedder et al. (1994) — Roedder, E., Whelan, J.F., and Vaniman, D.T. 1994 Fluid Inclusion Studies of Calcite Veins from Yucca Mountain, Nevada, Tiffs: Environment of Formation *Proc. Int Con , Amer. Nucl. Soc.* "High-Level Radioactive Waste Management". La Grande Park, Illinois pp. 1854-1860

Rollinson (1993) — Rollinson, H. 1993 Using Geochemical Data: Evaluation, Presentation, Interpretation Pearson Education Limited. 352 p.

Romberger (1986) — Romberger, S.B. 1986 Ore Deposits #9, Disseminated Gold Deposits. *Geiscience Canada*, **13**, pp. 23-31.

Rosinski and Snow (1961) — Rosinski, I. and Snow, J. 1961 Mathematical survey of the coagulation *J Matarol* **18**, p. 739.

Russell (1987) — Russell, C.E 1987 Hydrologic Investigations of Flow in Fractured Tuffs, Rainier Mesa, Nevada Test Site *M S Thesis, University of Nevada-Reno*, Reno, Nevada

Rye and Ohmoto (1974) — Rye, R. O. and Ohmoto, H 1974 Sulfur and Carbon Isotopes and Ore Genesis: A Review *Econ Geol.* **69**, pp. 826-842.

Ryzhenko and Krainov (2000) — Ryzhenko, B.N. and Krainov, S.R. 2000 Influence of the weight relationships of the reacting rocks and water on the chemical composition of natural water solutions in systems, open for CO_2 *Geochemistry*. **8**, pp. 725-737. (*In Russian*)

Ryzhenko et al. (1996) — Ryzhenko, B N., Barsukov, V.L., and Kniazeva, S.N. 1996 Chemical characteristics (composition, pH, Eh) of the rock/water systems: I. Systems "granite/water" and "syenite/water". *Geochemistry*. **5**, pp 436-454. (*In Russian*)

Ryzhenko et al. (2000) — Ryzhenko, B N , Barsukov, V.L., and Kniazeva, S N. 2000 Chemical characteristics (composition, pH, Eh) of the rock/water systems: III. Systems "pyroxenite/water" and "dunite /water". *Geochemistry*. **6**, pp. 618-642. (*In Russian*)

S

Sabelfeld et al. (1996) — Sabelfeld, K.K., Rogasinsky, S V., Kolodko, A.A., Levykin, A I. 1996 Stochastic algorithms for solving Smolukhovski coagulation equation and applications to aerosol growth simulation. *Monte Carlo Methods and Applications*, **2**, 1, pp. 41-87.

Salomons and Mook (1986) — Salomons, W and Mook, W.G. 1986 Isotope geochemistry of carbonates in the weathering zone. In: P. Fritz and J.Ch. Fontes, Eds *Handbook of Environmental*

Isotope Geochemistry 2. The terrestrial Environment, B. Elsevier, Amsterdam pp 239-269.

Sass (1998) — Sass, J. 1998 Thermal tracking of water flow under Yucca Mountain *Proc. Int Con , Amer. Nucl. Soc.* "High-Level Radioactive Waste Management". La Grande Park, Illinois. pp. 269-271.

Sass (1999) — Sass, J 1999 Thermal Manifestation of Hydrologic Phenomena in the Great Basin of the Southwestern United States. *Supplement to EOS*, April 27, 1999

Sass and Lachenbruch (1982) — Sass, J.H and Lachenbruch, H 1982 Preliminary Interpretation of Thermal Data from the Nevada Test Site *USGS Open File Report 82-973*, Denver, CO.

Sass et al. (1971) — Sass, J., Lachenbruch, A , Munroe, R., Greene, G., and Moses, T. (Jr) 1971 Heat flow in the Western United States *Journ of Geophys. Res.* **76**, 26, pp. 6376-6413.

Sass et al (1980) — Sass, J.H , Lachenbruch, H.A , and Mase, T. 1980 Analysis of Thermal Data from Drill Holes UE-25a3 and UE-25a1, Calico Hills and Yucca Mountain, Nevada Test Site. *USGS Open File Report 80-826*, Denver, CO

Sass et al. (1983) — Sass, J. H., Lachenbruch, H.A., Grubb, H., and Mase T. 1983 Status of Thermal Observations at Yucca Mountain, Nevada. *USGS Letter Report to DOE.*

Sass et al (1987) — Sass, J.H., Lachenbruch, A.H., Dudley, W W., Priest, S S , and Munroe, R J. 1987 Temperature, Thermal Conductivity, and Heat Flow near Yucca Mountain, Nevada: Some Tectonic and Hydrologic Implications *US Geological Survey Open-File Report 87-649*, Denver, CO. - 118 p.

Sass et al (1995) — Sass, J.H , Dudley, W.W., and Lachenbruch, A.H. 1995 Regional thermal setting, chap 8, *in* Major Results of Geophysical Investigations at Yucca Mountain and Vicinity, Southern Nevada, H.W. Oliver, D A. Ponce and W.C. Hunter, Eds. *U.S Geol Survey Open File Rep. 95-74*, 23 pp.

Schmitt (1993) — Schmitt, R A , 1993. Technical Report, Radiation Center Project No 926. In Livingston D E , Trace Element and REE Composition of Five Samples of the Yucca Mountain Calcite/Silica Deposits. *Special Report No. 8*, Submitted to the Nuclear Waste Project Office, State of Nevada.

Schuraytz et al. (1989) — Schuraytz, B J., Vogel, T.A., and Younker, L.W. 1989 Evidence for dynamic withdrawal from a layered magma body: The Topopah Spring Tuff, southwestern Nevada *J. Geophys. Res* **94-B5**, pp. 5925-5942.

Schwartz et al. (1976) — Schwartz, H P., Harmon, R S , Thompson, R, and Ford, D.C. 1976 Stable isotope studies of fluid inclusions in speleothems and their paleoclimatic significance. *Geochim Cosmochim Acta* 40, 657-665.

Scott and Castellanos (1984) — Scott, R. and Castellanos, M 1984 Preliminary report on the geologic character of the drill hole USW GU-3/G-3. *USGS, Open-file report, 84-491.*

Senderov and Khitarov (1970) — Senderov E.E. and Khitarov N.I. (1965) Zeolites, Their Synthesis and Conditions of Formation in Nature. Moscow, Nauka 283 p. (*In Russian*)

Shafranovsky (1968) — Shafranovsky, I I. 1968. Lectures on crystal morphology. Moscow, Vyshaya Shkola, 174. (*In Russian*)

Shannon and Prewit (1969) — Shannon, R.D. and Prewit, C T. 1969 Effective ionic radii in oxides and fluorides. *Acta Cristallographica* **25**, pp. 925-1047.

Sharp (1992) — Sharp, Z.D 1992 In situ laser microprobe techniques for stable isotope analysis. *Chemical Geology*. 101. pp 3-19.

Sharp and Cerling (1996) — Sharp, Z D. and Cerling, T.E. 1996 A laser GC-IRMS technique for in situ stable isotopic analyses of carbonates and phosphates. *Geochim et Cosmochim. Acta* **60**, 15, pp. 2909-2916

Shepherd et al. (2000) — Shepherd, T.J., Naden, J., Chenery, S.R., Milodowski, A E , Gillespie, M R 2000 Chemical analysis of palaeogroundwaters: a new frontier for fluid inclusion research *Journal of Geochemical Exploration* 69–70 pp 415–418.

Sheppard (1971) — Sheppard, R. A 1971 Zeolites in sedimentary deposits of the United States - a review. *Am Chem Soc Adv Chem Ser. Ed.* **101**, pp. 279-310.

Sherbina and Naumov (1963) — Sherbina, V.V. and Naumov, G B 1963 Basic features of uranium, governing its geochemistry. *In*. A P. Vinogradov, Ed Basic features of uranium geochemistry Academy of Sciences of the USSR Press, Moscow. pp. 5-26. (*In Russian*)

Shieh and Taylor (1969) — Shieh, Y.N. and Taylor, H.P. Jr. 1969 Oxygen and carbon isotope studies of contact metamorphism of carbonate rocks. *J. Petrol.* **10**, p. 307-331.

Shock and Helgeson (1988) — Shock, E.L and Helgeson, H C. 1988 Calculation of the thermodynamic and transport properties of aqueous species at high pressures and temperatures: Correlation algorithms for ionic species and equation of state predictions to 5 kb and 1000 °C. *Geochim et Cosmochim Acta* **52**, pp. 2009-2036.

Shock et al (1997) — Shock, E.L , Sassani, D.C., Willis, M , and Sverjensky, D.A. 1997 Inorganic species in geologic fluids: correlations among standard molal thermodynamic properties of aqueous ions and hydroxide complexes. *Geochim et Cosmochim Acta.* **61**, 5, pp

907-950.

Sholkovitz et al (1994) — Sholkovitz, E., Landing, W.M., Lewis, B.L. 1994. Ocean particle chemistry the fractionantion of rare-earth elements between suspended particles and seawater. *Geochim Cosmochim. Acta*, **58**, pp 1567-1580.

Shvarov (1999) — Shvarov, Y.V. 1999 Algoritmization of numeric equilibrium modeling of the dynamic geochemical processes *Geochemistry.* **6**, pp. 646-652 (*In Russian*)

Sibson et al. (1975) — Sibson, R.H , Moore, J.M., and Rankin, A H. 1975 Seismic Pumping - a Hydrothermal Fluid Transport Mechanism *Journal Geological Society of London*, **131**.

Slate et al (1999) — Slate, J. L , Berry, M E., Rowley, P. D., Fridrich, C. J., Morgan, K. S., Workman, J. B., Young, O. D., Dixon, G. L , William, s V. S., McKee, E. H , Ponce, D. A., Hildenbrand, T. G., Swadley, W. C., Lundstrom, S. C., Ekren, E. B , Warren, R. G., Cole, J. C., Fleck, R. J., Lanphere, M. A , Sawyer, D. A., Minor, S A., Grunwald, D. J., Laczniak, R J , Menges, C. M., Yount, J. C. and Jayko, A. S. 1999 Digital geologic map of the Nevada Test Site and vicinity, Nye, Lincoln, and Clark Counties, Nevada, and Inyo County, California. *USGS, Open-File Report 99-554-A*, 56 p.

Smirnov (1969) — Smirnov, V.I. 1969 Velocity of coagulation and condensation growth of the aerosol particles Gidrometeoizdat, Moscow. (*In Russian*)

Smirnov and Dublyansky (2000) — Smirnov, S and Dublyansky, Y. 2000 Secondary mineral assemblages in fractures and lithophysal cavities at Yucca Mountain, Nevada, USA. *GSA Abstracts with Program.* **32**, 7. p. A-260

Smirnov and Dublyansky (2001-a) — Smirnov, S Z. and Dublyansky, Y.V. 2001-a Ontogenetic mineralogy of secondary minerals from the vadose zone of Yucca Mountain, Nevada Report Submitted to the Agency for Nuclear Projects, State of Nevada, May 2001. Part I 114 p + Appendices

Smirnov and Dublyansky (2001-b) — Smirnov, S. and Dublyansky, Y., 2001-b Ontogenetic Mineralogy of Secondary Minerals at Yucca Mountain, Nevada. *Proc. Int. Con , Amer. Nucl. Soc* "High-Level Radioactive Waste Management", Las Vegas, Nevada

Smirnov et al. (2002) — Smirnov, S., Dublyansky, Y., Mel'gunov, M , and Mel'gunova, E. 2002 REE geochemistry of the fluorite from Yucca Mountain, USA: fingerprinting multiple sources of matter in hydrothermal fluids. 2002 International Goldschmidt Conference on Geochemistry. Zurich, 14-25 August 2002

Smith (1991) — Smith, M.R. 1991 Natural Radionuclide/Trace Element Hydrochemistry - Characterization of the Yucca Mountain Saturated (well water) and Unsaturated (pore water) Zone Ground Waters. *Pacific Northwest Laboratory*, Richland, Washington.

Smith and Shaw (1975) — Smith, R.L , and Shaw, H R. 1975 Igneous-Related Geothermal Systems *In* D E White and D.L Williams, *Eds* Assessment of Geothermal Resources of the United States – 1975. U.S. Geological Survey Circular 726 pp 58-83.

Smith et al (2002) — Smith, E I , Keenean, D.L , and Plank, T. 2002 Episodic Volcanism and Hot Mantle: Implications for Volcanic Hazard Studies at the Proposed Nuclear Waste Repository at Yucca Mountain, Nevada. GSA Today, **12**, 4, pp. 4-10

Smolukhovski (1936) — Smolukhovski, M 1936 Three presentations on diffusion, Brownian motion and coagulation of colloidal particles Brownian motion. Moscow. pp. 332-415. (*In Russian*)

Smyth and Bish (1988) — Smyth, J R. and Bish, D. L 1988 Crystal Structure and Cations Sites of the Rock Forming Minerals Allen and Unwin.

Smyth and Caporuscio (1981) — Smyth, J. R and Caporuscio, F. A 1981 Review of the thermal stability and and cation exchange properties of the zeolites mineral clinoptilolite, mordenite and analcime: application to radioactive waste isolation in silicic tuffs. *Los Alamos Natl Lab., Report LA-8841-MS*

Somerville et al (1992) — Somerville M R., Frazier, G A , and C. B., Archambeau, 1992. Yucca Mountain Hydrothermal History. *Quarterly Report No 1*. Submitted to the Nuclear Waste Project Office of the State of Nevada

Spengler et al (1981) — Spengler, R.W., Byers, F.M , Jr., and Warner, J.B. 1981 Stratigraphy and structure of volcanic rocks in drill hole USW-G1, Yucca Mountain, Nye County, Nevada *U S Geological Survey Open File Report 82-1338*. 264 p

Stahl (1977) — Stahl, W.J 1977 Carbon and nitrogen isotopes in hydrocarbon research and exploration *Chemical Geology*, **20**, pp. 121-149.

Stankeev (1986) — Stankeev, E. A. 1986. Genetic mineralogy. Moscow, Nedra, 272. (*In Russian*)

Strikland-Constable (1971) — Strikland-Constable, R.F. 1971 Kinetics and mechanism of crystallization Nedra, Leningrad. (*In Russian*)

Stuckless et al. (1991) — Stuckless, J S , Peterman, Z.E., and Muchs, D.R. 1991 U and Sr isotopes in Ground Water and Calcite, Yucca Mountain, Nevada: Evidence Against Upwelling Water *Science*, **254**. pp. 551-554

Stuckless et al (1998) — Stuckless, J S , Marshall, B.D , Vaniman, D.T., Dudley, W.W., Peterman, Z.E., Paces, J.B , Whelan, J.F., Taylor, E.M., Forester, R.M., and O'Leary, D.W., 1998 Comments on "Overview of calcite/opal deposits at or near the proposed high-level nuclear waste site, Yucca Mountain, Nevada, USA: pedogenic, hypogene, or both" by C.A Hill, Y.V. Dublyansky, R.S. Harmon, C M. Schluter. *Environmental Geology*. 43(1). pp 70-78.

Sullivan and Pescatore (1994) — Sullivan, T.M. and Pescatore, C. 1994 Release of Radon Contaminants from Yucca Mountain: The Role of Buoyancy Driven Flow. *Report to the U.S DOE on contract DE-AC02-79CH00016* Brookhaven National Laboratory – Environmental and Waste Technology Center. 31 p. + Appendices

Sun and Semkow (1998) — Sun, H and Semkow, T.M. 1998 Mobilization of thorium, radium and radon radionuclides in ground water by successive alpha-recoil. *Journ of Hydrology*, **205**, pp. 126-136.

Sunagawa (1953) — Sunagawa I. 1953 Variation of crystal habit of calcite, with special reference to the relation between crystal habit and crystallization stage. *Rep. Geol Surv. Japan* No. 155.

Sunagawa (1982) — Sunagawa, I. 1982. Morphology of crystals in relation to growth conditions. *Estudios geol* **38**, pp 127-134.

Sutugin et al. (1971) — Sutugin, A.G., Kotsev, E I., Fouks, N.A. 1971 Formation of the condensation highly disperse non-coagulated aerosols. *Zourn Colloid.* **33**, 4, pp. 585-591. (*In Russian*)

Sutugin et al. (1978) — Sutugin, A.G , Puchkov, A.S , Luchnicov, A.A. 1978 Evolution of coagulation systems. *Colloid Zh* **40**, p. 285

Sverjensky (1984) — Sverjensky, D A. 1984 Eiropium redox equilibria in aqueous solutions. *EPSL*, **67**, pp 70-78.

Sverjensky et al. (1991) — Sverjensky, D.A., Hemley, J J , and D'Angelo, W.M 1991 Thermodynamic assessment of hydrothermal alkali feldspar- mica-aluminosilicate equilibria. *Geochim et Cosmochim Acta*. **55**, pp. 989-1004.

Sverjensky et al (1997) — Sverjensky, D A , Shock, E.L., and Helgeson, H.C 1997 Prediction of the thermodynamic properties of aqueous metal complexes to 1000°C and 5 kb. *Geochim. et Cosmochim. Acta*. **61**, 7, pp.1359-1412

Szabo and Kyser (1990) — Szabo, B.J. and Kyser, T.K. 1990 Ages and stable-isotope compositions of secondary calcite and opal in drill cores from tertiary volcanic rocks of the Yucca Mountain, Nevada *Geol Soc. Amer. Bull.* **102**, pp. 1714-1719.

Szabo and O'Malley (1985) Szabo, B J. and O'Malley, P. A. 1985 Uranium-Series Dating of Secondary Carbonate and Silica Precipitates Relating to Fault Movements in the Nevada Test Site Region and of Caliche and Travertine Samples from the Amargosa Desert. *United States Geological Survey Open-File-Report 85-47.*

Szabo et al. (1981) Szabo, B J , Carr, W. J., and W.C, Gottschall, 1981. Uranium-Thorium Dating of Quaternary Carbonate Accumulations in the Nevada Test Site Region, Southern Nevada *United States Geological Survey Open-File-Report 81-119.*

Szymanski (1989) Szymanski, J.S 1989 Conceptual Considerations of the Yucca Mountain Groundwater System with Special Emphasis on the Adequacy of this System to Accommodate a High-Level Nuclear Waste Repository. Internal Report, U.S Department of Energy, Nevada Operations Office, Las Vegas, Nevada.

Szymanski (1992) Szymanski, J. S. 1992 The origin and history of alteration and carbonatization of the Yucca Mountain ignimbrites. *U S Department of Energy, Internal Report.*

T

Talma and Netterberg (1983) Talma, A.S. and Netterberg, F. 1983 Stable isotope abundances in calcretes. In: R.C.L. Wilson, Ed Residual deposits: Surface Related Weathering Processes and Materials Geological Society of London pp. 221-233.

Taylor and McLennan (1985) Taylor, S R , and McLennan, S.M. 1985 The continental crust: its composition and evolution Blackwell, Oxford.

Tesoriero and Pankow (1996) Tesoriero, R J. and Pankow, J.F. 1996 Solid solution partitioning of Sr, Ba, and Cd to calcite. *Geochim et Cosmochim Acta*, **60**, pp. 1053-1063.

Thompson (1998) Thompson, J. L , ed , 1998, Laboratory and field studies related to radionuclide migration at the Nevada test site: Los Alamos National Laboratories, *Report LA-13419-PR*, 31 p

Thorstensen et al (1989) Thorstensen, D. C., Weeks, E. P., Haas, H., and Woodward J. C. 1989 Physical and Chemical Characteristics of Topographically Affected Airflow in an Open Borehole at Yucca Mountain, Nevada. Proceedings, the Focus '89 Nuclear Waste in the Unsaturated Zone, September 18-21, Las Vegas, Nevada

Tikunov (1989) Tikunov, Y.V. 1989 On the mobilization of uranium in vitric volcanogenic rocks. Acta of the Institute of Geology and Geophysics, Academy of Sciences of the USSR, Novosibirsk, № 750, pp. 122-130. (*In Russian*)

Truesdel and Jones (1974) Truesdel, A.H. and Jones, B.F. 1974 WATEQ: A computer program for calculating chemical equilibria of natural waters· *U S Geol Survey Jour Research* **2** pp 233

chemical equilibria of natural waters: *U.S Geol. Survey Jour. Research*, **2**, pp. 233-248.

Turi (1986) — Turi, B. 1986 Stable Isotope Geochemistry of Travertines. In P. Fritz and J.Ch Fontes, Eds. *Handbook of Environmental Isotope Geochemistry. 2. The terrestrial Environment, B.* Elsevier, Amsterdam. pp. 207-238.

U

U.S DOE (1988) — U.S. DOE (U. S. Department of Energy) 1988 Site Characterization Plan, Yucca Mountain Site, Nevada Research and Development Area. U. S. Department of Energy, Office of Civilian Radioactive Waste Management, Washington, D C

U S. DOE (1993-a) — U.S. DOE (U.S. Department of Energy) 1993 Report on the Origin of Calcite-Silica Deposits at Trench 14 and Busted Butte and Methodologies Used to Determine Their Origin. *Report YMP193-11-R.* U.S. Department of Energy, Yucca Mountain Site Characterization Project, 64 pp. + Appendices

U.S. DOE (1993-b) — U.S DOE (U. S. Department of Energy) 1993 Transmittal Letter of December 20, 1993 "Second Installment of Data Reported in U. S. Geological Survey (USGS) Monthly Reports" from Nelson, R M to R R. Loux (Agency for Nuclear Projects, State of Nevada)

U.S DOE (1998) — U.S. DOE (U. S Department of Energy) 1998 Viability Assessment of a Repository at Yucca Mountain. Vol 1. Introduction and Site Characterization. *DOE/RW-0508.* U. S. Department of Energy, Office of Civilian Radioactive Waste Management, Washington, D C.

U.S. DOE (1999) — U.S. DOE (U.S. Department of Energy) 1999 Draft Environmental Impact Statement for a Geologic Repository for the Disposal of Spent Nuclear Fuel and High-Level Radioactive Waste at Yucca Mountain, Nevada. *DOE/EIS-0250D.*

U.S. DOE (2001) — U.S. DOE (U. S Department of Energy) 2001 Yucca Mountain Science and Engineering Report. Technical Information Supporting Site Recommendation Consideration *DOE/RW-0539.*

USGS (1993) — USGS (U.S Geological Survey) 1993 Monthly Report of Ongoing Work. January 1993.

USGS (1997) — USGS (U.S Geological Survey) 1997 USGS Level 4 Milestone SPC23FM4; Appendix E: U-Pb dating (L.A Neymark, main author) pp E-1-E-11.

V

Vaniman (1993) — Vaniman, D.T. 1993 Calcite deposits in fractures at Yucca Mountain, Nevada *Proc. Int Con , Amer. Nucl Soc.* "High-Level Radioactive Waste Management". La Grande Park, Illinois. pp. 1935-1939.

Vaniman and Chipera (1996) — Vaniman, D T. and Chipera, S.J. 1996 Paleotransport of lanthanides and strontium recorded in calcite compositions from tuffs at Yucca Mountain, Nevada, USA. *Geochim. et Cosmochim Acta* **60**, pp. 4417-4433.

Vaniman and Whelan (1994) — Vaniman, D.T., and Whelan, J.F. 1994 Inferences of Paleoenvironment from Petrographic, Chemical, and Stable-Isotope Studies of Calcretes and Fracture Calcites *Proc Int. Con , Amer. Nucl Soc* "High-Level Radioactive Waste Management" La Grande Park, Illinois pp. 2730-2737.

Vaniman et al. (1984) — Vaniman, D., Bish, D , and Levy, S. 1984 Progress report: Studies of the origins of soil and fault-related mineralogy in the vicinity of Yucca Mountain. *TWS-ESS-1-11/84-22.* 6 p.

Vaniman et al (1988) — Vaniman, D. T., Bish, D. L., and Chipera, S 1988. A Preliminary Comparison of Mineral Deposits in Faults Near Yucca Mountain, Nevada, with Possible Analogs. *Los Alamos National Laboratory Report, LA-11289-MS.*

Vaniman et al. (1995) — Vaniman, D. T., Chipera, S., and Bish, D. L. 1995 Petrography, Mineralogy, and Chemistry of Calcite-Silica Deposits at Exile Hill, Nevada, Compared with Local Spring Deposits. *Los Alamos National Laboratory Report, LA-13096-MS* 70 p

Vaniman et al (2001) — Vaniman, D. T., Chipera, S. J., Bish, D L., Carey, W. and Levy, S. S. 2001. Quantification of unsaturated-zone alteration and cation exchange in zeolitized tuffs at Yucca mountain, Nevada, USA. *Geochim. et Cosmochim Acta.* **65**, 20, pp. 3409-3433.

Veimarn (1906) — Veimarn, P.P. 1906 Colloidal state as general state of the matter. *Journ. Russ Phys - Chem. Soc.* **38**.

Veizer (1983) — Veizer, J. 1983 Trace elements and isotopes in sedimentary carbonates. In Carbonates· Mineralogy and Chemistry (R.J. Reeedr, Ed) *Min. Soc. Amer Rev. in Mineralogy*, **11**, pp. 265-299.

Voloschuk and Sedunov (1975) — Voloschuk, V.M. and Sedunov, Y.S 1975 Processes of coagulation in disperse systems Gidrometeoizdat. Leningrad. (*In Russian*)

Von Herzen and Lee (1969) — Von Herzen, R.P., and Lee, H.K. 1969 Heat Flow in Oceanic Regions *In*: The Earth's Crust and Upper Mantle, *Geophysical Monograph, 13.* American

Geophysical Union

Vosel and Kalinin (1999) — Vosel, S V. and Kalinin D.V. 1999 Thermodynamic analysis of formation of crystal-like noble-opal structures. *Russian Geology and Geophysics*, **40**, 4, pp 606-614.

W

Wang and Merino (1992) — Wang Y. and Merino E. 1992 Dynamic model of oscillatory zoning of trace elements in calcite: Double layer, inhibition, and self-organization *Geochim et Cosmochim. Acta* **56**, pp. 587–596

Warren et al. (1984) — Warren, R G., Byers, F.M., and Caporuscio, F.A , 1984 Petrography and mineral chemistry of units of the Topopah Spring, Calico Hills and Crater Flat Tuffs, and some other volcanic units, with emphasis on samples from drill hole USW G-1, Yucca Mountain, Nevada Test site Los Alamos Natl. Lab. Report LA-10003-MS

Wedepohl (1971) — Wedepohl, K. H. 1971. Geochemistry. Holt, Rinehart, and Winston, Inc

Weeks (1991) — Weeks, E.P. 1991 Does the Wind Blow through Yucca Mountain? *In*· D D. Evans and T.J. Nicholson, (Eds) Workshop V: Flow and Transport in Unsaturated Fractured Rock – Related to High-Level Radioactive Waste Disposal NUREG/CR-0040. pp. 43-53.

Weiss (1990) — Weiss, S. I. 1990 Yucca Mountain Project Monthly Report Task No. 3 - August, 1990 The State of Nevada Nuclear Waste Project Office, Agency for Nuclear Projects

Weiss et al. (1994) — Weiss, S.I., Noble, D C., Jackson, M.R., Connors, K.A , and McKee, E.H. 1994 Multiple Episodes of Hydrothermal Activity and Epithermal Mineralization in the Southwestern Nevada Volcanic Field and Their Relations to Magmatic Activity, Volcanism and Regional Extension. Appendix A in: Evaluation of Geologic Relations and Seismotectonic Stability of the Yucca Mountain Area Nevada Nuclear Waste Site Investigations - Progress Report, Center for Neotectonic Studies, Mackay School of Mines, University of Nevada Reno. September 1994 Inconsecutive pages.

Wells (1976) — Wells, P.V. 1976 Macrofossil analysis of wood rat (*Neotoma*) middens as a key to the Quaternary vegetation history of arid America. *Quaternary Research*. 6, pp. 223-248.

Whelan and Moscati (1998) — Whelan, J F. and Moscati, R.J. 1998 9 M Y. record of Southern Nevada climate from Yucca Mountain secondary minerals. *Proc Int. Con , Amer. Nucl. Soc.* "High-

Level Radioactive Waste Management". La Grande Park, Illinois. pp. 12-15

Whelan and Stuckless (1991) Whelan, J.F., and Stuckless, J S., 1991 Paleohydrologic Implications of the Stable Isotope Composition of Secondary Calcite within the Tertiary Volcanic Rocks of Yucca Mountain, Nevada *Proc. Int Con., Amer. Nucl. Soc.* "High-Level Radioactive Waste Management". La Grande Park, Illinois, pp. 1572-1581.

Whelan et al. (1994) Whelan, J.F., Vaniman, D T., Stuckless, J.S. and Moscati, R.J. 1994 Paleoclimatic and Paleohydrologic Records from Secondary Calcite: Yucca Mountain, Nevada. *Proc. Int Con , Amer. Nucl Soc.* "High-Level Radioactive Waste Management". La Grande Park, Illinois. pp 2738-2745.

Whelan et al (1998-a) Whelan, J F., Moscati, R.J., Roedder, E., and Marshall, B.D. 1998 Secondary Mineral Evidence of Past Water Table Changes at Yucca Mountain, Nevada. *Proc Int Con., Amer. Nucl. Soc.* "High-Level Radioactive Waste Management". La Grande Park, Illinois pp. 178-181.

Whelan et al. (1998-b) Whelan, J.F., Moscati, R.J., Allerton, S B M , and Marshall, B D., 1998, Applications of Isotope Geochemistry to the Reconstruction of Yucca Mountain. Nevada, Paleohydrology – Status of Investigations: June 1996. *U S Geol. Survey Open-File Report 98-83.* 41 p.

Whelan et al (1999) Whelan, J.F., Paces, J B , Moscati, R.J., Neymark, L.A., Marshall, B.D , and Peterman, Z.E. 1999 Paragenesis and Oxygen Isotopes of Calcite in Unsaturated Zone of Yucca Mountain, Nevada: Evidence of an Early Thermal Event. *Supplement to EOS*, April 27, 1999. p S7

Whelan et al. (2000) Whelan, J., Paces, J., Neymark, L., Marshall, B , Peterman, Z , Moscatti, R., and Roedder, E. 2000 Calcite fluid inclusion, paragenetic, and oxygen isotopic records of thermal event(s) at Yucca Mountain, Nevada *GSA Abstracts with Program.* **32**, 7. p A-259

Whelan et al. (2001) Whelan, J , Roedder, E., and Paces, J. 2001 Evidence for an Unsaturated-Zone Origin of Secondary Minerals in Yucca Mountain, Nevada *Proc. Int. Con , Amer. Nucl. Soc.* "High-Level Radioactive Waste Management". La Grande Park, Illinois.

Whipple et al (1998) Whipple, C.G , Budnitz, R.J , Ewing, R.C., Moeller, D.W., Payer, J.H., and Whiterspoon, P.A 1998 Yucca Mountain Total System Performance Assessment Peer Review Panel Report. *Third Interim Report.* 45 p.

Whipple et al (1999) Whipple, C., Budnitz, R., Ewing, R , Moeller, D., Payer, J., and Whiterspoon, P. 1999 Final Report, Total System Performance Assessment Peer Review Panel *Civilian Radioactive Waste Management and Operating Contractor.* Las Vegas,

NV. February 11, 1999.

White (1957) — White, D.E 1957 Thermal waters of volcanic origin *Bull. Soc. Geol Amer.* 68, pp. 1637-1658

White and Chuma (1987) — White, A F., and Chuma, H.J. 1987 Carbon and Isotopic Mass Balance Models of Oasis Valley-Fortymile Canyon Groundwater Basin, Southern Nevada. *Water Resources Research*, **23**, 4

White and Williams (1975) — White, D.E. and Williams, D.L 1975 Introduction *In*: D.E. White and D L. Williams, *Eds.* Assessment of Geothermal Resources of the United States – 1975. U.S Geological Survey Circular 726. pp. 1-4.

White et al (1980) — White, A. G., Claassen, H C., and Benson, L. V. 1980 The Effect of Dissolution of Volcanic Glass on the Water Chemistry in a Tuffaceous Aquifer, Rainier Mesa, Nevada. *USGS Water Supply Paper WSP 1536-Q*, Washington, D C.

Wilson and Cline (2001) — Wilson, N. and Cline, J. 2001 Paragenesis, Temperature and Timing of Secondary Minerals at Yucca Mountain. *Proc Int Con , Amer. Nucl Soc.* "High-Level Radioactive Waste Management". La Grande Park, Illinois.

Wilson et al. (2000) — Wilson, N.S.F , Cline, J.S , Rotert, J. and Amelin Y.V. 2000 Timing and temperature of fluid movement at Yucca Mountain, NV: Fluid inclusion analyses and U-Pb and U-series dating *GSA Abstracts with Program*, **32**, 7. p. A-260.

Wohletz and Heiken (1992) — Wohletz, K. and Heiken, G. 1992 Volcanology and Geothermal Energy. University of California Press, Berkeley, Los Angeles, Oxford. 432 p.

WoldeGabriel (1993) — WoldeGabriel, G. 1993 K/Ar Dating of Clinoptilolite, Mordenite, and Associated Clays from Yucca Mountain, Nevada. *Proceedings, International Zeolite Conference*, Boise, Idaho, June 20-28, 1993,

WoldeGabriel et al. (1993) — WoldeGabriel, G., Broxton, D.E , Bish, D.L , and Chipera, S.J. 1993 Mineralogy and clinoptilolite K/Ar results from Yucca Mountain, Nevada , USA· A potential high-level radioactive waste repository site. *Los Alamos Natl. Lab Rept LA-12652-MS*

Y

Yang (1992) — Yang, I C., 1992. Flow and Transport Through Unsaturated Rock - Data from Two Test Holes, Yucca Mountain, Nevada *Proc Int Con , Amer. Nucl Soc.* "High-Level Radioactive Waste Management". La Grande Park, Illinois.

Yang et al. (1996) Yang, I C., Rattray, G W., and Yu, P. 1996 Interpretation of chemical and isotopic data from boreholes in the unsaturated zone at Yucca Mountain, Nevada. *U.S Geological Survey Water-Resources Investigations Report 96-4058*. 58 p

Yang et al. (1998) Yang, I C., Yu, P. Rattray, G.W., Fararese, J.S , and Ryan, J.N. 1998 Hydrochemical Investigations in characterizing the unsaturated zone at Yucca Mountain , Nevada *USGS Water-Resources Investigation Report 98-4132*, Denver, CO, 33. p

Yarborough (1980) Yarborough, K.A. 1980 The National Park Service cave radiation research and monitoring program *Proc. Natl. Cave Management Symposium*, Carlsbad, New Mexico. pp 27-40.

Z

Zartman and Kwak (1993-a) Zartman, R. E., and Kwak, L. M 1993 Preliminary Study of Lead Isotopes in the Carbonate-Silica Veins of Trench 14, Yucca Mountain, Nevada *U. S Geological Survey Open-File-Report 93-690*

Zartman and Kwak (1993-b) Zartman, R E. and Kwak, L M. 1993 Lead Isotopic Composition of Paleozoic and Late Proterozoic Marine Carbonate Rocks in the Vicinity of Yucca Mountain, Nevada *Proc. Int. Con , Amer. Nucl Soc* "High-Level Radioactive Waste Management". La Grande Park, Illinois. pp 1953-1959

Zhang and Dawe (2000) Zhang, Y. and Dawe, R. A. 2000. Influence of Mg^{2+} on the kinetics of calcite precipitation and calcite crystal morphology. *Chemical Geology*. **163**, pp. 129-138

Zielinski (1980) Zielinski, R.A 1980 Uranium in Secondary Silica: A Possible Exploration Guide. *Economic Geology*. **75**, pp. 592-602.

Zielinski (1982) Zielinski, R.A 1982 Uraniferous opal, Virgin Valley, Nevada· Conditions of Formation and Implications for Uranium Exploration *Journal of Geochemical Exploration*. **16**, pp 197-216

Zielinski and Rosholt (1978) Zielinski, R.A and Rosholt, J.N 1978 Uranium in Waters and Aquifer Rocks at the Nevada Test Site, Nye County, Nevada. *USGS Jour. Res* , **6**, 489.

Zukin et al. (1987) Zukin, J.G., Hammond, D E., Ku, T.L., and Elders, W.E 1987 Uranium-Thorium Series Radionuclides in Brines and Reservoir Rocks from Two Geothermal Boreholes in the Salton Sea Geothermal Field, Southeastern California. *Geochim et Cosmochim. Acta*, **551**.

Zverev et al. (1975) Zverev, V.L., Dolidze, N.I , Spiridonov, A.I. 1975 Anomaly of even isotopes of uranium in groundwaters of the seismically active regions of Georgia.

Geochemistry. 11, pp. 1720-1723. (*In Russian*)

Zverev et al (1980) Zverev, V.L , Tokarev, A.N , Timinski, V.G , and Shvets, V.M. 1980 Radioisotope geochemistry. Moscow, Nedra. 201 p (*In Russian*)